UNIVERSIDADE DA BEIRA INTERIOR
Engenharia

Simulation of 4D Trajectory Navigation

Francisco Emanuel Silva Lucas

Dissertação para obtenção do Grau de Mestre em
Engenharia Aeronáutica
(Ciclo de estudos integrado)

Orientador: Prof. Doutor Kouamana Bousson

Covilhã, outubro de 2017

Acknowledgments

I would like to thank professor Bousson for his expert advice throughout this difficult project. I also wish to thank my family, girlfriend and friends for their support and encouragement throughout my study.

Resumo

Um algoritmo foi desenvolvido para prever com exatidão a navegação de trajetórias aéreas 4D juntamente com uma interface gráfica do utilizador para permitir a simulação eficaz de várias trajetórias com diferentes parâmetros. Várias simulações foram efetuadas recorrendo a esta ferramenta, que foram depois analisadas e comparadas com valores das trajetórias reais, de forma a validar a sua precisão. A necessidade para tal ferramenta emergiu do aumento constante da procura relativamente ao espaço aéreo, a qual se espera que se mantenha até 2030. As iniciativas SESAR na Europa e NextGen nos EUA visam responder a esta necessidade recorrendo para isso à implementação de trajetórias 4D na navegação aérea geral. O modelo dinâmico escolhido foi o modelo cinético de ponto-massa que gera resultados suficientemente exatos sem requerer demasiada informação especifica de cada aeronave. Uma base de dados contendo a informação necessária para a simulação de várias aeronaves de transporte comercial com motores *turbofan* foi compilada. De forma a abranger o efeito da atmosfera na simulação foi incorporada na ferramenta uma base de dados com informação atmosférica histórica mundial. A informação de intenção necessária para a simulação é o percurso da aeronave na forma de *waypoints* e alguns parâmetros de voo específicos de cada fase de voo. A ferramenta foi criada com a linguagem de programação *Python* e a biblioteca *open source* para a criação de *interfaces* gráficas do utilizador *Kivy*. Três voos foram simulados com o intuito de serem analisados e validados ao serem comparados com valores reais, de forma a estudar a exatidão da ferramenta. Os resultados gerais obtidos foram positivos com 2.27% de erro médio relativamente à duração média dos voos e 9.19% de erro médio relativamente à posição da aeronave ao longo do voo. A exatidão da ferramenta foi satisfatória dado a quantidade de fontes de erro na previsão de trajetórias de voo, no entanto, são importantes mais melhoramentos para que a ferramenta seja implementada com sucesso em sistemas reais de gestão de tráfego aéreo.

Palavras-chave

Trajetórias 4D; Navegação de trajetórias; Simulação de trajetórias, Interface gráfica do utilizador

Abstract

An algorithm to accurately predict 4D trajectory navigation was developed alongside a graphical user interface (GUI) to allow the easy simulation of several trajectories with different parameters. Several simulations were conducted using this tool which were then analyzed and compared with actual flight values in order to validate its accuracy. The need for such a tool emerges from the ever increasing demand regarding the air transportation system, that is expected to maintain positive growth rates up until 2030. The programs of SESAR in Europe and NextGen in the USA were initiated to respond to this need and at their heart lies the implementation of 4D trajectories. A point-mass kinetic model was chosen to simulate the aircraft's movement, as it provides sufficiently accurate results without requiring too much aircraft specific information. A database containing the information of several large turbofan commercial aircraft was compiled. In order to model the effect of the weather on the simulation, a large world wide historical weather database was incorporated into the tool. The intent information required for simulation is the flight's course (in waypoints) and certain flight phase specific parameters. The tool was created using the Python programming language and the open source library for GUI development Kivy. Three real flights were simulated and their performance was analyzed. A comparison between the simulated and the actual flight's values was made in order to validate the tool's accuracy. The results were satisfactory with the three flights averaging a 2.27% error regarding average flight duration as well as a 9.19% median error regarding the aircraft's position throughout the flight. Overall the tool proved to be satisfactorily accurate given the amount of possible error sources for flight trajectory prediction however, further improvements are important for implementation in real active air traffic management systems.

Keywords

4D-Trajectories; Trajectory navigation; Trajectory simulation; Graphical User Interface

Contents

List of Figures

List of Tables

List of Acronyms

4DT	4 Dimensional Trajectories
AA	American Airlines
ADREP	Accident/Incident Data Reporting
ADS-B	Automatic Dependent Surveillance-Broadcast
ANSP	Air Navigation Service Provider
AR	Aspect Ratio
ATC	Air Traffic Control
ATM	Air Traffic Management
BADA	Base of Aircraft Data
CTA	Controlled Time of Arrival
EAM	Extended Arrival Management
FAA	Federal Aviation Administration
FL	Flight level
FMS	Flight Management System
GPS	Global Positioning System
GUI	Graphical User Interface
IATA	International Air Transportation Association
ICAO	International Civil Aviation Organization
ITP	In Trail Procedures
JSON	JavaScript Object Notation
LTO	Landing and Takeoff
MTOW	Maximum Takeoff Weight
NAS	National Airspace System
NCAR	National Center for Atmospheric Research
NCEP	National Center for Environmental Prediction
NextGen	Next Generation Air Transportation System
NNEW	NextGen Network Enabled Weather
NOAA	National Oceanic and Atmospheric Administration
NOTAM	Notice to Airmen
NVS	National Airspace System Voice Switch
RAM	Random Access Memories
RBT	Reference Business Trajectory
RVR	Runway Visual Range
SES	Single European Sky
SESAR	Single European Sky ATM Reserach
SFC	Specific Fuel Consumption
SOA	Service Oriented Architecture
SWIM	System Wide Information Management
TBFM	Time Based Flow Management
TBO	Trajectory Based Operation
TP	Trajectory Prediction
TSFC	Thrust Specific Fuel Consumption
UA	United Airlines
UTC	Coordinated Universal Time

Nomenclature

a	Acceleration	$[m/s^2]$
b	Wing Span	$[m]$
c	Sound Speed	$[m/s]$
$C_{D0_{flap}}$	Flaps Parasitic Drag Coefficient	$[-]$
C_{D0}	Parasitic Drag Coefficient	$[-]$
C_L	Lift Coefficient	$[-]$
C_Lg	Lift Coefficient on the Ground	$[-]$
c_{SFC}	Specific Fuel Consumption	$[N.s/kg]$
d	Angular distance	$[^o]$
D	Total Drag	$[N]$
D_0	Parasitic Drag	$[N]$
d_a	Distance To Arrival Airport	$[m]$
D_g	Drag on the Ground	$[N]$
D_i	Induced Drag	$[N]$
e	Oswald Efficiency Factor	$[-]$
g	Gravitational Acceleration	$[m/s^2]$
h	Altitude	$[m]$
h_g	Distance Between Wing and Ground	$[m]$
R_e	Earths Radius	$[m]$
K	Induced Drag Coefficient	$[-]$
$K_{profile}$	Airfoil's Induced Drag Factor	$[-]$
L	Lift	$[N]$
L_g	Lift on the Ground	$[N]$
$\dot{m}$	Mass flow	$[kg/s]$
M	Mach Number	$[-]$
m_a	Aircraft Mass	$[kg]$
m_{fuel}	Fuel Mass	$[kg]$
S	Wing Area	$[m^2]$
T	Thrust	$[N]$
t	Simulation Time Step	$[s]$
T_A	Available Thrust	$[N]$
T_e	Elapsed Simulation Time	$[s]$
T_R	Required Thrust	$[N]$
u_{wind}	Wind u component	$[m/s]$
V	Speed	$[m/s]$
v_{wind}	Wind v component	$[m/s]$
W	Aircraft Weight	$[N]$
$W_{intensity}$	Wind intensity	$[m/s]$

Greek letters

δ	Engine Power Setting	$[-]$
ϕ	Ground Effect Parameter	$[-]$

ψ	Trajectory Angle	[^{o}]
$\psi_{correction}$	Wind Correction Angle	[^{o}]
ψ_{ref}	Reference Trajectory Angle	[^{o}]
ψ_{ref_c}	Corrected Reference Trajectory Angle	[^{o}]
ψ_{wind}	Wind Angle	[^{o}]
φ	Longitude	[^{o}]
γ	Flight Path	[^{o}]
γ_G	Givry correction angle	[^{o}]
γ_{ref}	Reference Flight Path	[^{o}]
λ	Latitude	[^{o}]
μ	Ground attrition coefficient	[$-$]
ρ	Air Density	[kg/m^3]

Chapter 1

Introduction

1.1 Motivation

The global air transportation system is a cornerstone of the world's economy, that in turn is constantly growing. According to ICAO there was a 6% increase of the number of passengers carried on scheduled services in 2016, reaching the 3.7 billion mark. The previous year's relative growth was even more impressive at 7.1%. As a matter of fact, air traffic has sustained an almost constant growth in the last decade as seen in figure 1.1, and is expected to maintain positive growth rates up to 2030 [1]. However, in order to accompany this constant growth in a sustainable manner the Air Traffic Management (ATM) systems in use today must be updated and drastically transformed. At the heart of this transformation lies the change from clearance based Air Traffic Control (ATC) operations in use today, to trajectory based operations. Trajectory based operations require a change of mentality when it comes to the definition of aircraft trajectories. The implementation of 4 dimensional trajectories (4DT), which are trajectories defined in both time and space, will allow air traffic controllers to properly predict the effect that a disturbance in the air traffic flow will have in the near future, which when combined with the ability to accurately predict trajectories will permit optimal correcting actions to be done accordingly [2] [3] [4]. For this reason the ability to predict aircraft trajectories is crucial to properly optimize the ever-more complex ATM systems in use today.

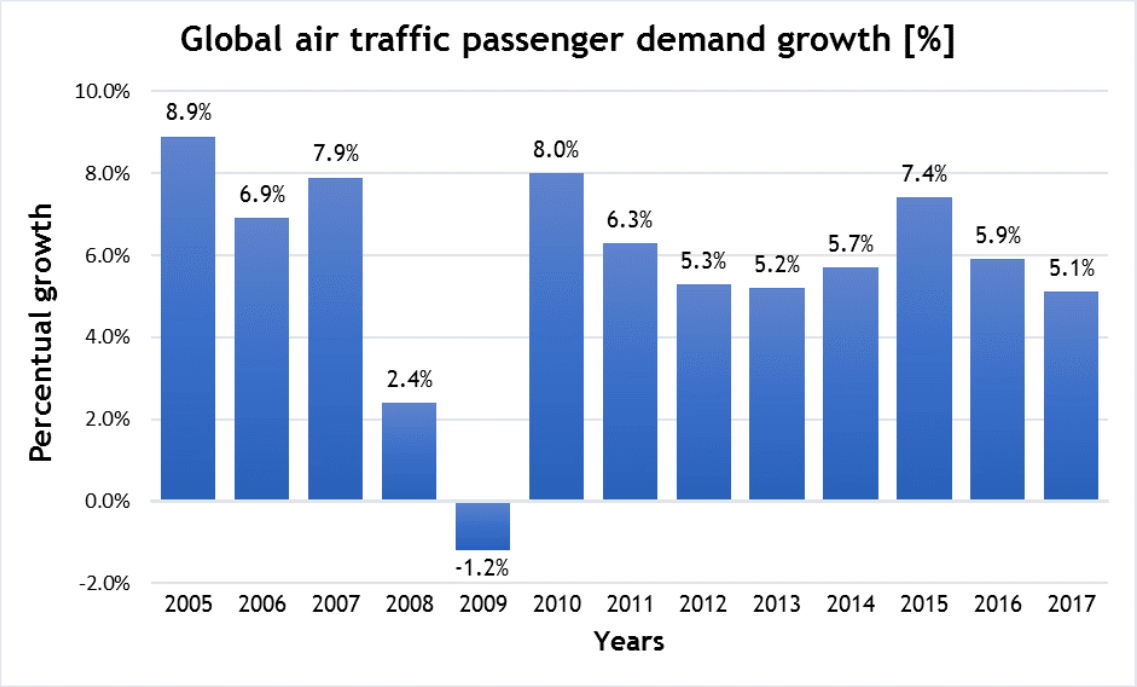

Figure 1.1: Annual growth of global air traffic passenger demand from 2005 to 2017, according to IATA and ICAO [5].

1.2 Main Goals

The main goal of the present work is to create a tool for aircraft trajectory prediction (TP) and analysis and to use it to study a number of 4D trajectories of certain aircraft. This tool may also be used, to some extent, to study or compare aircraft performance. The tool focuses on large civil transport turbofan powered aircraft. There was a significant effort placed in making the tool user friendly so that it may be used and improved upon by future users.

The TP tool was created using the Python programming language, version 3.4 [6]. It contains a graphical user interface (GUI) created with the use of the cross-platform framework for GUI development Kivy, version 1.9.1 [7]. The TP tool also contains databases containing atmospheric information derived from historical data sets made available by the National Oceanic and Atmospheric Administration (NOAA) [8]. A database containing the information of several aircraft was also compiled, which includes both flight phase dependent information as well as actual aircraft characteristics. This information was mainly obtained from the online data set appendices [9] of the book Civil Jet Aircraft Design [10] and from Eurocontrol's vast aircraft performance database [11].

1.3 Task Overview

This thesis is divided in five chapters. The first chapter discloses the motives behind this work and to this end it contains an introduction to trajectory based operations and 4D trajectories and their importance to the present days ATM systems. The programs of SESAR (Single European Sky ATM Research) and NextGen (Next Generation Air Transportation System) were used as examples of the implementation and importance of 4D trajectories. This chapter will also contain a review of previous works related to aircraft trajectory prediction and a simple introduction of trajectory predictors in general.

The second chapter contains a detailed explanation of the models and algorithms used in the creation of the TP tool. It will also contain a more comprehensive description of every aspect of the tool and its implementation. This chapter allows the reader to fully understand all aspects that the tool takes into account when simulating trajectories, which is especially important from a user standpoint as it allows him to understand the strengths and weaknesses of the tool.

The third chapter will present information of a number of flights simulated using the TP tool and a detailed description and analysis of those simulation's results. Several flight parameters will be analyzed and compared between the chosen flights, which will have varying lengths and aircraft models.

Using chapter's three simulation results, chapter four will contain the validation of the TP tool, by comparing the simulated flight values with the actual values of position and speed. The comparison and analysis of the actual and simulated values is especially important to illustrate which aspects of the TP tool should be improved upon.

The fifth and final chapter will include concluding remarks regarding the TP results and validation as well as the difficulties encountered and future work proposals.

1.4 Trajectory predictor fundamentals

The main goal of a trajectory predictor is to be able to accurately describe an aircraft's state and position during flight from its initial position to its final destination. Despite existing several different and valid approaches to building a trajectory predictor almost all of them share the following components [12]:

1. Initial condition: The aircraft's initial condition must always be included, regardless of the complexity of the used model. The actual parameters necessary will depend on the the used model type.
2. Intent or trajectory information: The information regarding the aircraft's desired trajectory or flight plan can be included in several different forms, but it must always be present. It may come in the form of a full control setting schedule, a flight plan or simply a projection of the state vector with fixed heading and speed. Other important information can also be included such as operational procedures that are flight phase dependent or certain restrictions such as maximum speeds or altitudes.
3. Environmental information: Given the very significant impact of external environmental factors on a flights trajectory they should always be included, even if in simple formats. The most important parameter of this kind is wind velocity.
4. Aircraft information: Relevant aircraft information such as weights or thrust modeling is usually included even if in simple formats. Alternatively some models use fixed speed values for certain phases.

The initial steps of a trajectory predictor involve the treatment of the given information and is usually referred to as the preparation process. A common way to express the flight plan is by a list of waypoints, which are simply named geographical positions. These positions must be processed and converted to actual geographical points in Cartesian or geodetic coordinates before the simulation start, which is known as route conversion. After completing the route conversion the initial intent for the aircraft must be calculated which will depend on the aircraft's initial state. This mechanism is usually known as lateral path initialization. Other steps may also be required depending on the complexity of the predictor such as getting the initial environmental state or applying certain constraints.

Following these initial steps lies the core of trajectory prediction which will take into account the aircraft's current state, follow appropriate aircraft dynamics while considering environmental and aircraft-specific information as well as any other simulation specified constraints to obtain the next aircraft state. The final result will be the aircraft's state and position expressed as a function of time from start to finish.

A simplified example of the process described above can be seen in figure 1.2. The flight intent information is present in the form of a simplified flight plan that includes the flight number (AAA123), the aircraft model (B757-200), the initial condition and a list of the trajectory's waypoints. The lateral path, or the approximation between the initial position and the first waypoint, can be observed, as well as certain constraint specifications.

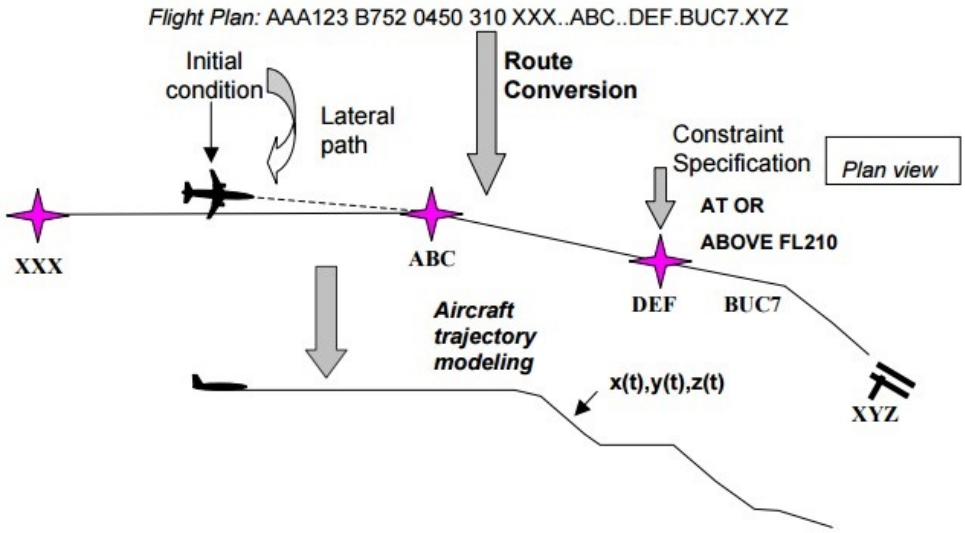

Figure 1.2: A flight plan example schematic [12].

1.4.1 Dynamical models

Trajectory predictors can employ several types of dynamical systems which in turn require different types of intent or aircraft specific information. Although certain models demonstrate higher fidelity than others the TP accuracy is not solely dependent on the dynamical model used, it highly depends on the input data reliability and the consideration of many operational conditions. Keeping this in mind the following are the most commonly used dynamical systems from the most to the least accurate [12].

1. Six degree of freedom model - This model takes into account the forces and moments that affect the airframe along all axes of motion. These moments are dependent on the aircraft's state and control settings and therefore require knowledge of the control laws that govern the aircraft. This method requires accurate working relationships between the moments and the aircraft's state and control input, normally obtained from the aircraft's manufacturer which often proves difficult to acquire.

2. Point mass model (kinetic) - Unlike the previous model this approach considers the aircraft as a single point and requires only the modeling of the resulting longitudinal forces, thrust and drag, assuming the lift normally compensates the weight. The main difficulty of this method is acquiring information reliable enough to accurately calculate the thrust and drag in different operational conditions. The engine's SFC (specific fuel consumption) is also an important parameter to calculate fuel spent as a function of thrust and time. This method provides accurate information for regular large commercial aircraft flights where straining maneuvers are not very common and therefore the calculation of moments is of less importance.

3. Macroscopic model (kinematic) - This simplified model does not calculate the forces acting on the aircraft, therefore being a kinematic approach. It instead uses constant, predetermined fixed values for various parameters that are often flight phase dependent, such as climb/descent rate, accelerations and others that may, for example, be a function of altitude. The main advantage of this model is that it does not require thrust and drag

data and can instead use average values from known flights, which in many cases are readily available. This approach is of relatively easy implementation and can provide acceptable results for already well established flights. However, it lacks flexibility since it requires accurate values for each individual flight phase.

1.4.2 Error sources

Although errors or simplifications of the used TP dynamical model account to significant inaccuracies, there are other outside error sources that are very significant, of which the most significant ones are described below [12] [13].

1. Inaccurate initial condition errors due to, for example, sensor errors or simple lack of detail in communication.
2. Errors in atmospheric models or forecasts.
3. Several types of missing intent information such as separation or approach maneuvers, unreliable course waypoints or inaccurate target speeds. Very often this type of intent information is simply not known before the flight (or not properly communicated) and therefore cannot be used for ground trajectory prediction. Many times, even in-flight trajectory prediction may suffer from this problem when, for example, path changes issued by voice are not inputted into the system.
4. Path deviation will always occur to some extent, when the aircraft deviates from the predicted lateral path.

1.5 4D trajectories and trajectory based operations

A 4D trajectory offers precise information about an aircraft's flight path in both space and time, while also taking into account some position uncertainty. These trajectories have different levels of specificity depending on their implementation, but most of them use a system of waypoints specified in latitude and longitude, as well as altitude and, of course, time. The time variable however is somewhat flexible to compensate for uncertainties such as wind speeds or airport queue times. Some trajectories employ controlled time of arrivals (CTA's) which are a system of time windows to cross several waypoints in order to have extra control on traffic flow [14].

Trajectory based operations (TBO) are based on the notion of 4D trajectories and on the planning and execution of those trajectories in a broad, strategical, sense. In a more specific, tactical sense TBO include the adjustment and evaluation of individual trajectories to ensure a synchronized, efficient and safe access to the airspace taking into account weather, environmental, defense, security and departure/arrival airport constraints. These individual trajectories are often combined into aggregate flows and are generated, negotiated and managed by ATM systems. This system allows the reduction of overly conservative and non-optimal actions, without compromising security. With proper integration, it also takes into account the airlines, aircraft's or flight crew's specific needs and limitations and tailors the generated trajectories to their needs and preferences. When conflicts that require controller interference do arrive, they

will be controlling the overall flow of traffic instead of an individual aircraft taking into account not only the immediate effects on traffic, but the long term effects as well. This system also allows for efficient high density arrival/departure operations, improving airport efficiency and capacity at times of peak demand. Current aircraft separation operations are managed by air traffic controllers using radar screens to visualize current trajectories and making operational judgments to resolve conflicts, however further use of TBO will change this process by inserting a much higher degree of automation and support for these maneuvers and in some cases it may be possible to delegate the separation maneuvers to the aircraft's crew. The main benefits of TBO are the following [2] [15]:

1. Capacity increase - Proper and global use of TBO will allow a very significant increase in capacity of the airspace, even in high traffic regions. The combination of proper trajectory planning that takes into account all requirements of the users will allow access to more of the airspace more of the time. Part of this capacity increase comes from the reduction of excessive separation without compromising security, thanks to the predictability of the system. High-density arrival/departure procedures will also highly benefit from this system.
2. Efficiency and environment - The operational management of TBO allow for a much more efficient control and spacing of flights, which will result in more consistent flight schedule integrity. In departure/arrival zones this increase in predictability and efficiency will allow an increased use of noise sensitive flights paths. While the increased efficiency will reduce fuel consumption the superior predictability will allow for a closer to optimal fuel loading.
3. Reduced cost per operation - After the initial implementation cost TBO will increase air service providers overall productivity which will result in a general reduction of per-operation costs.

1.6 Previous works

There has been great activity in the past few years regarding trajectory prediction due to the development of the NextGen and SESAR programs and their innovations regarding flight management systems (FMS) and Automatic Dependent Surveillance – Broadcast (ADS-B) capabilities that provide accurate details useful for trajectory prediction.

Most existing trajectory predictors are used as a tool to be employed within the Air Traffic Management system to facilitate both automation and decision making. Aircraft separation is an especially important component that depends on decision making. Existing algorithms to predict aircraft separation and associated conflicts are mostly simplified and consider the aircraft to have constant altitude, velocity and acceleration however, effort is being made to accurately predict conflicts regarding aircraft with transitioning altitudes.

In order to generate viable and efficient 4D trajectories it is necessary to calculate the aircraft's optimal control and state throughout its flight taking into account any possible restraints. One way to do this is using a pseudospectral based trajectory optimization method for the trajectory generation and then a predictive control law to drive the aircraft along the generated trajectory with minimum deviation [16]. Another approach based on a quintic spline approximation method

to find the minimum length trajectory between two consecutive waypoints has shown positive results [17].

From an extensive literary review [18], it was observed that the majority of papers in this field are concerning lateral, longitudinal and vertical profiles as well as flight plan and surveillance. Out of the 282 papers reviewed 20 of them shown special promise due to their innovative approaches in the areas of holding, modeling turns, vertical modeling and general mathematical flight models. Despite this, there are many sub themes related the global trajectory prediction theme that have been the subject of research as shown in figure 1.3 which contains each sub theme and their frequency in the 282 reviewed papers.

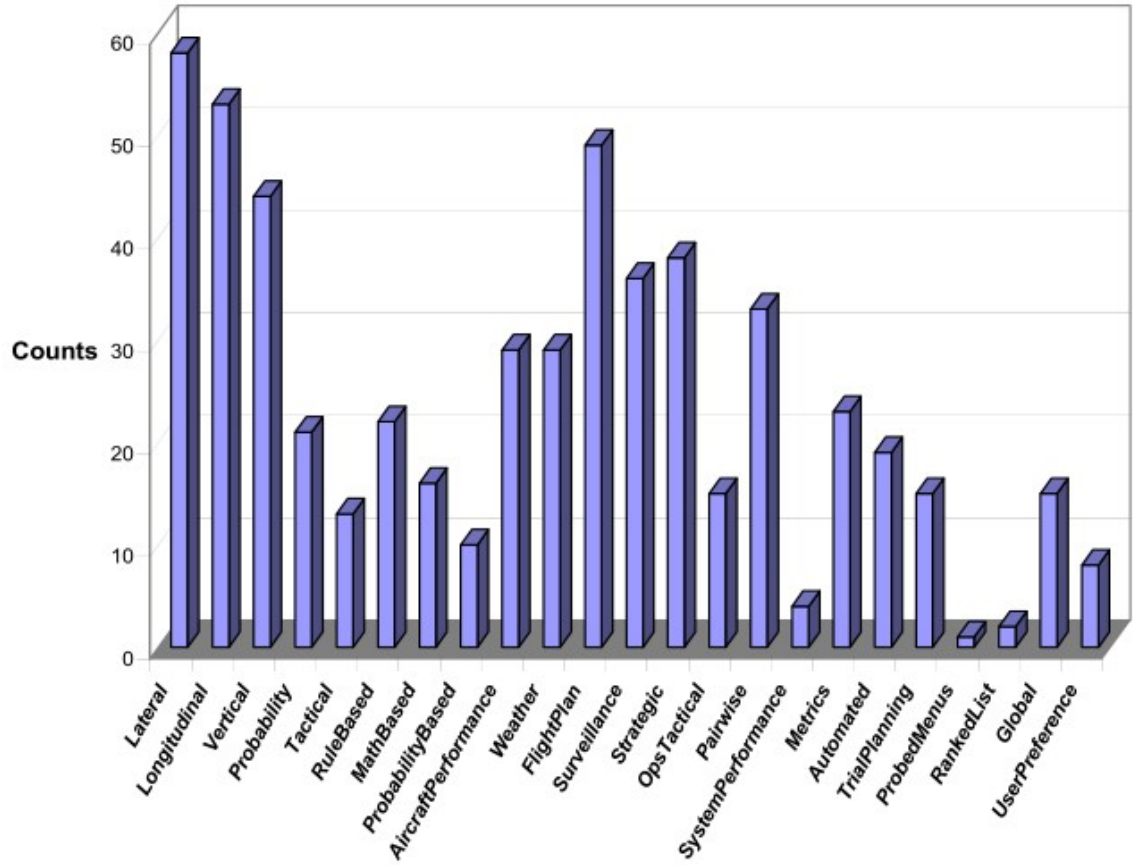

Figure 1.3: A chart demonstrating the frequency of common topics found on the reviewed 282 papers [18].

The vast majority of these papers focused on methods for estimating flight state variables, and not TP as a whole. The broadcasting of real time meteorological data combined with on board sophisticated flight systems was the major driver for a great part of these works, as well as the shift toward autonomous flight rules when, for example, aircraft separation could be handled by the crew and not by an air traffic controller, which would require great TP capabilities combined with somewhat autonomous conflict handling.

When it comes to the mathematical models used, the majority of them were of the point-mass type, mostly due to the reasons disclosed previously. Another somewhat common model was the kinematic model, that does not calculate forces and focuses only predefined values. A full

six degree of freedom model was only found once despite being the most accurate if employed correctly [19].

The majority of existing papers on this subject are of the academic level which is reflected on their low levels of maturity, since it requires many resources and years of research, prototyping, testing and validation for these concepts to be introduced in the operational system. Despite the tendency of moving some of the responsibility of aircraft separation from the ground to the cockpit the air traffic controller is still, and will remain to be, the final decision maker to such procedures, hence the need to track aircraft during all stages of flight.

It is obvious that TP has greatly benefited from modern computer capabilities and the availability of accurate data that allows TP tools to take into account different aircraft performances as well as other external factors such as weather and separation requirements. This results in a direct increase of TP fidelity that can lead to a lesser separation standard and the resulting increase in overall flight space capacity and flight delay reduction.

Some future areas of research that could prove to be very beneficial are vertical modeling, hold modeling and models of closure rates may improve overall TP and conflict resolution fidelity.

1.7 NextGen and SESAR

As a response to the need to reform the ATM systems in place two programs emerged: SESAR in Europe and NextGen in the USA. A central part of these programs is the introduction of trajectory based operations as the norm, replacing the more commonly used clearance based operations system.

1.7.1 NextGen

The American FAA (Federal Aviation Administration) has determined that the ever-increasing congestion in the air transportation system of the USA will cost the American economy 22 billion dollars by 2022 [20]. The Next Generation Transport System (NextGen) program was devised to be to phased in three time frames: Research and Development activities (2007-2011), aircraft equipage and deployment capabilities (2012-2018) and fully integrated ATM system operating across all air transport domain (2019-2025) [21]. Much like SESAR this project's main goal is to revamp the ATM in use today to accommodate the ever increasing needs of air traffic users. The four main elements of the NextGen program are the following [22]:

1. ADS-B implementation - Ads-b is a system that will allow its users to broadcast very accurate and varied information out of which the most important is the current aircraft position using GPS (Global Positioning System). This will allow both the air traffic controllers and the aircraft to visualize the position of nearby (and distant) aircraft in real time.
2. NextGen Data Communications (Data comm) - While most communication between air traffic controllers and aircraft crew is made today by voice, the ability to transfer information by other means (and in a faster, more automated way) would be valuable to allow controllers to handle larger amounts of traffic. Data comm will facilitate this transfer of

information regarding operations such as instructions, advisories, reports and flight crew requests, significantly improving air traffic controllers productivity and the associated capacity and safety benefits.

3. NextGen network enabled weather (NNEW) - The main goal of NNEW is to combine the different thousands of sources of weather observations and ground sensors and combining them into a single concise real time picture available to all air traffic users. This would highly contribute to better decision making and would reduce weather related delays, which are responsible for 70% of overall FAA delays.

4. National airspace system voice switch (NVS) - NVS goal is to combine the many different voice systems in use today in the National Airspace System (NAS) into a single set of scalable air/ground and ground/ground voice communication switches system that can support a dynamic flow of air traffic, facilitating flexible communications routing.

1.7.1.1 Trajectory definition

NextGen 4DT are defined in space and time using waypoints to represent specific locations along with corresponding buffers to describe the aircraft's position uncertainty. These waypoints are earth referenced (they have a specific latitude and longitude) and they also contain broader altitude and time interval (rather then precise) descriptions. Some of these waypoints are associated with Controlled Time Of Arrivals (CTA's) which represent time windows for the aircraft to reach or cross certain waypoints and are needed to regulate air traffic flows in congested airspace, often on arrival/departure airspace [14].

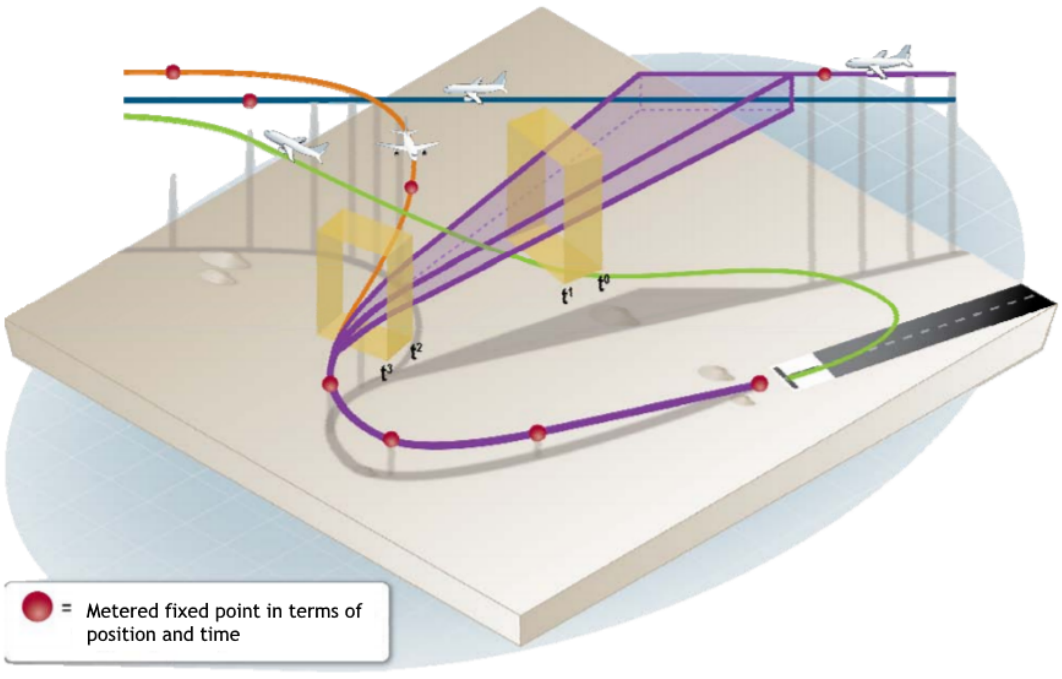

Figure 1.4: NextGen 4D trajectory definition schematic [2].

1.7.1.2 Benefits and Results: Metropolex

In order to improve ATM in metropolitan areas with multiple airports and complex air traffic flows (Metroplexes) the FAA has initiated the Metroplex program as part of NextGen. Working together with aviation stakeholders the FAA is improving regional traffic movement in these regions by optimizing airspace procedures based on precise satellite-based navigation. This new operating method has the possible benefits of reducing fuel burn and aircraft exhaust emissions while also optimizing on-time performance in the associated airports [23].

The FAA is now studying and analyzing the benefits of this program that has been implemented in 12 major airports. The FAA conducts post-implementation analysis using Radar track information to provide a projection of the expected benefits. These projected benefits are presented in table 1.1.

Table 1.1: Metroplex program general 2016 results [23].

Total operations	40,887
Fuel savings [millions of liters]	28.7
Value of fuel savings [millions of euros]	71.12
Carbon savings [thousands of metric tons of carbon]	246.1

1.7.1.3 Benefits and Results: ADS-B

ADS-B is a system developed in scope of NextGen that uses GPS satellites to determine aircraft location, ground speed and other data to provide traffic and weather real time information [24]. This information when combined with the benefits of 4DT has been put to work in the form of In-Trail Procedures (ITP), a ADSB-B application. This allows pilots of transoceanic flights to reach and maintain altitudes that are optimal for fuel consumption with less worry about aircraft separation. Traditionally since radar is not available in most oceanic airspace pilots are required to maintain around 80 to 100 nautical miles of separation, which often leads to flying in non-optimal altitudes. With this new method this separation may be reduced to 30 nautical miles [25].

According to an FAA report regarding the benefits of ITP dated December 15, it has been determined that aircraft equipped with this technology saved an average of 304 kg on transatlantic flights and 236 kg of fuel on transpacific flights. The users of this system not only benefit from this significant fuel economy, but they also gain higher awareness of the air traffic around them [25].

1.7.2 SESAR

The SES (Single European Sky) program was launched by the European commission in 2004 to reform the European airspace. SES's key objectives are the following [26]:

1. The restructuring of European airspace as a function of air traffic flow.

2. To create additional capacity.
3. To increase the overall efficiency of the ATM system.

SES's high level goals are political targets set by the European Commission whose scope is the full ATM performance outcome resulting from the implementation of SES pillars and instruments as well other industry development not driven directly by the EU [27]. Despite being ambitious, these goals represent a realistic view of what could be enabled by SESAR Technology Pillar [28]. They are as following [26]:

1. Enable a 3-fold increase in capacity which will also reduce delays both on the ground and in the air.
2. Improve safety by a factor of 10.
3. Enable a 10% reduction in the effects flights have on the environment.
4. Reduce the cost of ATM services to the airspace users by at least 50%.

SESAR's goals and vision rely heavily on the notion of trajectory-based operations and in the provision of air navigation services that allow the aircraft to fly its preferred trajectory without so many external constraints. In a way TBO are the glue between ATM components during tactical planning and flight operations by ensuring consistency between the desired trajectory and all the constraints that originate from the various ATM components and regions that shape it [15].

Another major ideology of SESAR's is that to properly increase ATM performance the systems in place should start looking at flights as a whole within a flow and network context, rather than segmented portions of its trajectory as it happens today. There should be improvements in every stage of flight, as demonstrated by image 1.5.

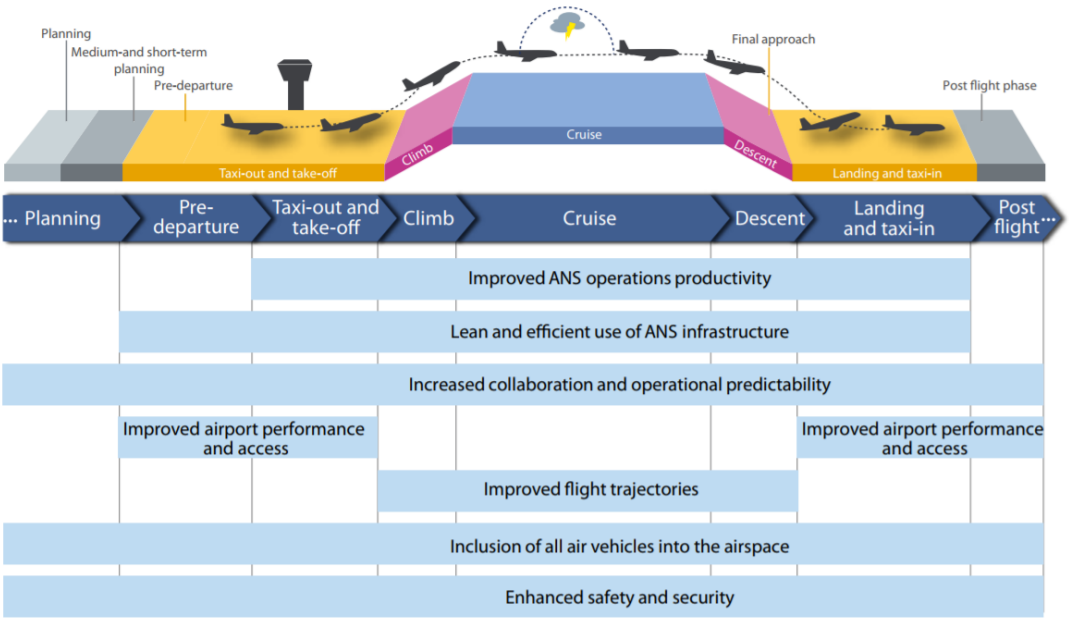

Figure 1.5: SESAR's target improvements for each flight phase [29].

1.7.2.1 Trajectory definition

SESAR's 4DT trajectories are decided on between the airspace users, the Air Navigation Service Providers (ANSP) and airport operators. This trajectory may be altered from the early planning stages to the day of departure since it takes into account constraints such as limited airspace or airport capacity or adverse weather conditions. The final version of this trajectory is referred as the Reference Business Trajectory (RBT) and is defined in three spatial coordinates and in time. After all alterations this is the trajectory which airspace users agree to fly and all service providers agree to facilitate. The cooperation between ATC, airports, airlines, cockpit, military and others is especially emphasized by SESAR [14].

1.7.2.2 Benefits and Results: Topflight program

During May, June and July of 2013 and April of 2014 more than 20 000 flights were involved in SESAR's Topflight program. The overall goal of this program was to put SESAR's 4D trajectories and ideals in place and analyzing their benefits. This was done by demonstrating SESAR procedures designed to allow transatlantic flights to closely follow its assigned 4D Reference Business Trajectories while meeting their times of arrival and remaining de-conflicted [30] [31].

During phase 1, 100 transatlantic flights were conducted that implemented the following SESAR optimization elements:

1. • Reduced taxi engine.
2. • Continuous climb operations.
3. • Business trajectories.
4. • Continuous climb and descent operations.
5. • Flexible use of airspace.
6. • Optimized oceanic profiles such as continuous cruise climb and variable speeds.

Out of these 100 flights 25% applied 100% of these core elements and 70% applied more than 60% of the core elements above. Up to 834 kg of fuel were saved in westbound flights and 301 kg of fuel were saved in eastbound flights.

The second phase focused on the benefits of Extended Arrival Management (EAM), which is a system that provides sequencing support of arrival traffic based on trajectory prediction, much faster than the systems in place today, resulting in less holding times and in decreased fuel consumption. Over 20 000 flights were involved in these trials and it was shown that this system can reduce ATM inefficiencies, reducing delays and saving between 40 to 150 kg of fuel each flight, thanks to the reduction of orbital holding time.

This exercise demonstrated that SESAR's innovations can be successfully put to work, even on congested routes and arrival/departure airspace and that the SESAR program has the potential to deliver great improvements to the European ATM system in use today.

1.7.3 SWIM

One of the most important requirements for an effective 4DT ATM system is the constant communication and information sharing between airspace monitors and users. System Wide Information Management (SWIM) is NextGen's and SESAR's response to this need. Its purpose is to transition from direct connections to a publisher-subscribe model which is know as Service Oriented Architecture (SOA). This new system will allow the user to receive several different data sets from a single point. It will also give the user access to new information not easily available today such as Time Based Flow Management (TBFM) and digital Notices to Airmen (NOTAM). The information shared by SWIM is divided in three categories: aircraft position and flight status, aeronautical information (which can be static or dynamic and is usually used for pre-flight planning) and up-to-date weather observations and forecasts [32]. SWIM's main benefits are the following:

1. Gate management - Knowing exactly when to expect an arriving flight allows ramp controllers to optimize gate use with fewer arrivals stuck waiting for a gate.
2. Surface traffic management - In low visibility conditions surface surveillance data highly improves the management of surface traffic. Better information about queu time for deicing or departure allows ramp controller to optimize tarmac usage times.
3. Reducing excessive departure delays - Information regarding real-time airborne and surface delays allows operation managers to make informed decisions about prioritizing departures.
4. Flight following and support - Using information on the Runway Visual Range (RVR) at the destination airport dispatchers inform pilots of local conditions and advise them of preferred arrival and approach procedures.
5. Resource management - Knowing exactly when the flight is arriving allows gate agents and ground crews to be optimally deployed.
6. Post-event review and process improvement - The vast information archived by SWIM allows investigators to identify problems and inefficiencies and to devise appropriate solutions.

This system is of special importance for in-flight trajectory prediction as it allows a very efficient and reliable source of information, playing a crucial role in the new tendency of moving separation maneuvers from the ground to the cockpit.

Chapter 2

Models and Algorithms

2.1 Weather database system

The unpredictability of the weather system presents a strong difficulty when it comes to trajectory prediction. Without resorting to real weather data of the specific time and place (which is very hard to acquire given the altitude of commercial flights) the second-best option is to utilize historical values or to use a prediction model. However, unlike temperature and atmospheric pressure the relation between wind speed and altitude is hard to be modeled at high altitudes as it depends widely on geographical position and other factors.

Given the difficulties of implementing an accurate wind model and of acquiring accurate weather values for the specific date and place of the flights, the best solution was found to be the use of reliable historical values. The weather database employed requires to have wind velocity information in different altitudes as well as geographical positions. Another important factor is the ability to access data relative to different times of the day and year. The database employed was NCEP/NCAR (National Center for Environmental Prediction and National Center for Atmospheric research) Reanalysis 1: pressure, made available by NOAA (National Oceanic and Atmospheric Administration) [8]. This database provided all the required information in various, easily accessible, netCDF4 format files. The available variables and temporal/spatial coverage was ideal as can be seen by its relevant characteristics in the table below.

Table 2.1: Weather database relevant characteristics.

Variables used	Air temperature, uwind, vwind[1]
Temporal coverage	4 times daily values from January 1, 1948 to the present
Spatial coverage	2.5x2.5 degrees global grid (144x73 resolution)
Altitude Levels	17 pressure levels from 1000 mb to 10 mb

This database was made possible by the cooperation between the NCEP and the NCAR in creating this project that comprises a long record of global analysis of atmospheric fields to support climate monitoring communities. The data utilized on this project was recovered from land surface devices, ship, rawinsonde (radiosondes tracked by a radio direction finding device to determine wind velocity), pibal (also known as ceiling balloon or pilot balloon), aircraft, satellite and other sources. The data assimilation system employed eliminates perceived climate jumps associated with changes in the data assimilation system. This database has shown to be especially accurate near and around mainland USA, mainly due to the larger availability of information sources in this area.

[1]Where uwind is the U component of the wind that is positive for a west to east flow (eastward wind) and vwind is the V component of the wind that is positive for a south to north flow (northward wind) [33].

Given its very large temporal and spatial density, in order to make the database file size smaller and faster to process a new database was derived by calculating the average variable value of each month at the 4 available times of day (6 hours apart). This allowed to vastly reduce the file size while also allowing the user to choose the approximate time of day and month of the flight.

Figures 2.1, 2.2 and 2.3 show a visualization of a portion of the information available on the database demonstrated in the form of three plots containing the mean global values of temperature, uwind and vvind for the year of 2016 at 200 mb pressure altitude or at approximately FL390.

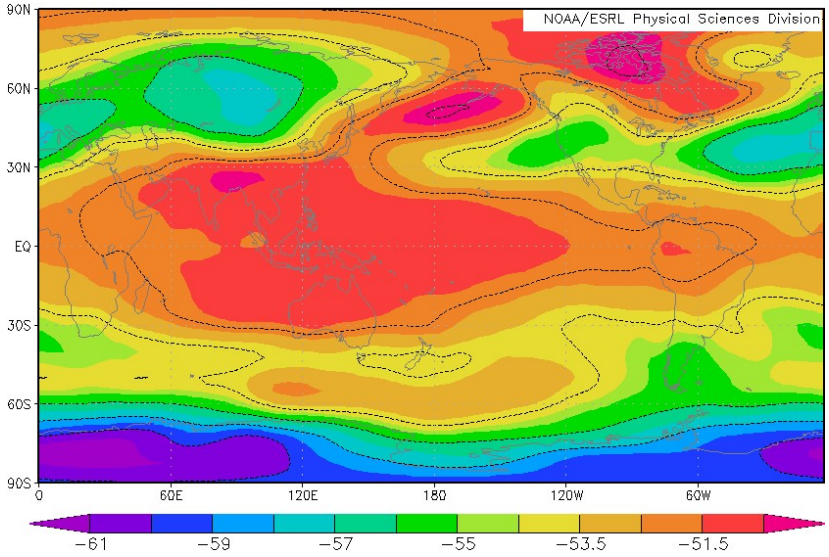

Figure 2.1: Temperature at 200 mb pressure level, approximately at FL 390.

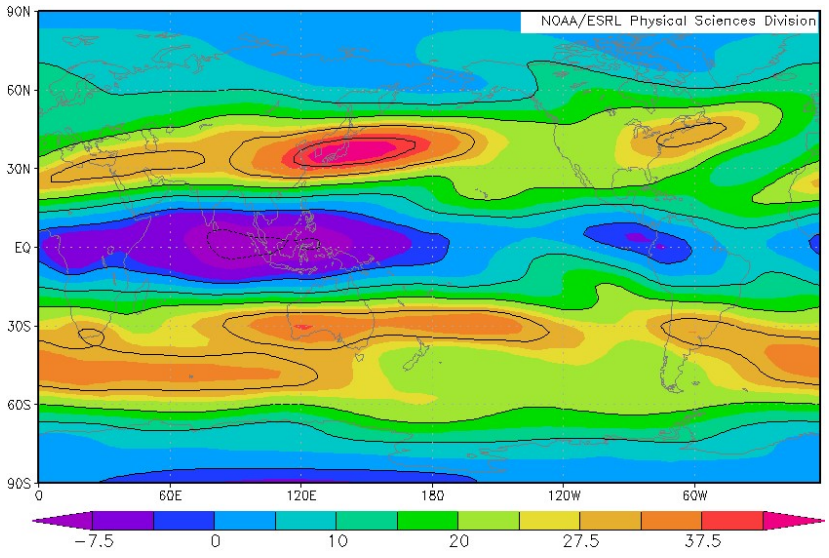

Figure 2.2: Uwind at 200 mb pressure level, approximately at FL 390.

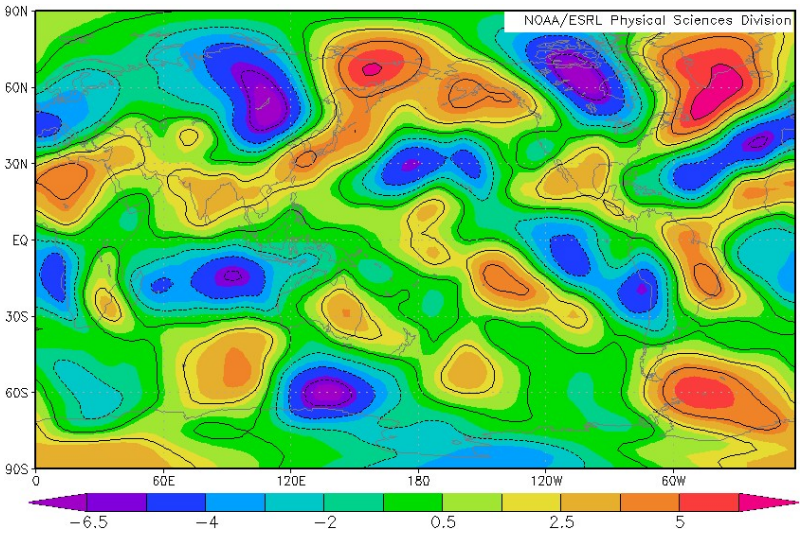

Figure 2.3: Vwind at 200 mb pressure level, approximately at FL 390.

2.2 Flight phase explanation

There are several accepted terms for each flight phase, that depend on their use as well as the organization that defined them. The flight phase terminology and definition used for the TP tool were adapted from IATA's (International Air Transport Association) taxonomy, ICAO's (International Civil Aviation Organization) Accident/Incident Data Reporting (ADREP) system [34] as well as Eurocontrol's flight phase definition as used on their aircraft performance database [11]. The adapted Eurocontrol's base of aircraft data (BADA) flight phases as defined in [35] were also used.

Each different flight phase requires several parameters for an accurate simulation such as target speed, target altitude or climb/descent rates. These values will always be respected unless it is not possible to do so. All climb and descent phases have a pre-determined thrust setting that will be maintained constant unless it must be altered in order to, for example, respect speed constraints, target altitudes or rates of climb/descent. The used terminology for each flight phase is the following:

1. **Takeoff**: This phase combines both the takeoff roll as well as the rotation and the takeoff phases. This phase's thrust setting is constant at the maximum value. The parameters this phase requires are rotation speed and initial obstacle altitude. The phase ends when the initial obstacle altitude is reached.

2. **Initial Climb**: During the initial climb the thrust setting is set to be slightly less than the maximum value in order to minimize the increased stress the engines are subject to at maximum power setting. This phase is the steepest of all climb phases and lasts until its target altitude is reached. It requires initial climb target speed, altitude and rate of climb.

3. **On Course Climb**: The on course (or en route) climb starts when the aircraft has reached a high enough altitude to safely proceed "on course" to its target destination. It requires on course climb target speed, altitude and rate of climb.

4. **Secondary Climb**: The secondary climb is a continuation of the en course climb, that is usually slightly less steep. It requires secondary climb target speed, altitude and rate of climb.

5. **Mach Climb**: The mach climb (also called cruise climb) is the final climb phase before reaching cruise altitude, and its generally the smoothest of all climb phases. Usually most altitude related airspeed restrictions no longer apply at this altitude so the aircraft will accelerate to high speeds, close to cruising speed. As the altitude increases it is necessary to gradually reduce the flight path angle in order to ensure a close to constant speed. This phase requires mach climb target Mach number, altitude and rate of climb.

6. **Cruise**: During cruise the aircraft is leveled off and unlike the previous phases its power setting is adjusted to maintain the cruise phase desired speed. The cruise phase ends when the aircraft is close enough to the airport as to ensure a smooth descent. This phase requires target Mach number and distance from airport to initiate descent.

7. **Initial Descent**: At the start of the initial descent the power setting will be set to idle and a descending flight path is taken. This phase is usually flown at high, close to cruise, speeds. It requires target Mach number, altitude and rate of descent.

8. **Main Descent**: During this phase it is sometimes required for the aircraft to level off to slow down to its target speed. Once a certain altitude has been reached it is safe to extend flaps, which are crucial to reach safe approach and landing speeds. This phase requires target speed, altitude and rate of descent.

9. **Approach Descent**: The final descent phase is also set to be flown at idle power, however it is often required to slightly increase power for approach maneuvers. During this phase it is essential to reduce the aircraft's speed to a safe speed for landing. This phase requires approach descent target speed.

10. **Landing**: During landing the aircraft is leveled off and its thrust is set to reverse mode. The simulation ends when, during this phase, the aircraft's speed reaches zero.

Image 2.4 was retrieved from Eurocontrol's aircraft performance database and contains the average flight phase parameters for the Boeing 777-200.

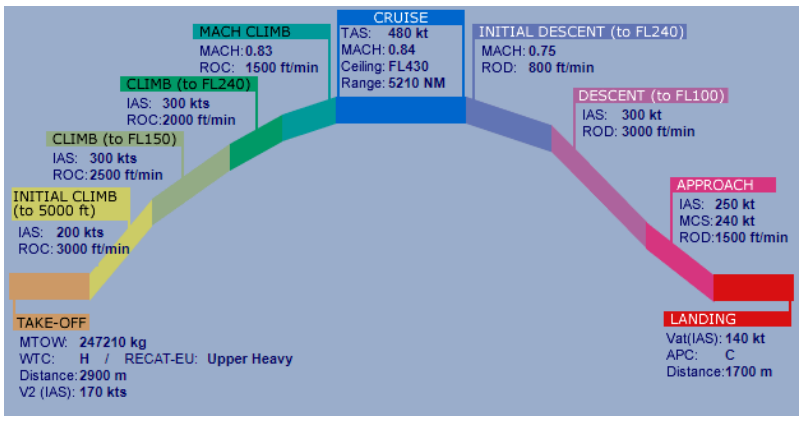

Figure 2.4: Eurocontrol's aircraft performance database flight phases for the Boeing 777-200 [11].

2.3 Aircraft information

The aircraft information employed is divided in two main areas: aircraft parameters and aircraft flight plan typical values. The aircraft parameters were mostly retrieved from the book Civil Jet Aircraft Design data sets that contains accurate information regarding the majority of large civil transport aircraft in use today [9]. The aircraft typical flight plan values were retrieved from Eurocontrol's Aircraft Performance database [11]. Using these sources a database of several aircraft was created and included on the TP tool, allowing the user to easily simulate several civil transport aircraft in use today. In order to contain this information the JSON (JavaScript Object Notation) file format was chosen due to its lightweight and simplicity of use, as well as its capabilities of being both easily readable and writable for humans and efficient for machines to parse and generate. The tool also allows the user to create a new aircraft entry based on existing entries or to create a completely new entry using only the GUI. Table 2.2 contains the required parameters for each aircraft.

Table 2.2: Required aircraft parameters for simulation.

Parameter name	**Parameter type**
Maximum take-off weight [kg]	Weights
Fuel Weight [kg]	Weights
Number of engines	Engines
Maximum sea level thrust [N]	Engines
Take-off engine specific fuel consumption [kg/s/N]	Engines
Cruising engine specific fuel consumption [kg/s/N]	Engines
Engine idle thrust percentage	Engines
Wing span [m]	Dimensions
Wing surface area [m^2]	Dimensions
Flap to wing span ratio	Dimensions
Takeoff lift coefficient	Aerodynamic
Maximum lift coefficient	Aerodynamic
Parasitic drag coefficient	Aerodynamic
Never exceed speed (V_{NE}) [m/s]	Safety
Maximum flight path angle [°]	Safety

The safety parameters of never exceed speed and maximum flight path angle are to be used as limits not to be exceeded during simulation. The way they are employed on the algorithm will be explained on the next section. Some of the parameters on table 2.3 are dependent on the actual flight requirements, therefore they should be treated as an average rather than a fixed value and should be adjusted, if needed, for each flight.

Table 2.3: Required flight parameters for simulation.

Takeoff speed [m/s]	Cruise altitude [m]
Initial climb speed [m/s]	Cruise target Mach number
Initial climb target altitude [m/s]	Initial descent target Mach number
Secondary climb speed [m/s]	Initial descent target altitude [m]
Secondary climb target altitude [m]	Main descent speed [m/s]
On course climb speed [m/s]	Main descent target altitude [m]
On course climb target altitude [m]	Approach descent speed [m/s]
Mach climb target Mach number	Touch down speed [m/s]

2.4 Airport database

An airport and aerodrome database was incorporated into the TP tool in order to allow the user to simulate a quick trajectory without predetermined waypoints between two known airports or aerodromes. The database chosen was Openflights Airport database that contains several thousand of the world's airports and aerodromes. This data was available in a generic information file. The used information for each airport entry was the airports name, IATA/ICAO code, latitude, longitude and altitude [36]. Below is an image taken directly from the TP tool showing all airport entries as red dots.

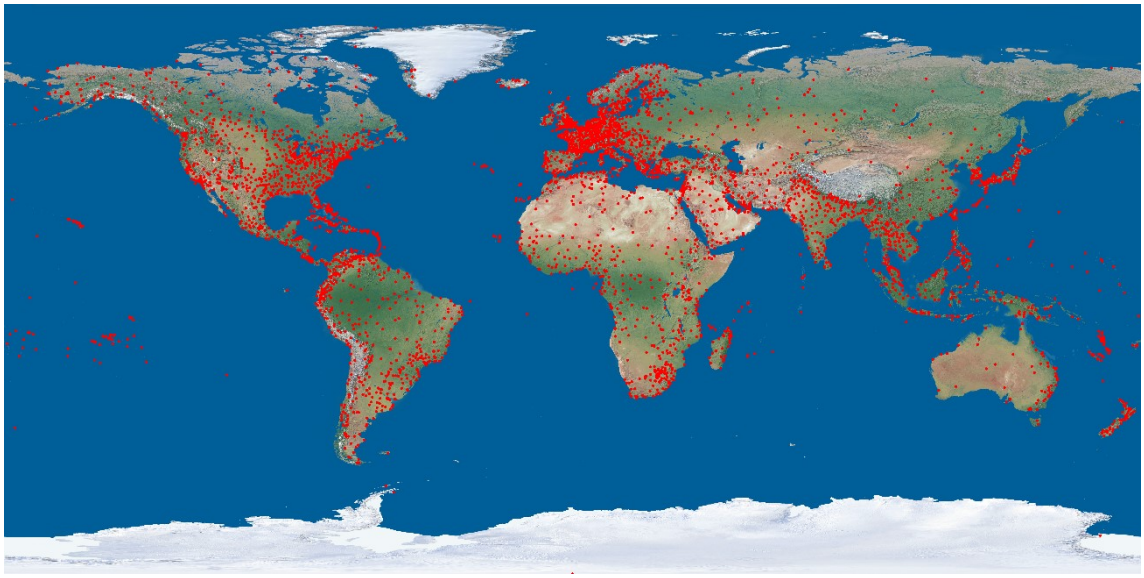

Figure 2.5: Airport database entries location.

2.5 Waypoint determination

The TP tool allows the user to simulate flight solely between a starting and a finishing waypoint and also to simulate a trajectory between a larger number of given waypoints, while calculating intermediate waypoints between them as needed, in order to approach the path to a orthodromic trajectory between intermediate waypoints.

In order to approximate the trajectory between two given points to a orthodromic one, intermediate waypoints are calculated on a great circle (or orthodrome) between those two points. The amount of waypoints calculated depends on the position of the two original waypoints. The algorithm below calculates the latitude and longitude of a point between the two given points that is at a fraction of the total distance between them on the same orthodrome. The only requirement is that the initial points are not antipodal, as that would cause the route to be undefined. In the algorithm below *f* is the fraction of the distance between the given points, *d* is the distance in degrees between the given points, λ_x and φ_x are the latitude and longitude of the given points and finally λ_f and φ_f are the coordinates of the calculated intermediate points [37].

1. A:
$$A = \frac{sin(d(1-f))}{sin(d)} \tag{2.1}$$
2. B:
$$B = \frac{sin(fd)}{sin(d)} \tag{2.2}$$
3. x:
$$x = Acos(\lambda_1)cos(\varphi_1) + Bcos(\lambda_2)cos(\varphi_2) \tag{2.3}$$
4. y:
$$y = Acos(\lambda_1)sin(\varphi_1) + Bcos(\lambda_2)sin(\varphi_2) \tag{2.4}$$
5. z:
$$z = Asin(\lambda_1) \tag{2.5}$$
6. Intermediate point latitude, λ_f:
$$\lambda_f = atan2(z, \sqrt{x^2 + y^2}) \tag{2.6}$$
7. Intermediate point longitude, φ_f:
$$\varphi_f = atan2(y, x) \tag{2.7}$$

The angular distance *d*, between the given points is calculated in the following way based on the spherical law of cosines [38] where the point P is the elevated pole and A and B are the given points as illustrated in figure 2.6:

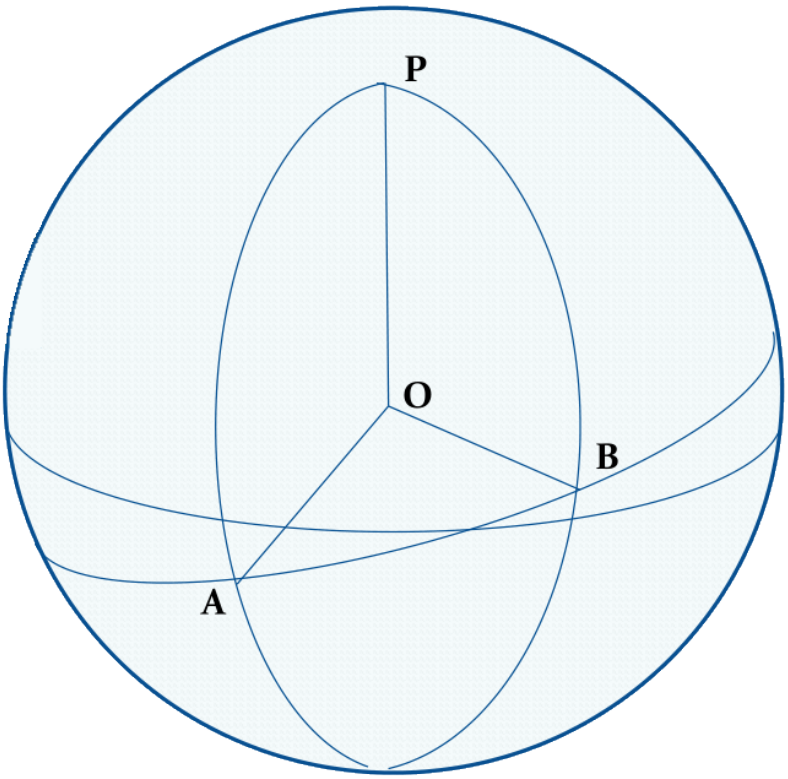

Figure 2.6: Scheme of the globe showing the points A and B on the same orthodrome, as well as the elevated pole P.

1. AB longitude variation, $\Delta\varphi$:

$$\Delta\varphi = \varphi_2 - \varphi_1 \tag{2.8}$$

2. Angular distance between A and P, PA[1]:

$$PA = 90 \pm \lambda_1 \tag{2.9}$$

3. Angular distance between B and P, PB[1]:

$$PB = 90 \pm \lambda_2 \tag{2.10}$$

4. Angular distance between A and B, d:

$$d = acos(cos(\Delta\varphi)sin(PA)sin(PB) + cos(PB)cos(PA)) \tag{2.11}$$

In order to determine when a intermediate waypoint is needed an iterative process determines the fraction between the initial point and the final point by calculating the Givry correction between the initial point and the would be intermediate point and comparing it to a maximum value, whose default is set to 10º. If the Givry correction is larger than the maximum value

[1]When calculating the angular distance of A and B from the elevated pole P (PA and PB), the mathematical operator depends on which elevated pole is selected (North or South) and on what hemisphere the points A and B are on. If the selected pole and the point's hemisphere is the same the operator is positive, otherwise its negative.

that intermediate waypoint is integrated in the trajectory path. In order to calculate the Givry correction (γ_G) between two waypoints only their coordinates are required, as can be seen below where A and B are the waypoints used:

$$\gamma_G = \frac{\Delta\lambda_{AB}}{2} sen\varphi_m \tag{2.12}$$

The medium latitude between points A and B (φ_m) is given by:

$$\varphi_m = \frac{1}{2}(\varphi_A + \varphi_B) \tag{2.13}$$

An example of the use of intermediate waypoints between given waypoints can be seen on figure 2.7, where the given waypoints are purple and the calculated intermediate waypoints are white.

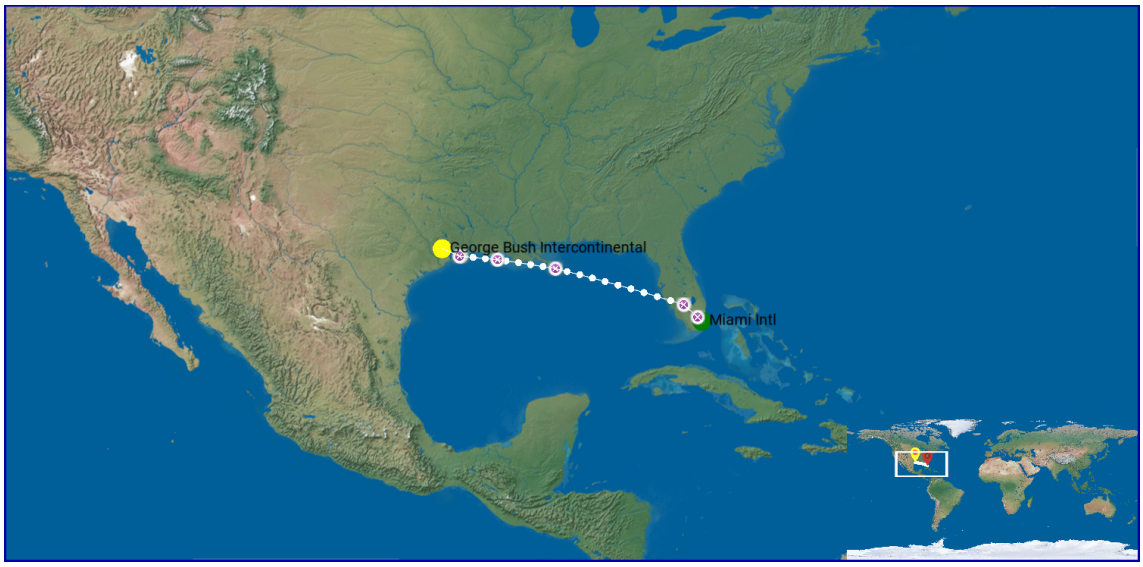

Figure 2.7: An example of calculated and given waypoints retrieved from the TP tool.

2.6 Main algorithm

In this section the main algorithm's loop will be explained step by step. Before the initiation of the loop a verification of the user input is applied, to make sure its valid. The required parameters are the aircraft characteristics described above, as well as the flight path waypoints or, at least, the initial and final waypoints. The month and time of day of the simulation, as well as attrition coefficients for the takeoff and landing phases should also be provided.

2.6.1 Time Step Calculation

Given the nature of commercial aircraft flights a variable time step (t) is valuable for their efficient (fast) simulation. This is due to the long duration of the cruise flight phase when maneuvers are limited and overall speed varies only slightly. Taking this fact into account a variable time step is used whose value depends mostly on the current flight phase and the distance to the target waypoint, diminishing the closest the aircraft is to the waypoint. Smaller

values of time step are especially important during ground phases for accurate calculation of landing and takeoff distances.

2.6.2 Update climate state

When the aircraft crosses the spatial grid of the weather database new values must be retrieved from it. This is done by checking the aircraft's current position and comparing it to its last position. Even if new database entries are not required, the weather database parameters are interpolated between entries to improve accuracy and to avoid sudden steep leaps in values.

2.6.3 Available Thrust

In this step, the maximum available thrust is calculated (at full throttle) for the current simulation state. As stated before, these simulations are based on high bypass ratio turbofan engines, since these are the most widely used for large civil transportation aircraft. These engine's thrust varies significantly with speed and altitude. Although it varies with every engine, it can be estimated by the equation below, where M is the Mach number, T_0 is the maximum available thrust at sea level and $\rho(h)$ and ρ_0 is the air density at the current altitude and at sea level, respectively. When M < 0.1, M = 0.1 should be used.

$$T_A = \frac{0.1}{M} T_0 \frac{\rho(h)}{\rho_0} \tag{2.14}$$

2.6.4 Drag

The current total drag is calculated in this step, by combining the parasitic and lift induced drag. This tool only takes into account subsonic drag since its focus is to simulate large transport aircraft whose highest Mach numbers during cruise are usually between 0.79 and 0.86. The parasitic and induced drags are calculated below where V is the current speed, W is the aircraft weight, S is the wing surface area, C_{D0} is the parasitic drag coefficient and γ is the aircraft's flight path angle.

1. Parasitic Drag (D_0):
$$D_0 = \frac{1}{2}\rho V^2 S C_{D0} \tag{2.15}$$
2. Induced Drag (D_i):
$$D_i = \frac{KW^2 cos^2\gamma}{\frac{1}{2}\rho V^2 S} \tag{2.16}$$
3. Total Drag (D):
$$D = D_0 + D_i \tag{2.17}$$

The parameter K is the induced drag coefficient and can be calculated with the equation bellow where AR is the wing aspect ratio, *e* is the Oswald efficiency number and $K_{profile}$ is the airfoil's induced drag factor.

$$K = \frac{1}{\pi ARe} + K_{profile} \tag{2.18}$$

2.6.5 Current Thrust and Power Setting

The way thrust and power setting is calculated in this simulation depends on the current flight phase. In phases where the power setting is constant the current thrust is simply calculated with that power setting value (δ) and the available thrust (T_A). The power setting values range from 0 (zero thrust) to 1 (maximum thrust), although during flight the minimum power setting acceptable is the idle power setting, whose default value is set to be 0.1, but may be changed by the user. The default thrust setting values used are ICAO's standard values in the Landing and Takeoff (LTO) cycle, which were defined for aircraft emission testing [39], and are shown below. These values however, are only a general approximation and sometimes differ significantly from the actual used values, which results in some intent prediction errors [40].

$$T = \delta T_A \tag{2.19}$$

- Takeoff: During takeoff the power setting is constant and set to the maximum value.
- Climb Phases: During climb the default power setting is set to slightly less than maximum value, at 0.85. It remains at this value unless more thrust is required to reach the current phase's target altitude.
- Cruise: Unlike the previous phases the power setting during this phase is not constant or predetermined. During the beginning of cruise the thrust setting is kept at the previous phase's setting while accelerating to the cruise phase target Mach number. Once the cruise target Mach number is reached the current thrust is set to be equal to the required thrust to maintain the current Mach number, and is updated every iteration, causing a changing power setting. In other words the required thrust is approximately equal to the previously calculated drag, in order to maintain a constant Mach number as the speed of sound varies only slightly on constant altitude.
- Descent Phases: During the descent phases the power setting is set to idle, except when the current aircraft speed is less than the phases target speed or the aircraft's stall speed. In this case the current thrust is set to the required thrust to maintain constant speed, much like during the cruise phase, except in this phase the weight component must be taken into account.
- Landing: During the landing phase the thrust is set to reversed mode, with an arbitrary value of percentage of available thrust that is user dependent.

2.6.6 Flight Path

The first step to calculate the flight path angle is calculating the desired flight path, called the reference flight path (γ_{ref}). This angle is calculated based on the excess thrust which is the difference between the current thrust and the thrust required to maintain this phase's target speed.

$$\gamma_{ref} = asin\left(\frac{T - T_{required}}{W}\right) \tag{2.20}$$

One exception to this happens if during the start of a descent phase a deceleration is required to reach the phases target speed, in which case the aircraft is leveled (γ=0) until that speed is reached. Another exception is during the final approach phase in which the descent angle must be smoother, and is therefore calculated based on the proximity to the airport, where h is the aircraft's altitude and d_a is the absolute distance to the airport.

$$\gamma_{ref} = asin\left(\frac{h}{d_a}\right) \tag{2.21}$$

After calculating the reference flight path the actual angle is calculated. In order to avoid instant variations of the flight path angle it is calculated using an arbitrary maximum flight path angle rate of change. The maximum value of the flight path angle is limited by the user inputted maximum flight path angle.

2.6.7 Acceleration

The acceleration is calculated in two separate ways: on the ground (takeoff and landing) and during flight.

- During flight, where m_a is the aircraft's mass:

$$a = \frac{T - D - Wsin(\gamma)}{m_a} \tag{2.22}$$

- On the ground:

  - Ground induced drag compensation, ϕ: This parameter compensates the reduced induced drag due to the proximity between the ground and the wing. The parameter h_g is the distance between the wing and the ground and b is the wing span.

$$\phi = \frac{\left(\frac{16h_g}{b}\right)^2}{1 + \left(\frac{16h_g}{b}\right)^2} \tag{2.23}$$

  - $C_{Lground}$: The lift coefficient during ground acceleration or deceleration $C_{Lground}$ is assumed to be constant at 0.8, although different values can be set by the user.

  - L_{ground}:

$$L_{ground} = \frac{1}{2}\rho V^2 S C_{Lground} \tag{2.24}$$

  - D_{ground}: The ground drag value takes into account the flaps contribution separately with the parameter $C_{d0_{flap}}$.

$$D_{ground} = \frac{1}{2}\rho V^2 S(C_{d0} + C_{d0_{flap}} + \phi K {C_{Lground}}^2) \tag{2.25}$$

  - Ground acceleration, a: Where μ is the floors attrition coefficient that has different values for landing or takeoff. These values can be set by the user, but are usually

between 0.03 and 0.08 during takeoff and between 0.06 and 0,5 during landing, when brakes are taken into account.

$$a = g\left(\frac{T}{W} - \mu\right) - \frac{g}{W}(D_{ground} - \mu L_{ground}) \tag{2.26}$$

2.6.8 Trajectory Angle

The calculation of the trajectory angle is divided in three parts: the initial reference trajectory angle ψ_{ref}, the corrected reference trajectory angle that takes into account the atmospheric winds effect ψ_{ref_c} and finally the actual trajectory angle ψ that is calculated using the predefined trajectory angle rate of change and ψ_{ref_c}.

1. Initial reference trajectory angle, ψ_{ref}: This initial step requires only the aircraft position and its current target waypoint position, and it is given by:

$$\psi_{ref} = arctan_2(\Delta\lambda, \Delta\varphi) \tag{2.27}$$

   - Where $\Delta\lambda$ is the differential longitude, in degrees, λ_w is the target waypoint's longitude and λ is the current longitude:

$$\Delta\lambda = \lambda_w - \lambda \tag{2.28}$$

   - And where $\Delta\varphi$ is the differential latitude:

$$\Delta\varphi = \varphi^{(2)} - \varphi^{(1)} \tag{2.29}$$

$$\varphi^{(1)} = ln\left(\left|tan\left(\frac{\varphi}{2} + 45^o\right)\right|\right) \tag{2.30}$$

$$\varphi^{(2)} = ln\left(\left|tan\left(\frac{\varphi_w}{2} + 45^o\right)\right|\right) \tag{2.31}$$

2. Corrected reference trajectory angle, ψ_{ref_c}: In order to correct the current trajectory to take into account the atmospheric winds a wind correction angle $\psi_{correction}$ must be calculated. The first step is to calculate the current wind angle and the wind intensity from the atmospheric parameters u_{wind} and v_{wind}.

   (a) Wind angle, ψ_{wind}:

$$\psi_{wind} = atan^2(u_{wind}, v_{wind}) \tag{2.32}$$

   (b) Wind intensity, $W_{intensity}$:

$$W_{intensity} = \sqrt{{u_{wind}}^2 + {v_{wind}}^2} \tag{2.33}$$

   (c) Wind correction angle, $\psi_{correction}$: Knowing the wind intensity, the aircraft's speed, the wind angle and the initial reference trajectory angle we can now calculate the wind correction angle:

$$\psi_{correction} = asin\left(\frac{W_{intensity} * sin(\psi_{reference} - \psi_{wind})}{V}\right) \tag{2.34}$$

(d) Corrected reference trajectory angle, ψ_{ref_c}:

$$\psi_{ref_c} = \psi_{correction} + \psi_{ref} \tag{2.35}$$

3. Final trajectory angle, ψ: After calculating the corrected reference trajectory angle, ψ_{ref_c}, the actual current trajectory is calculated. In order to avoid sudden instant variations of the trajectory angle it is calculated using an arbitrary trajectory angle rate of change.

It is important to note that during the initial climb phase the trajectory stays constant, only beyond a certain altitude does the aircraft begin to adjust its trajectory to reach the target waypoint. During ground phases the wind effects are not taken into account.

2.6.9 True Speed

In this step, we simply use the calculated acceleration and calculate the current iteration's speed. We also update the iteration's Mach number, where *c* is the speed of sound retrieved from the current climate state and t is the current time step.

$$V = V + at \tag{2.36}$$

$$M = \frac{V}{c} \tag{2.37}$$

2.6.10 Mass Flow

Knowing the specific fuel consumption (SFC, as c_{SFC}) the aircraft's current fuel consumption and consequently its mass variation is calculated here. The value of SFC used is interpolated between the aircraft engine's SFC values at sea level (takeoff) and at cruise altitude.

1. Mass flow, $\dot{m}$:
$$\dot{m} = -c_{SFC}T \tag{2.38}$$
2. Spent fuel mass, m_{fuel}:
$$m_{fuel_{current}} = m_{fuel_{previous}} + \dot{m}t \tag{2.39}$$
3. Aircraft mass, m_a:
$$m_{a_{current}} = m_{a_{previous}} + \dot{m}t \tag{2.40}$$

2.6.11 Aircraft Position

In order to calculate this iteration's change in position the effects of the aircraft's true speed and of the wind are calculated separately. This allows us to easily set the wind effect to zero if required, for example when the aircraft is on the ground. The longitude, latitude and altitude change of this iteration are also calculated separately and the aircraft's position is updated in the end and converted to geodetic coordinates [41]. The following equations are valid for both true aircraft speed and wind speed, therefore V can refer to either of these speeds. R_e is the earths radius.

- Latitude variation, $\Delta\lambda$:

$$\Delta\lambda = \left(\frac{Vcos\psi}{R_e}\right)t \tag{2.41}$$

- Longitude variation, $\Delta\varphi$:

$$\Delta\varphi = \left(\frac{Vsin\psi}{cos\lambda R_e}\right)t \tag{2.42}$$

- Altitude variation, Δh:

$$\Delta h = Vsin\gamma t \tag{2.43}$$

Using the equations above for both true aircraft speed and wind speed the last step is simply adding the resulting position variation to the current aircraft's position. The differential equations used were solved using the Runge Kutta-Butcher algorithm [42].

2.6.12 Target Verification

With the newly updated aircraft position it is necessary to verify if we have reached the current target waypoint, by calculating the distance between the aircraft and that target waypoint and comparing to an arbitrary interval value. If the target waypoint has been reached the next waypoint on the list is targeted. When the final waypoint has been reached, the current flight phase is landing and the aircraft's speed is 0, it means the aircraft has landed and the simulation is successful.

2.6.13 Elapsed Time

The final step of the iteration is to update the elapsed time (T_e) with the current simulation step (t).

$$T_{e_{current}} = T_{e_{previous}} + t \tag{2.44}$$

Chapter 3

Simulation

This chapter contains three simulations made using the TP tool, divided in two sections: the information required for simulation (flight intent, aircraft information and other relevant factors) and the actual simulation results. The flights were chosen based on their length (a short, medium and long flight), aircraft model, available trajectory information and the availability of reliable actual flight information to be used in the tool's validation discussed on the next chapter. All simulations were conducted on a PC with an Intel Core i7 Processor (8x 2.60 GHz) and 16gb DDR5 RAM running the Windows 10 operating system.

3.1 Flight Information

The information required for simulation that was discussed on the previous chapter is shown here for all three flights. Flights departing from or arriving to the USA were preferred because their flight plan was of easier access and the atmospheric database employed seems to be more accurate in this region. The majority of the flight plan information was retrieved from the website flightaware.com, who in turn obtains it from several government sources, airlines, commercial data providers and ADS-B receivers [43].

3.1.1 General Information

The flights general information will be present here, such as flight designations (that will be used later on the chapter), as well as aircraft model and airports.

Table 3.1: Flight AA97 (A) general information.

	Flight A (short distance)
Flight number	AA97
Departure airport	Miami international airport (MIA/KMIA)
Arrival airport	Houston, George Bush intercontinental airport (IAH/KIAH)
Date	March 7, 2017, 10:29 (UTC)
Aircraft Model	Airbus A319-115
Flight time	2 hours 21 minutes
Average flight time	2 hours 26 minutes
Great circle distance	1549.4 km

Table 3.2: Flight UA632 (B) general information.

	Flight B (medium distance)
Flight number	UA632
Departure airport	Washington Dulles international airport (IAD/KIAD)
Arrival airport	Los Angeles international airport (LAX/KLAX)
Date	March 7, 2017, 7:48 (UTC)
Aircraft Model	Boeing 757-224
Flight time	5 hours 13 minutes
Average flight time	5 hours 22 minutes
Great circle distance	3674.0 km

Table 3.3: Flight AA142 (C) general information.

	Flight C (long distance)
Flight number	AA142
Departure airport	New York, John F. Kennedy international airport (JFK/KJFK)
Arrival airport	London, Heathrow airport (LHR/EGLL)
Date	March 9, 2017, 15:33 (UTC)
Aircraft Model	Boeing 777-223 (ER)
Flight time	5 hours 52 minutes
Average flight time	6 hours 8 minutes
Great circle distance	5539.5 km

3.1.2 Aircraft Information

The majority of the aircraft information (including engine specific information) found here was retrieved from the previously mentioned Civil Jet Aircraft Design data sets [9].The aircraft's parasitic drag coefficient (C_{d0}) was estimated, based on average values for similar aircraft. The maximum flight path angle used is the usual maximum for large passenger transport aircraft whose typical values are between the 15 to 20 degrees range.

Table 3.4: Analyzed flights aircraft information.

	Flight A	**Flight B**	**Flight C**
Aircraft Model	Airbus A319-115	Boeing 757-224	Boeing 777-223 (ER)
Maximum Takeoff Weight [kg]	64 000	115 900	242 670
Design fuel load [kg]	13 020	40 190	71 170
Wing span [m]	33.91	38.05	60.9
Wing surface area [m^2]	122.4	185.25	427.8
Flap to wing span ratio	0.78	0.6	0.6
Estimated parasitic drag coefficient (CD_0)	0.019	0.014	0.015
Maximum flight path angle [°]	20	20	20

Table 3.5: Analyzed flights aircraft engine information.

	Flight A	Flight B	Flight C
Model / Type	CFM56-5A1	RB211-535E4B	RR Trent-892
Number of engines	2	2	2
Static sea level thrust [Kn]	99.7	191.3	413.8
SFC at sea level [kg/s/N]	$9.34x10^{-6}$	$1.72x10^{-5}$	$1.66x10^{-5}$
SFC at 35 000 ft (10668 m) [kg/s/N]	$1.69x10^{-5}$	$1.69x10^{-5}$	$1.576x10^{-5}$

3.1.3 Flight Phase Information

Most flight phase information was taken from Eurocontrol database that contains flight phase and aircraft specific average values for speed and rate of climb or descent, as well as the altitude at which these phases take place [11]. Because these values are averages relative the the aircraft, some of them, such as cruise altitude, were adapted to the specific flights being simulated. The used attrition values for the landing and takeoff runways are typical values.

Table 3.6: Analyzed flights flight plan information.

	Flight A	Flight B	Flight C
Takeoff speed [m/s]	69.45	74.6	87.5
Initial climb speed [m/s]	84.88	90.0	102.9
Initial climb target altitude [m/s]	1524.0	1524.0	1524.0
Secondary climb speed [m/s]	149.19	154.3	154.3
Secondary climb target altitude [m]	4572.0	4572.0	4572.0
On course climb speed [m/s]	149.19	154.3	154.3
On course climb target altitude [m]	7315.2	7315.2	7315.2
Mach climb target Mach number	0.78	0.78	0.83
Cruise altitude [m]	11582.4	11582.4	11887.2
Cruise target Mach number	0.79	0.80	0.86
Initial descent target Mach number	0.78	0.80	0.75
Initial descent target altitude [m]	7315.2	7315.2	7315.2
Main descent speed [m/s]	149.19	138.9	154.3
Main descent target altitude [m]	3048	3048	3048
Approach descent speed [m/s]	118.32	113.28	128.6
Touch down speed [m/s]	66.88	66.88	72.02

Table 3.7: Analyzed flights takeoff and landing information.

	Flight A	Flight B	Flight C
Departure altitude [m]	3	95	4
Arrival Altitude [m]	30	38	25
Departure takeoff attrition coefficient	0.05	0.05	0.05
Arrival landing attrition coefficient (with brakes)	0.5	0.5	0.5

3.1.4 Waypoints

For flight B (UA632) and C (AA142) the course waypoints were retrieved from flightaware.com and were shown to be viable. However the available flight A (AA97) courses were not as accurate. For this reason flight's A course was estimated by the author using flightradar.com values. The trajectory images shown below are the representations of the simulated course taken directly from the TP tool, where the given waypoints are purple and the calculated intermediate waypoints are white. The maximum Givry correction angle between waypoints used was 10º. It can be noted that both flight A and C are mostly oceanic while flight B is continental in its totality. This fact is reflected on the amount of given waypoints per distance traveled that are much larger on the continental flight B than on the transatlantic flight C, as expected. It is also important to note that there is somewhat more flexibility on transoceanic flights than on most continental ones, hence the interest in simulating both cases. The images below were taken directly from the TP tool.

Table 3.8: Flight AA97 (A) waypoints.

	Latitude	**Longitude**
Departure waypoint (MIA)	N25°47'36"	W80°17'26"
N/A	N26° 1' 24.236"	W80° 30' 44.276"
N/A	N26° 44' 39.674"	W81° 19' 7.082"
N/A	N28° 50' 9.265"	W88° 45' 43.697"
N/A	N29° 21' 2.927"	W92° 7' 42.193"
N/A	N29° 32' 36.83"	W94° 19' 39.576"
Arrival waypoint (IAH)	N29°59'04"	W095°20'29"

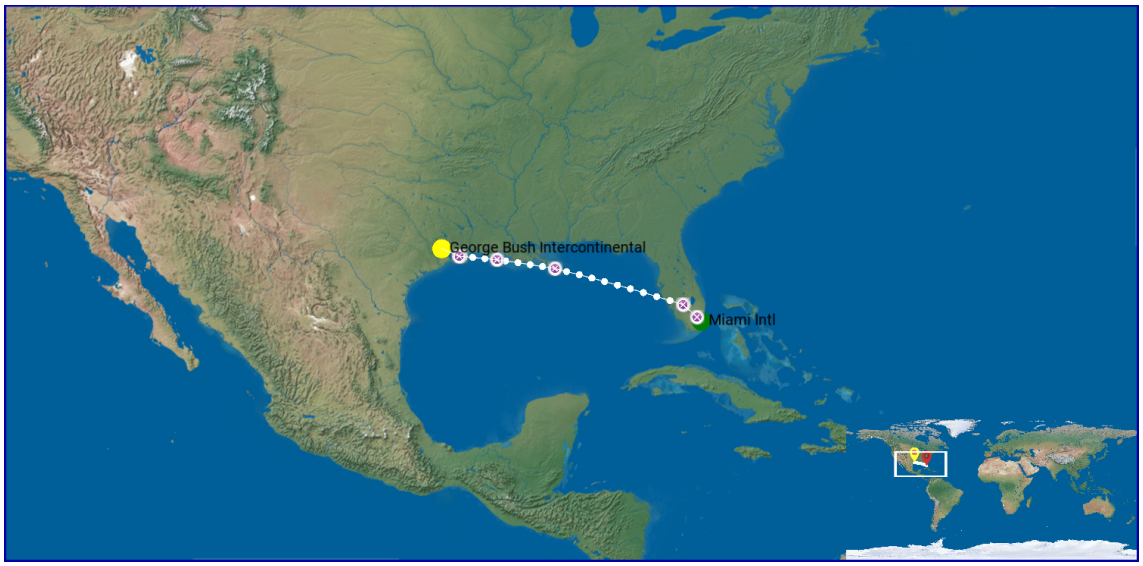

Figure 3.1: Flight AA97 (A) simulated trajectory.

Table 3.9: Flight UA632 (B) waypoints.

	Latitude	Longitude
Departure waypoint (IAD)	N38°56'40"	W77°27'21"
1 (RAMAY)	N38°57.67'0"	W78°12.96'0"
2 (HACKS)	N39°7.75'0"	W81°5.60'0"
3 (MECAN)	N40°5.19'0"	W83°30.49'0"
4 (KG660)	N40°59.99'0"	W85°59.99'0"
5 (MOPER)	N41°25.87'0"	W87°47.18'0"
6 (KG72K)	N42°0.02'0"	W90°0.00'0"
7 (CAPPR)	N42°13.08'0"	W92°25.61'0"
8 (KP72E)	N42°0.02'0"	W95°59.98'0"
9 (KP69C)	N41°30.02'0"	W98°0.01'0"
10 (KATLN)	N40°56.65'0"	W101°23.57'0"
11 (KD57W)	N39°29.99'0"	W103°59.99'0"
12 (ELWAY)	N38°24.94'0"	W106°20.60'0"
13 (KD45S)	N37°30.01'0"	W108°0.00'0"
14 (TBC)	N36°7.26'0"	W111°16.17'0"
15 (JASSE)	N36°4.28'0"	W111°48.74'0"
16 (DNERO)	N35°2.12'0"	W114°54.29'0"
Arrival waypoint (LAX)	N33°56'33"	W118°24'29"

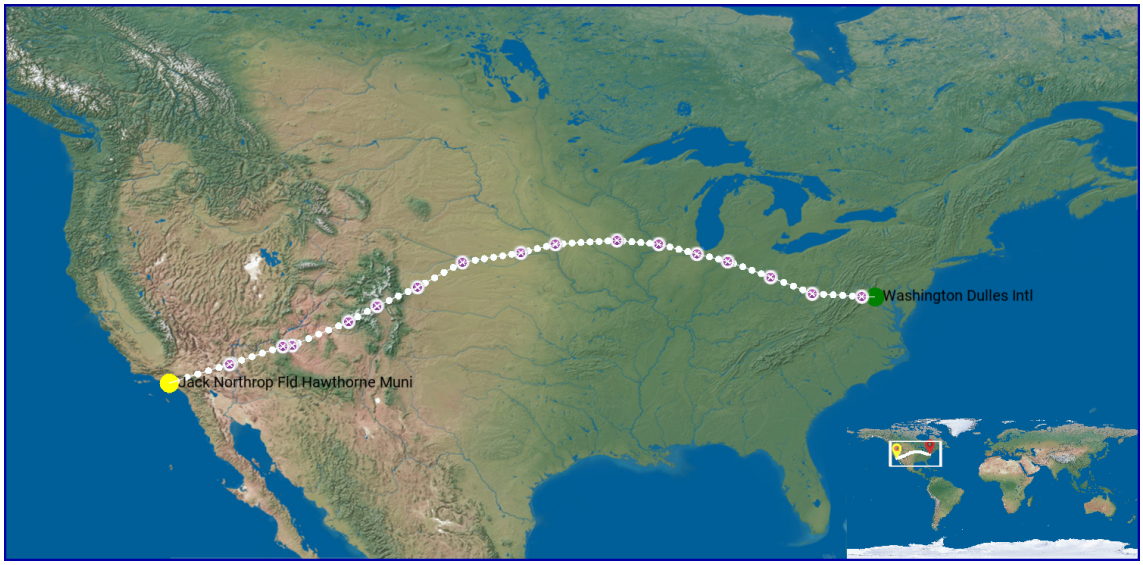

Figure 3.2: Flight UA632 (B) simulated trajectory.

Table 3.10: Flight AA142 (C) waypoints.

	Latitude	Longitude
Departure waypoint (JFK)	N40°38'23"	W73°46'44"
1 (BETTE)	N40°33.50'0"	W73°0.82'0"
2 (ACK)	N41°16.80'0"	W70°1.52'0"
3 (KANNI)	N42°38.10'0"	W67°0.12'0"
4 (PORTI)	N46°29.90'0"	W52°0.12'0"
5 (4750N)	N47°0.01'0"	W49°59.88'0"
6 (4940N)	N48°59.97'0"	W40°0.12'0"
7 (5030N)	N50°0.01'0"	W30°0.00'0"
8 (5220N)	N51°59.90'0"	W19°59.88'0"
9 (LIMRI)	N51°59.90'0"	W15°0.00'0"
10 (XETBO)	N51°59.90'0"	W13°59.88'0"
11 (SLANY)	N52°9.41'0"	W5°50.51'0"
12 (STU)	N51°59.69'0"	W5°2.34'0"
13 (BEDEK)	N51°22.20'0"	W1°33.52'0"
Arrival waypoint (LHR)	N51°28'39"	W00°27'41"

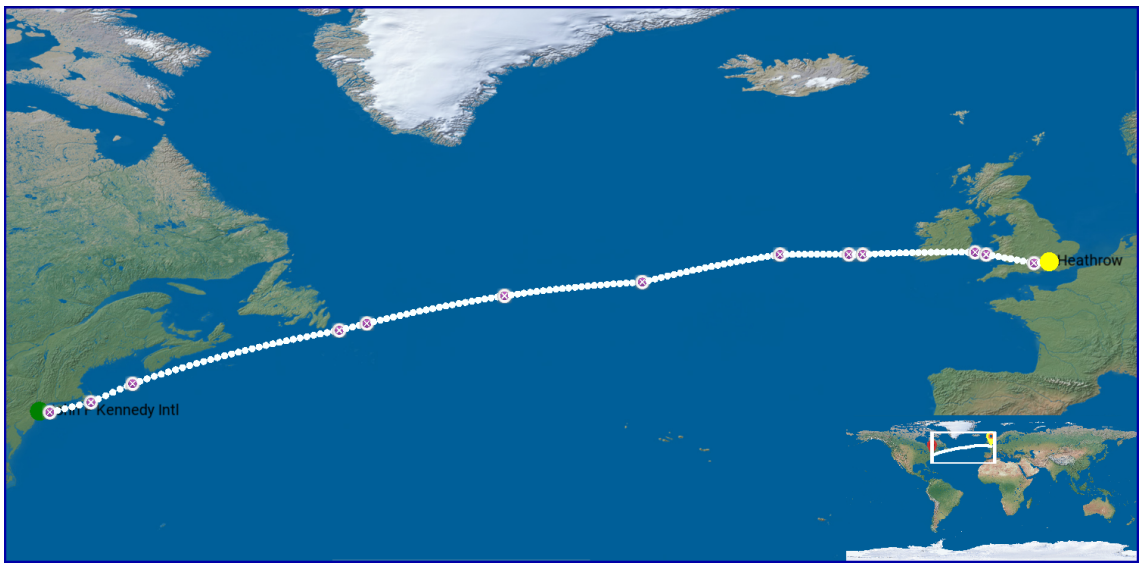

Figure 3.3: Flight AA142 (C) simulated trajectory.

3.2 Results

This subsection will contain an analysis and comparison of the most important flight parameters between the three simulated flights. The wind's impact on each flight will also be analyzed separately. All of the following data was taken directly from the TP tool and edited using Python programming language [6], more specifically using the matplotlib package [44] to generate the plots.

3.2.1 General Results

Table 3.11: General simulation results.

	Flight AA97 (A)	Flight UA632 (B)	Flight AA142 (C)
Total flight time	2 hours 28 minutes	5 hours 12	6 hours 2 minutes
Distance traveled [km]	1580.42	3831.47	5676.31
Fuel spent [kg]	4846.92	16872.09	38268.11
Fuel spent [% of total]	37.23	41.98	53.77
Takeoff roll distance [m]	1498.17	1780.83	2745.64
Landing distance [m]	1469.87	1265.47	1448.89
Simulation time [s]	2.13	4.02	4.00

Both the flight time and distance traveled were near the expected results. The fuel spent as a percentage of total aircraft fuel was slightly lower than expected which will be discussed in further detail later on. The takeoff roll and landing distances were also in the acceptable range, the comparison between them and their expected real values will be present in the validation chapter. Finally, the simulation time was acceptable, however further optimization might be required if the need to simulate a very large number of trajectories arises.

3.2.2 Altitude

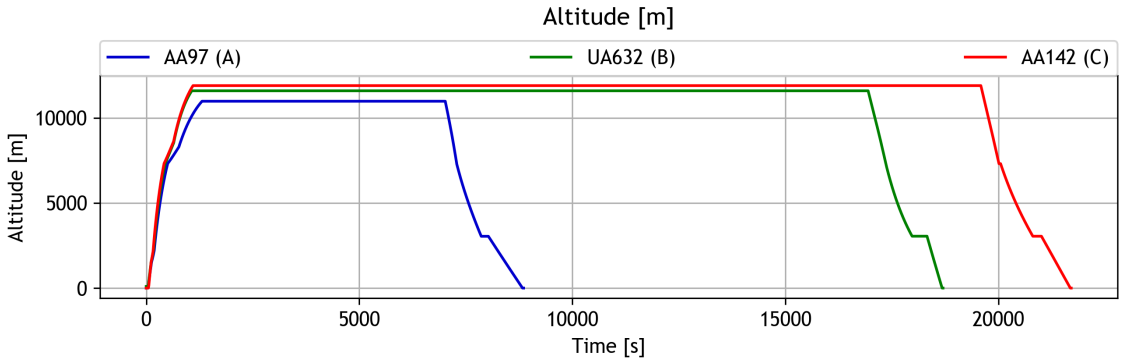

Figure 3.4: Simulated altitudes throughout the flight.

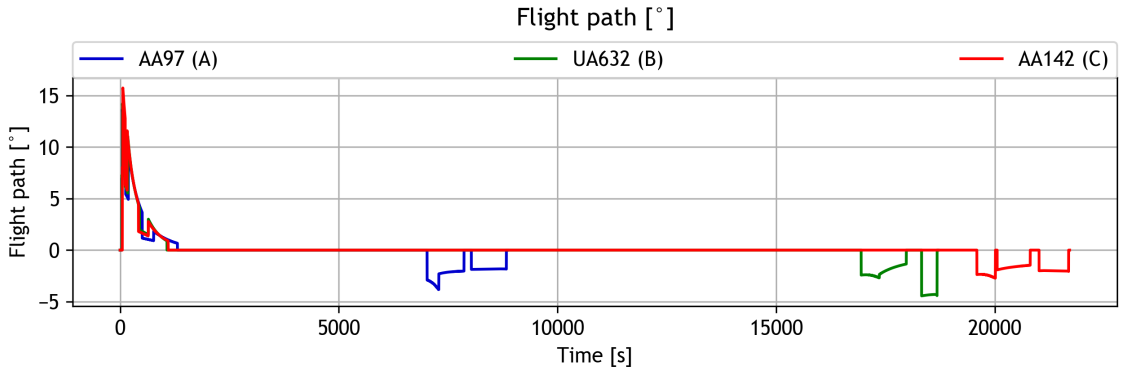

Figure 3.5: Simulated flight path angle throughout the flight.

The change in the rate of climb can be observed between the climb phases as it diminishes significantly from the steeper initial climb to the smoother final mach climb, which is also reflected in the change of the flight path angle. Between the initial descent and the main descent and between the main descent and approach descent there is a short period of time when the aircraft maintained constant altitude in order to reach the target speed before initiating the next descent phase.

Overall the flight path angle varied as intended during both climb and descent. The approach descent flight path angle is dependent on the distance between the aircraft and the airport at the start of that phase.

3.2.3 Speed

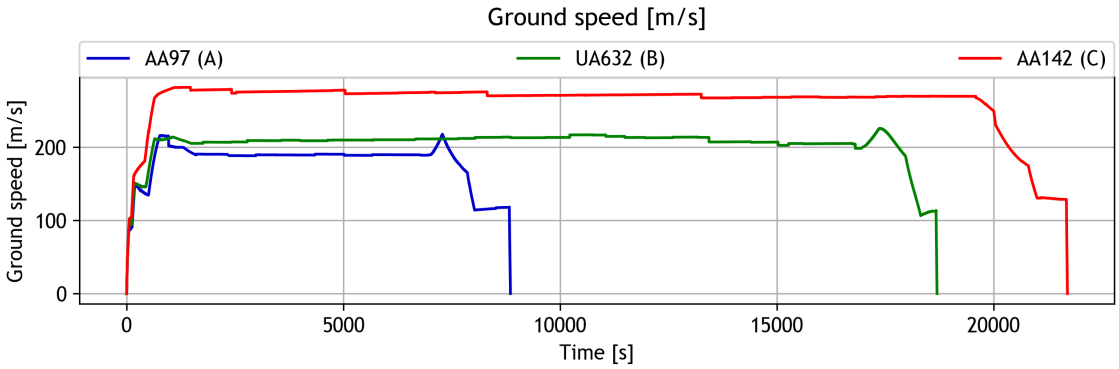

Figure 3.6: Simulated ground speed throughout the flight.

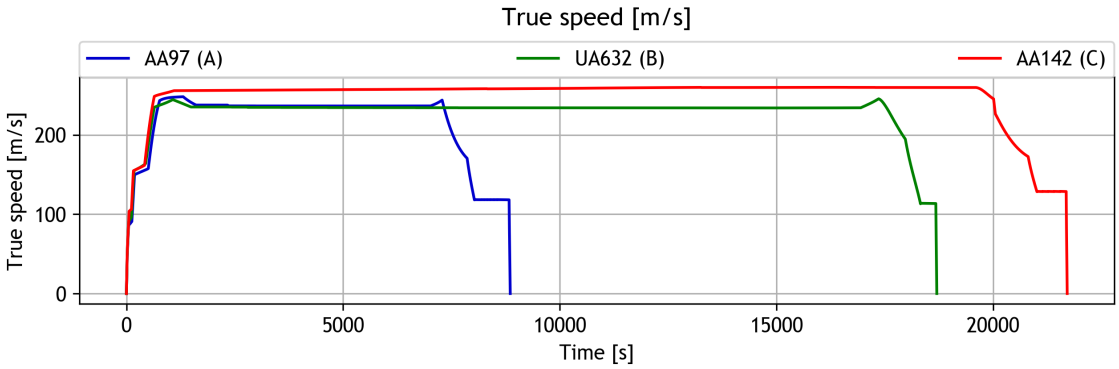

Figure 3.7: Simulated true speed throughout the flight.

The oscillations of the ground speed are mostly due to phase transitioning and wind speed variation, while most of the true speed oscillations are due to phase transitioning. The slight increase in speed at the beginning of the cruise phase is due to the sudden change in attitude while at climb power setting. Similarly, the true speed increase at the beginning of the descent phase is the result of the sudden change in attitude while at cruise speed and power setting. During descent the speed is held constant for a certain time, because during that phase the flight path adjusts itself to maintain null acceleration. The impact of the wind speed will be discussed in the following subsection.

3.2.4 Wind

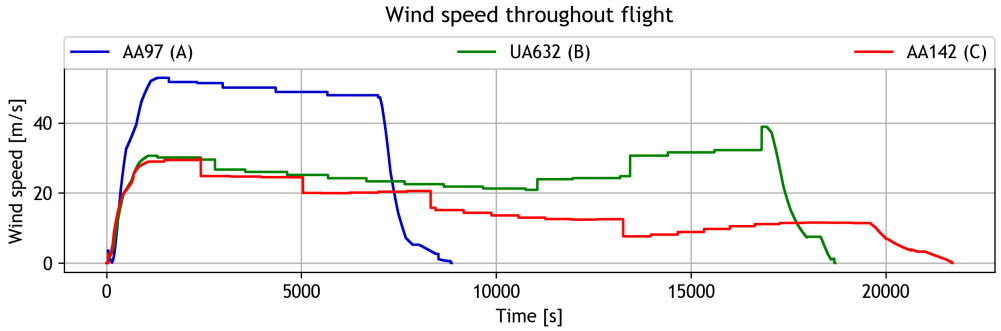

Figure 3.8: Simulated wind speed throughout the flight.

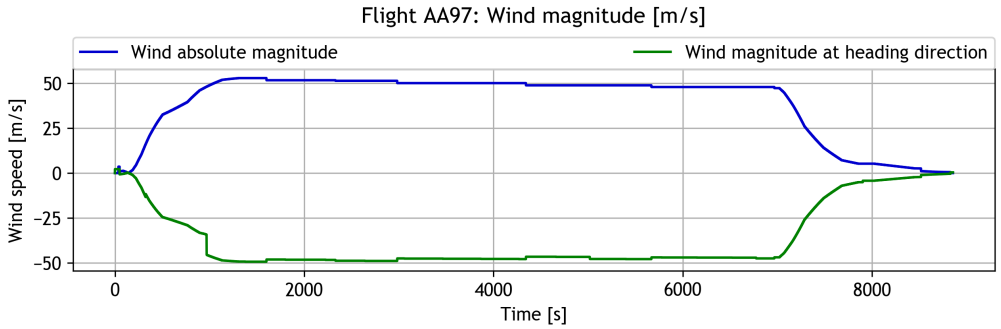

Figure 3.9: Simulated flight AA97 (A) wind (absolute and at trajectory angle) throughout the flight.

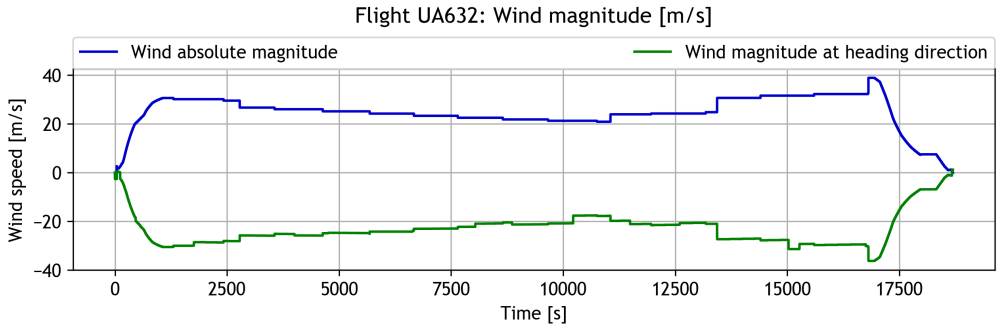

Figure 3.10: Simulated flight UA632 (B) wind (absolute and at trajectory angle) throughout the flight.

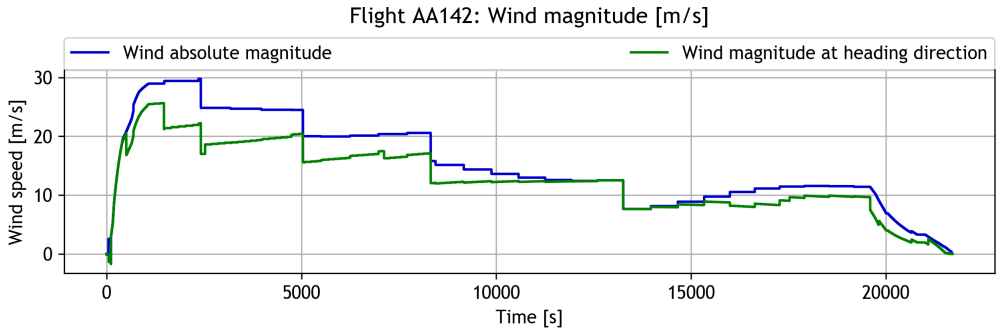

Figure 3.11: Simulated flight AA142 (C) wind (absolute and at trajectory angle) throughout the flight.

Table 3.12: Overall wind impact on flight.

	Flight AA97 (A)	Flight UA632 (B)	Flight AA142 (C)
Duration impact [minutes]	+ 24.66	+ 32.86	- 17.9
Duration impact [%]	+ 20.06 %	+ 11.79 %	- 5.95 %
Fuel spent impact [kg]	+ 752	+ 1514	- 1678
Fuel spent impact [%]	+ 18.36 %	+ 9.85 %	- 4,38 %

As expected it can be observed that the wind increases with altitude, however it's also vastly dependent on the geographic position, especially in the case on the transatlantic flight AA142 where the wind speed diminishes significantly while at the same altitude during cruise. Both flight AA97 and flight UA632 had strong headwinds which delayed the flight, while flight AA142 had a significant tailwind. The wind impact on the flights duration was of approximately +20.06% for the AA97 flight, +11.79% for the UA632 flight and -5.95% for the AA142 flight. An obvious consequence of the impact of flight time is the effect of fuel consumption which was significant for all flights, as shown on table 3.12. The heavy impact of the wind on the shorter flight A will lead to some difficulties in its accurate prediction given the oscillations of wind speeds with seasons and other variables. These significant impacts easily justify the need to take wind speed into account for trajectory prediction and optimization.

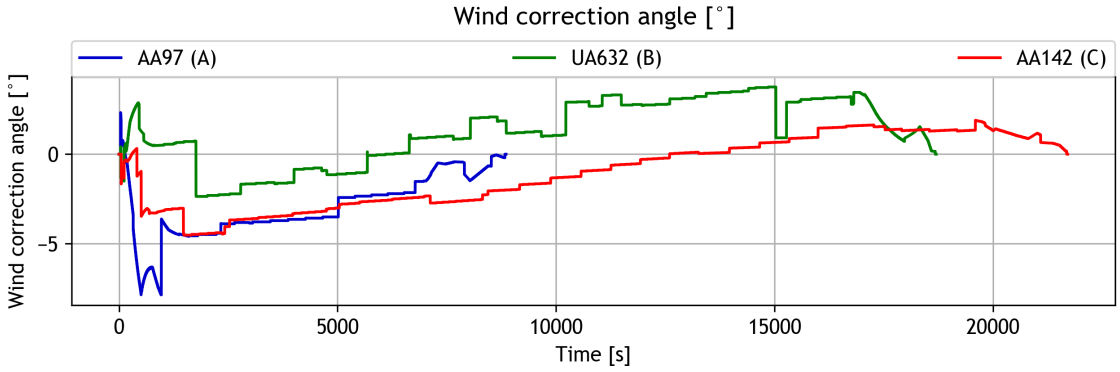

Figure 3.12: Simulated wind correction angle throughout the flight.

The wind correction angle is the alteration of the aircraft's heading that ensures it remains on course even with strong adverse winds. The amplitude of this angle is dependent of the relation between wind speed and aircraft speed as well as their directions. In this case, it was strongest during flight AA97 reaching around -8 degrees. During actual flights this angle may have much larger amplitudes due to strong wind oscillations that do not happen in this simulated case.

3.2.5 Thrust

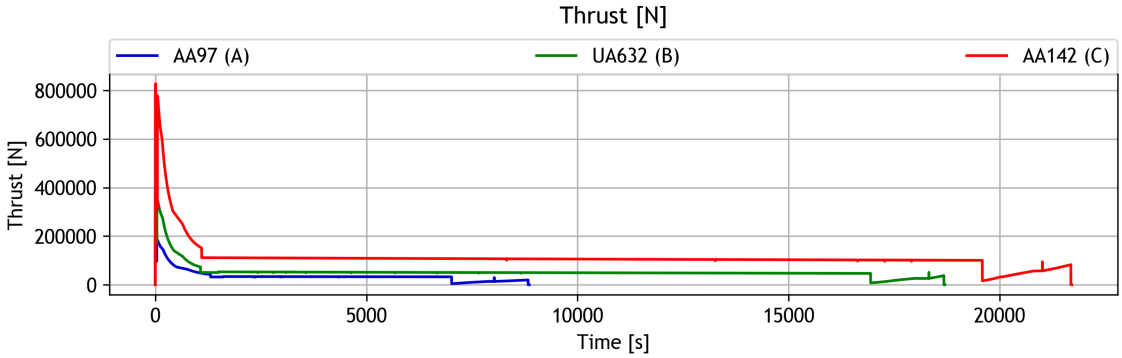

Figure 3.13: Simulated thrust throughout the flight.

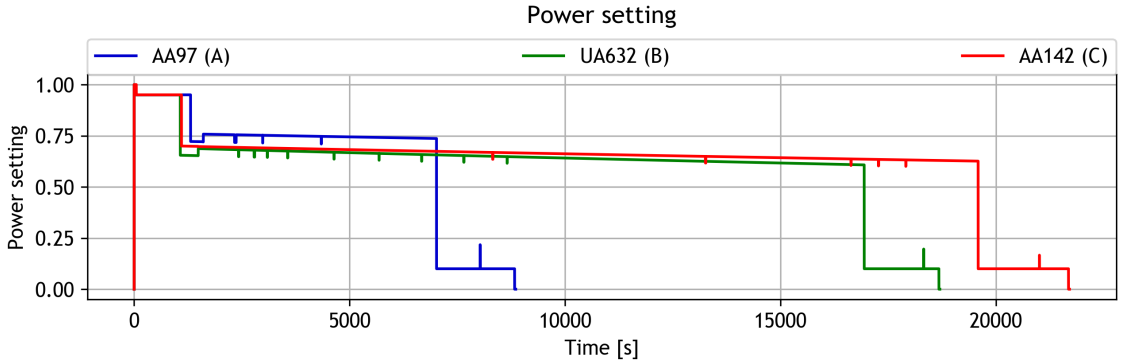

Figure 3.14: Simulated power setting throughout the flight.

The power setting varies as explained in the previous chapter with full power at takeoff followed by a very slight reduction during the climb phases and an adjustment to the desired speed during cruise. During cruise the power setting reduces slightly due to the aircraft's weight loss (and consequent lift induced drag reduction) in order to maintain constant speed. During the majority of the descent phases the power is set to idle. This differs from a real life setting in which during the approach descent power is required for loiter and approach maneuvers.

The cruise power setting is lower than expected which could be due to an underestimation of the aircraft's drag coefficients or an overestimation of the available engine thrust at cruise altitudes.

3.2.6 Fuel Spent

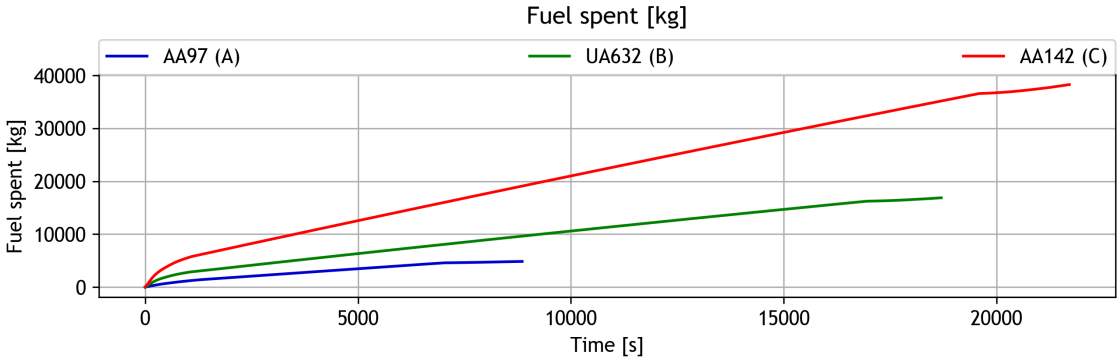

Figure 3.15: Simulated spent fuel weight throughout the flight.

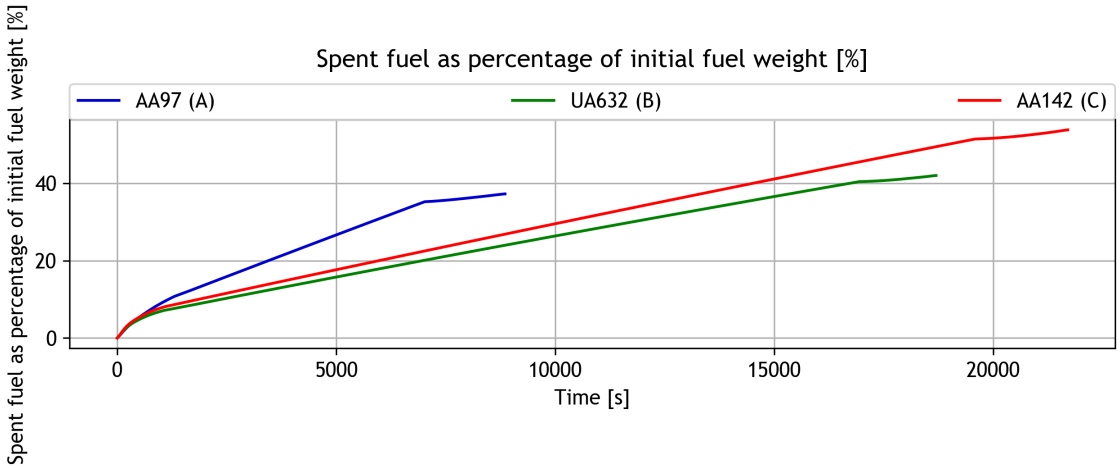

Figure 3.16: Simulated spent fuel as percentage of total fuel throughout the flight.

As expected the longer transatlantic flight spent a much higher amount of fuel, not only due to its larger duration, but also because of its higher thrust requirements. Both flight A and flight B spent around 40% of its total fuel capacity while the longer flight C spent around 56% of its fuel capacity. These values are however subject to inaccuracies due to difficulty in getting the exact SFC value at certain altitudes. Another important factor to take into account is that for this simulation the aircraft carries the maximum amount of fuel possible at MTOW which is rarely the case, as it is often not required and leads to unnecessary drag and consequently higher fuel consumption.

Chapter 4

Validation

To validate the used methods of trajectory prediction the flight trajectories discussed on the previous chapter were compared with values from actual flights. These values were obtained from the website flightradar24.com which in turn acquired them mostly from automatic dependent surveillance-broadcast (ADS-B) systems [45]. Aircraft equipped with ADS-B capabilities (roughly 70% of all commercial passenger aircraft) get their current position from a GPS source while a on-board transponder transmits this information (and more) to nearby receivers, such as ground stations or other aircraft, as seen on figure 4.1. The information required for this validation was the aircraft's ground speed and its location (latitude, longitude and altitude). The ADS-B system receives this signal in intervals of varying lengths usually from 5 to 50 seconds when good coverage is available. This temporal density allows an accurate comparison with the simulation's results. Due to the limitations of the on-board transponders and ground receivers range some remote areas of the globe are not covered by the system even though flightradar24 maintains over 7000 receivers worldwide [45].

In order to provide an accurate comparison, despite the random time intervals in which the actual flight information is received, the values of both the simulation and the actual flight were interpolated in 10 second intervals and the absolute differences between them, as well as the original values themselves, were plotted and analyzed. As in the previous chapter the information was plotted using Python programming language [6], specifically the package pyplot from the matplotlib library [44].

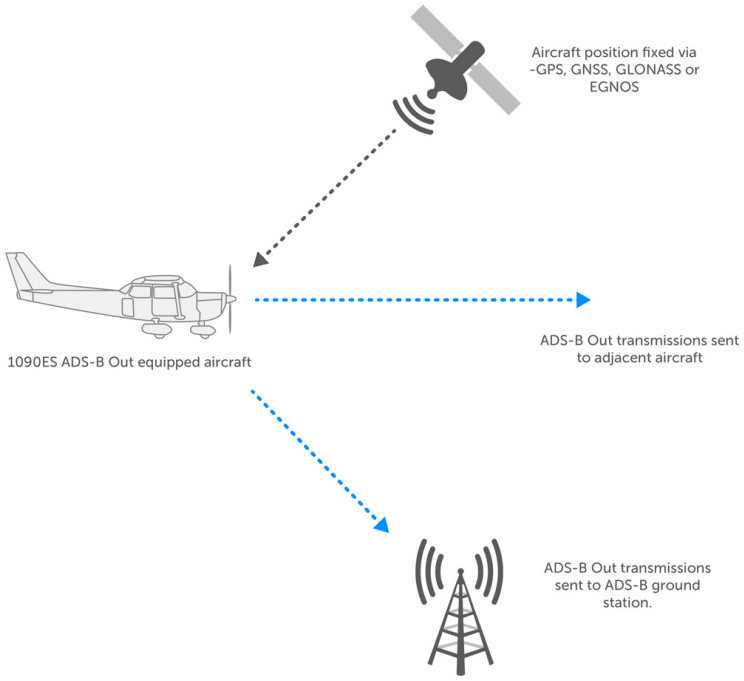

Figure 4.1: ADS-B operation diagram.

4.1 Altitude

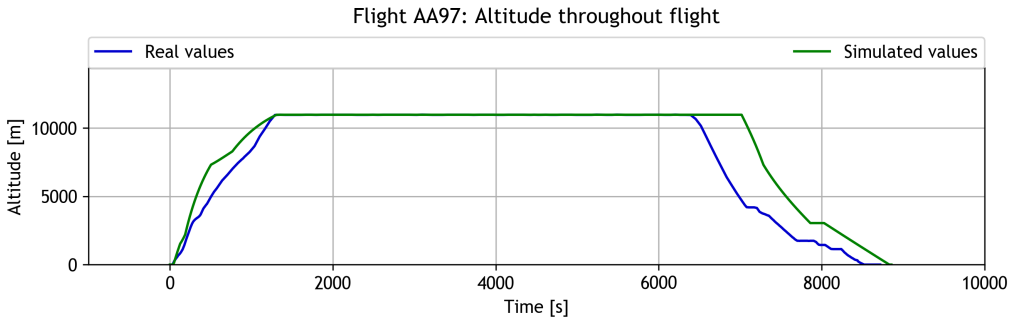

Figure 4.2: Flight AA97 (A) actual and simulated altitude throughout flight.

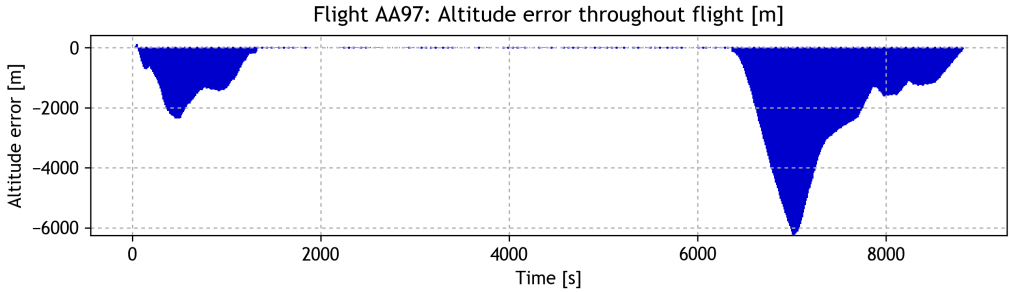

Figure 4.3: Flight AA97 (A) altitude error throughout flight.

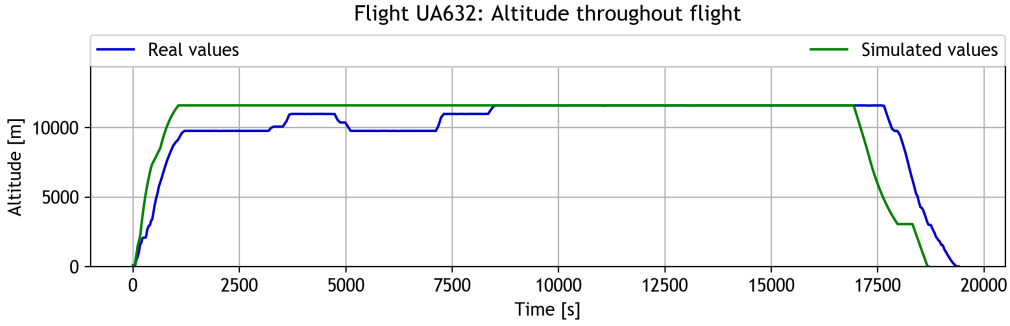

Figure 4.4: Flight UA632 (B) actual and simulated altitude throughout flight.

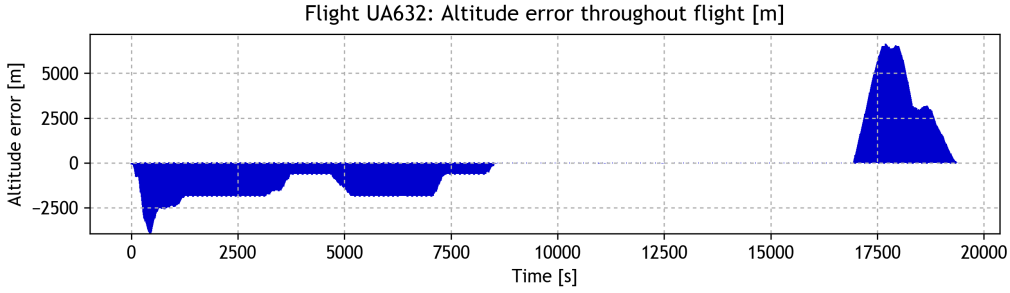

Figure 4.5: Flight UA632 (B) altitude error throughout flight.

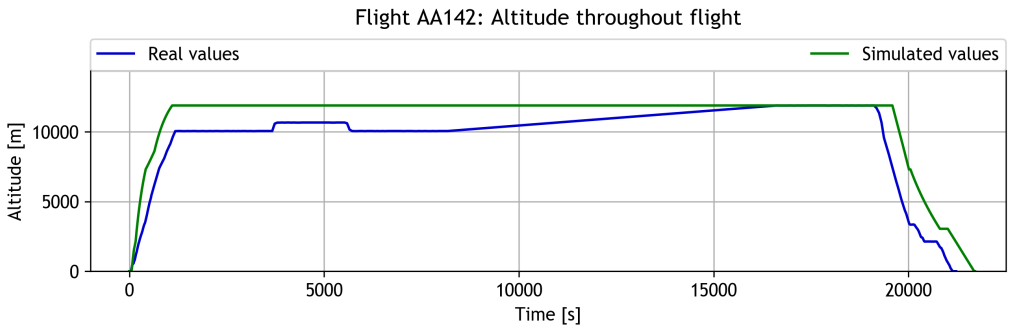

Figure 4.6: Flight AA142 (C) actual and simulated altitude throughout flight.

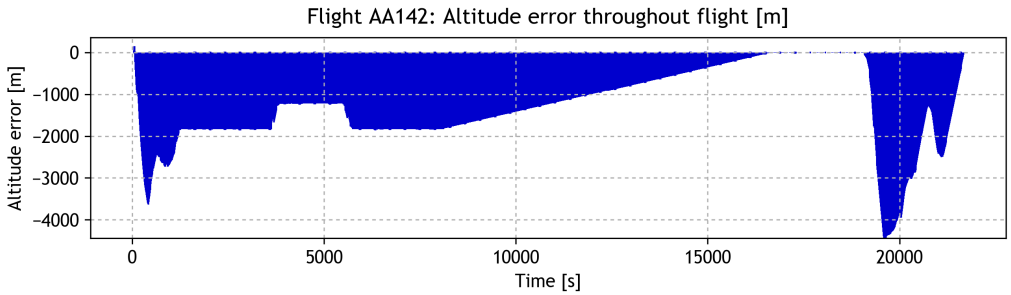

Figure 4.7: Flight AA142 (C) altitude error throughout flight.

Table 4.1: Altitude general error [m].

	Flight AA97 (A)	**Flight UA632 (B)**	**Flight AA142 (C)**
Mean	-833.66	-225.92	-1302.23
Median	-7.95	-8.66	-1269.78
Standard deviation	1375.51	1798.87	924.85
Maximum	95.10	6646.04	128.01
Minimum	-6256.01	-3942.59	-4441.49

The main differences in altitudes are a result of flight planning and aircraft separation maneuvers. It is usual for aircraft to fly at non-optimal altitudes in order to meet aircraft separation requirements. During flight the aircraft may climb or descent to the optimal cruise altitude when possible. These changes in altitude are hard to predict beforehand are a significant problem for flight prediction tools. It is also important to note that the transatlantic flight C had no ADS-B coverage throughout some of its duration (approximately between the 8000 and 16000 second flight times) which resulted in the linear altitude change during that period, that did not occur that way and is only a simplification made by flightradar24.

It can be observed that during climb in all three cases the simulated climb gradient was almost always significantly higher than the real one. This can be partly explained by an overestimation of the available thrust during climb. The only exception is during the initial climb phase when the climb gradients remains approximate. Another significant source of error is that the difference of the climb gradient between climb phases is not as big as expected as it remained almost constant throughout the actual flight's climb phases, especially in the case of flight A.

Regarding the differences between the times to initiate the descent, they can be attributed to the overall ground speed differences during flight and also to the exact distance to reach the

airport required to start the descent phase, which is hard to emulate accurately as it depends on several factors.

During the final descent phases, it can be seen in both the actual and simulated case that there are periods of time when the altitude is maintained constant. In the simulated cases this is to decrease the aircraft's speed before continuing the descent. In the actual cases however, these periods of time may also be due to loitering periods while waiting for landing clearance or due to approach maneuvers to position the aircraft for the final approach and landing.

4.2 Speed

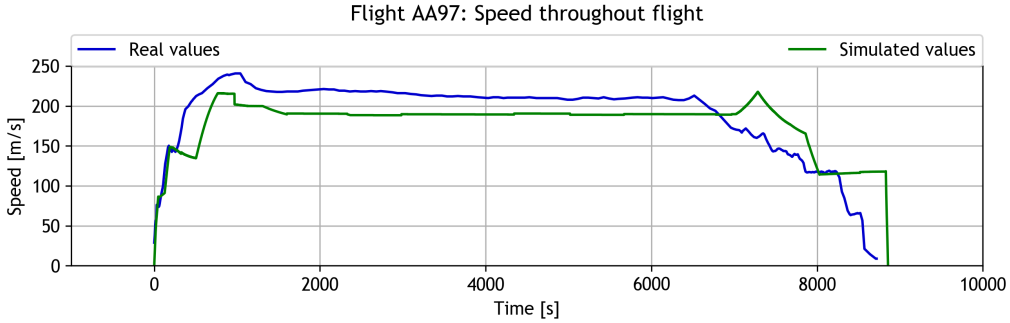

Figure 4.8: Flight AA97 (A) actual and simulated ground speed throughout flight.

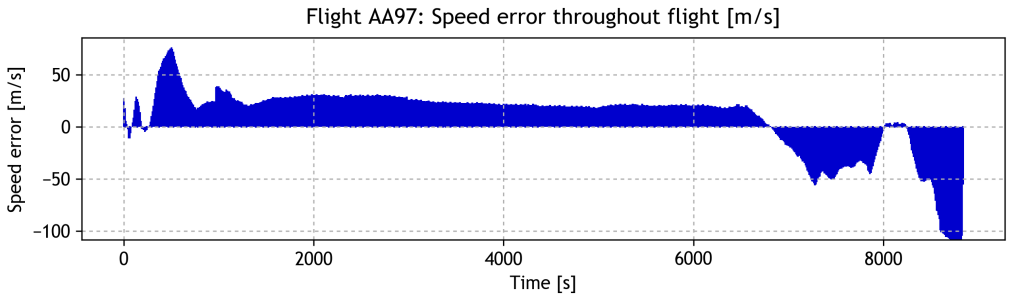

Figure 4.9: Flight AA97 (A) absolute speed error during flight.

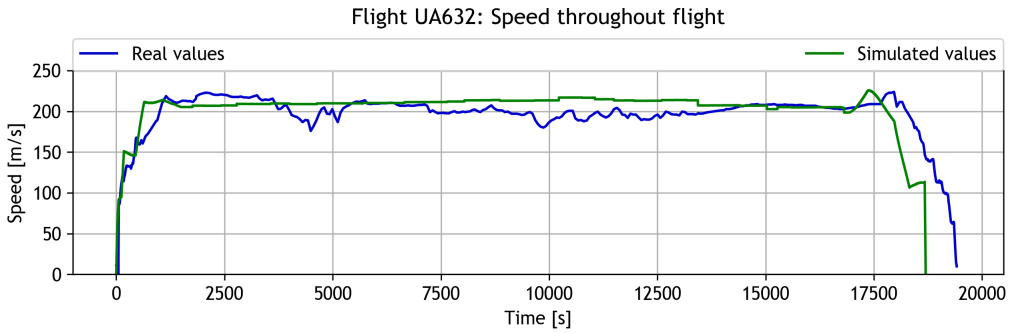

Figure 4.10: Flight UA632 (B) actual and simulated ground speed throughout flight.

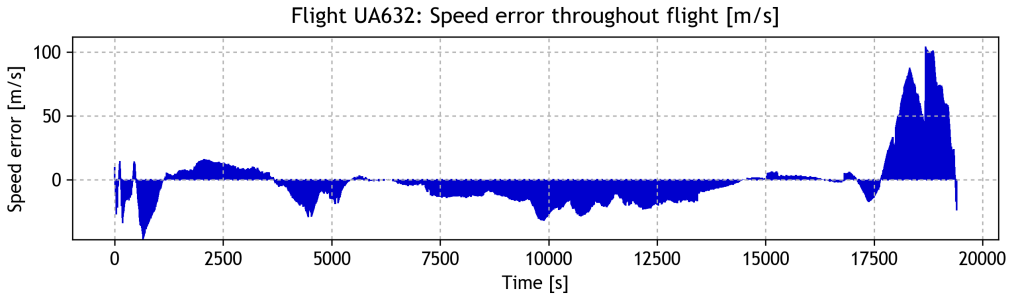

Figure 4.11: Flight UA632 (B) absolute speed error during flight.

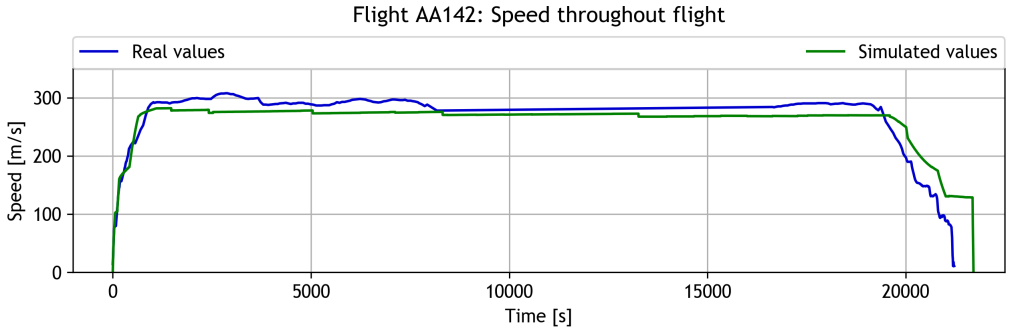

Figure 4.12: Flight AA142 (C) actual and simulated ground speed throughout flight.

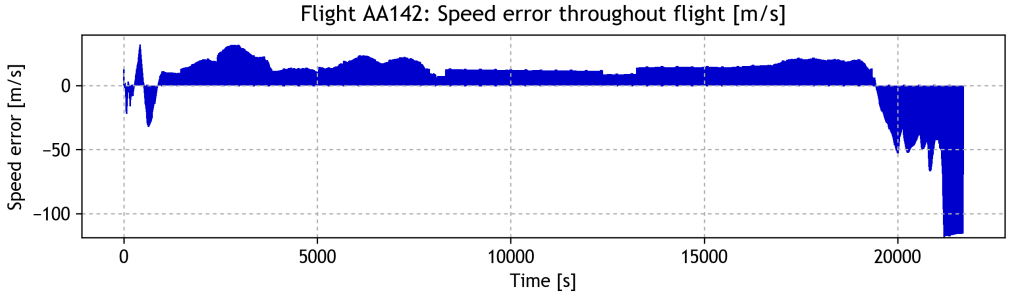

Figure 4.13: Flight AA142 (C) absolute speed error during flight.

Table 4.2: Speed general error [m/s].

	Flight AA97 (A)	**Flight UA632 (B)**	**Flight AA142 (C)**
Mean	9.35	-2.04	7.02
Median	20.64	-5.00	13.84
Standard deviation	31.96	23.09	25.69
Maximum	76.15	104.21	32.03
Minimum	-108.52	-47.05	-118.80

Part of the speed errors can be attributed to wind speed oscillations. Initially during the climb phases the speeds are very approximate to each other. However, this ceases to be the case around the final mach climb phase. This is especially true in flight's A and B cases. This difference in speed during this phase is partly due to the higher flight path angle of the simulated cases that was mentioned in the previous section as well as a somewhat abrupt change in the

wind database values between flight levels.

During the descent phase there are two main issues. The first is that the actual descent takes place at different times. This is due to the speed differences throughout the flight and also due to differences in distance between aircraft and airport to begin the initial descent, as mentioned before. The second issue is similar to that of the climbing phases, in that the descent angle is most likely different between cases. The period of time during the simulated descent when the speed remains nearly constant can be attributed to the descent angle during this time that adjusts itself to maintain approximately constant speed while descending, which does not occur in the actual case.

4.3 Geographic Position

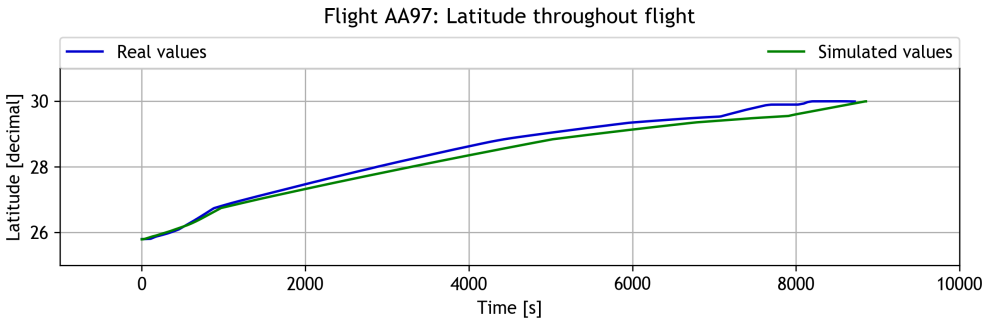

Figure 4.14: Flight AA97 (A) actual and simulated latitude throughout flight.

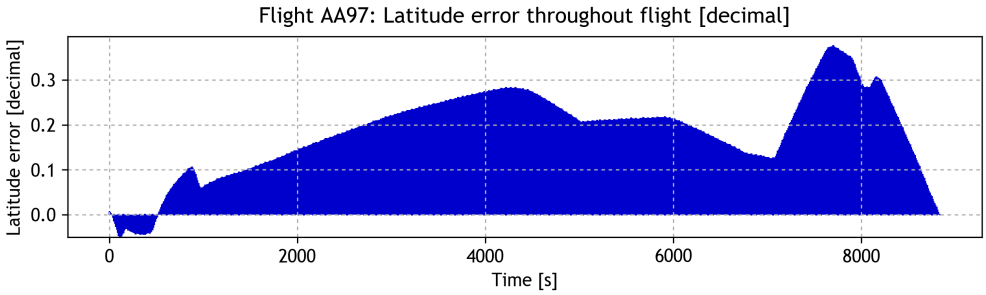

Figure 4.15: Flight AA97 (A) latitude error throughout flight.

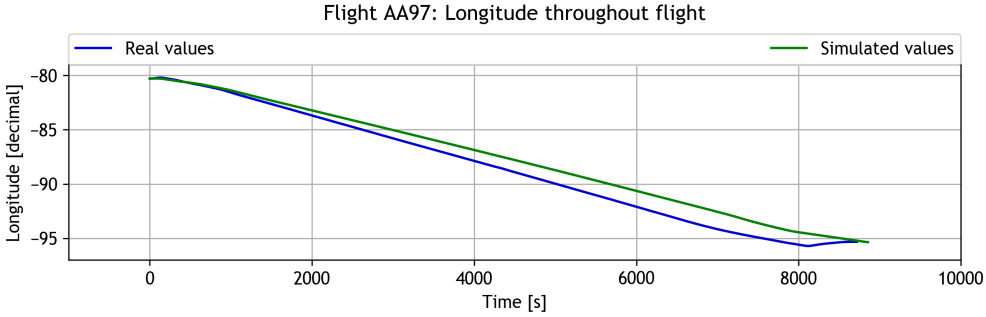

Figure 4.16: Flight AA97 (A) actual and simulated longitude throughout flight.

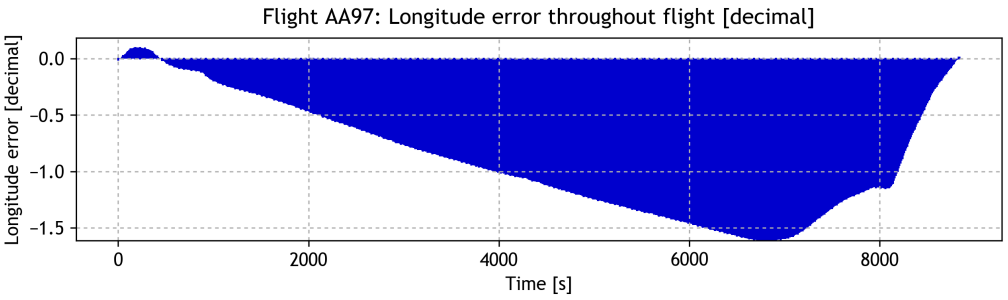

Figure 4.17: Flight AA97 (A) longitude error throughout flight.

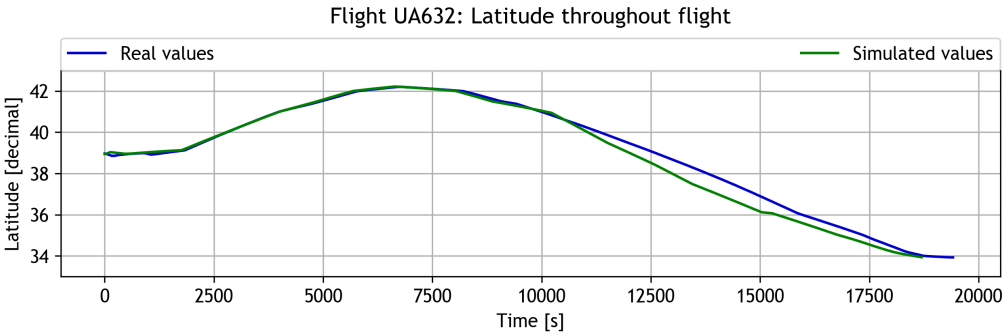

Figure 4.18: Flight UA632 (B) actual and simulated latitude throughout flight.

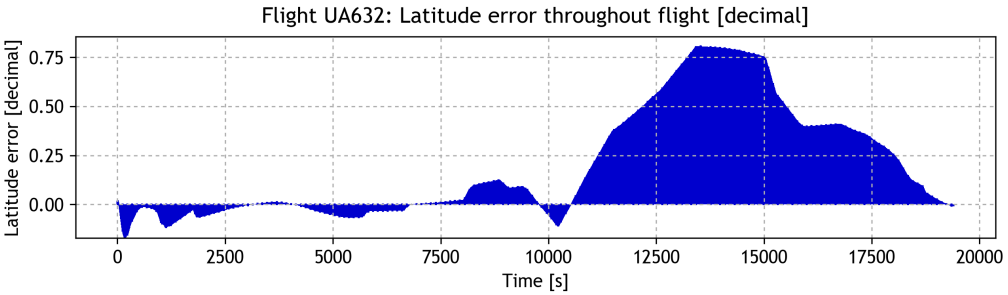

Figure 4.19: Flight UA632 (B) latitude error throughout flight.

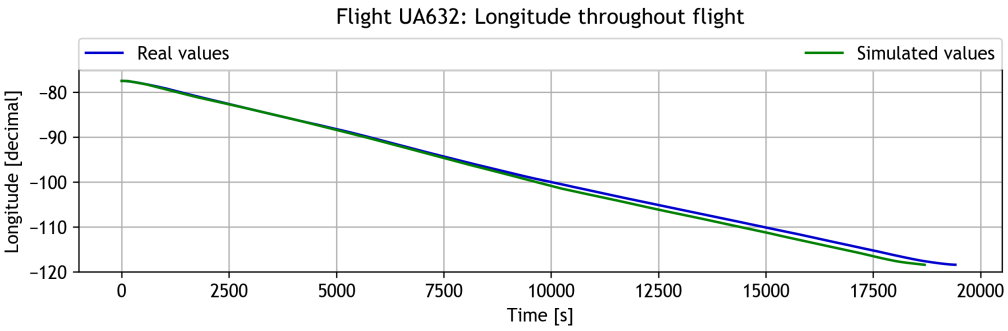

Figure 4.20: Flight UA632 (B) actual and simulated longitude throughout flight.

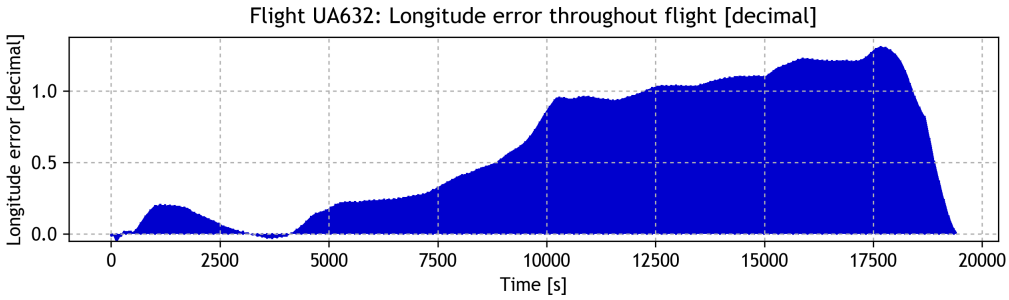

Figure 4.21: Flight UA632 (B) longitude error throughout flight.

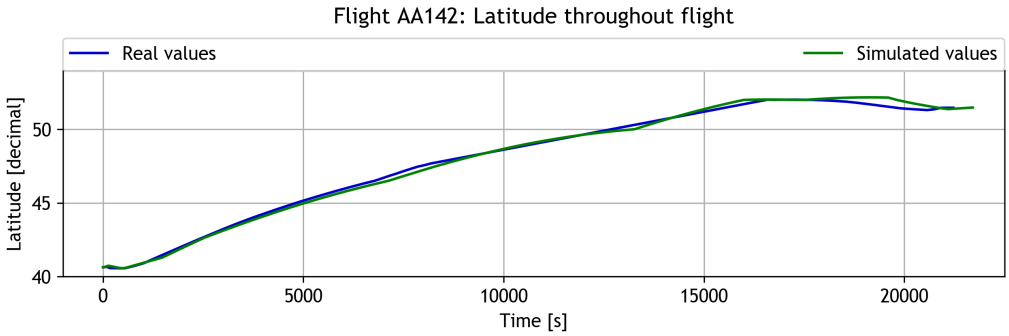

Figure 4.22: Flight AA142 (C) actual and simulated latitude throughout flight.

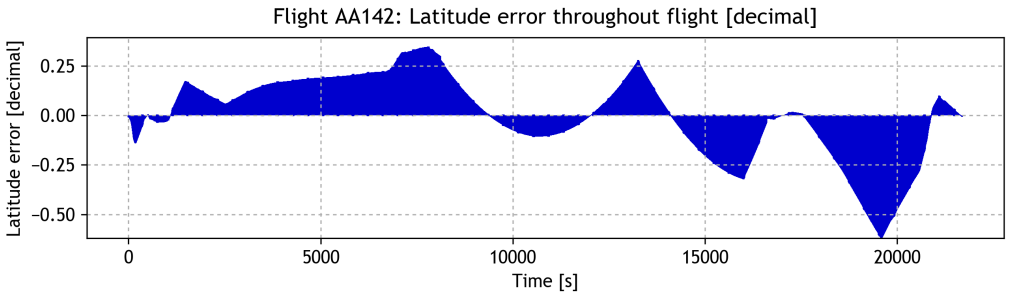

Figure 4.23: Flight AA142 (C) latitude error throughout flight.

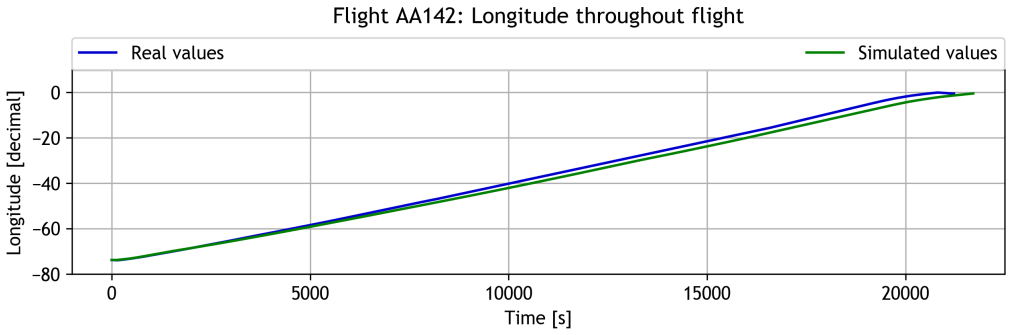

Figure 4.24: Flight AA142 (C) actual and simulated longitude throughout flight.

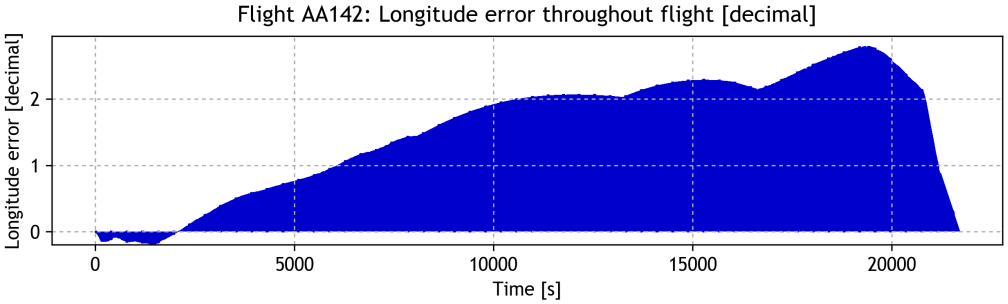

Figure 4.25: Flight AA142 (C) longitude error throughout flight.

Table 4.3: Latitude general error [decimal].

	Flight AA97 (A)	**Flight UA632 (B)**	**Flight AA142 (C)**
Mean	0.18	0.19	0.00
Median	0.21	0.05	0.02
Standard deviation	0.09	0.28	0.21
Maximum	0.38	0.81	0.34
Minimum	-0.05	-0.17	-0.62

Table 4.4: Longitude general error [decimal].

	Flight AA97 (A)	**Flight UA632 (B)**	**Flight AA142 (C)**
Mean	-0.87	0.62	1.52
Median	-0.96	0.57	1.92
Standard deviation	0.51	0.46	0.89
Maximum	0.10	1.31	2.79
Minimum	-1.62	-0.05	-0.20

The differences in these graphs are once again mainly a result of speed errors and actual trajectory inaccuracies. Although every flight plan includes a set of waypoints there is a significant tolerance when it comes to actual distance from these waypoints that the aircraft has to respect, which accounts for some of these errors. Other errors may be due to approach and climbing maneuvers. In flight's A case sufficiently accurate trajectory waypoints were not available, therefore they had to be estimated which could also be a contributing factor to these differences. The next sub-section will contain a more detailed analysis on the positional error throughout the flight.

4.4 Absolute Distance Analysis

Figure 4.26: Flight AA97 (A) absolute distance error throughout flight.

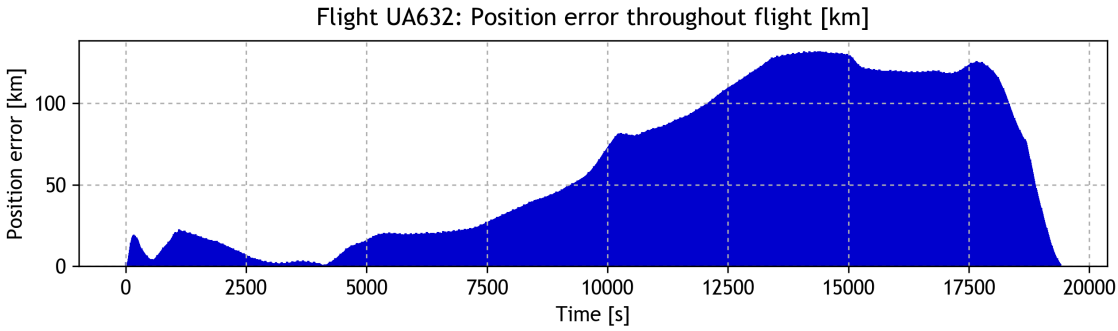

Figure 4.27: Flight UA632 (B) absolute distance error throughout flight.

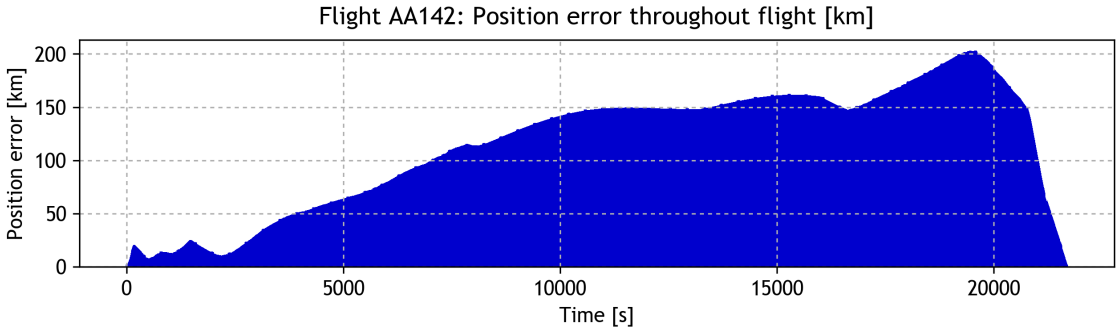

Figure 4.28: Flight AA142 (C) absolute distance error throughout flight.

Table 4.5: Absolute distance general error [km].

	Flight AA97 (A)	**Flight UA632 (B)**	**Flight AA142 (C)**
Mean	88.82	61.90	113.90
Median	98.40	48.88	141.44
Standard deviation	48.90	47.81	57.36
Maximum	157.73	131.88	203.00
Minimum	0.38	0.63	1.17

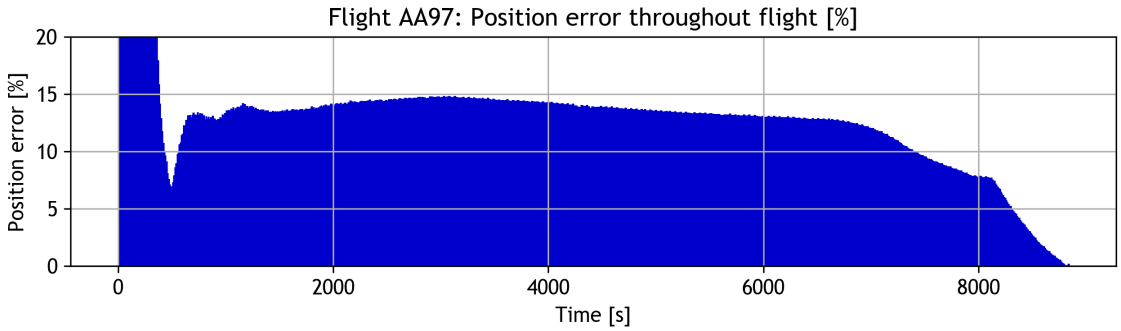

Figure 4.29: Flight AA97 (A) percentage distance error throughout flight.

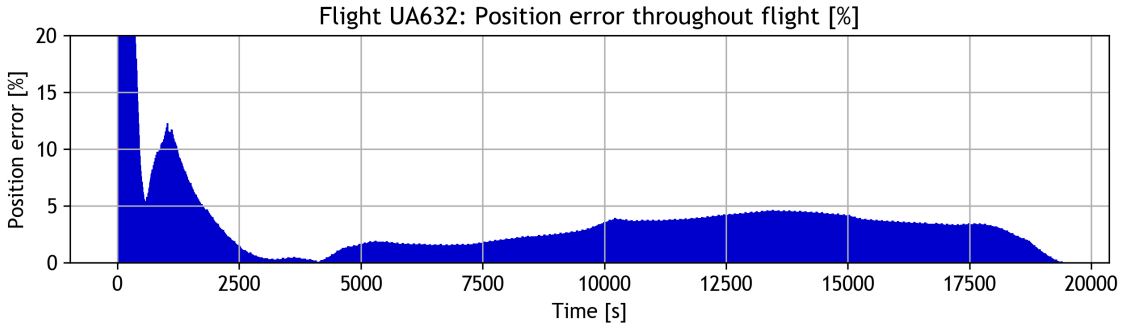

Figure 4.30: Flight UA632 (B) percentage distance error throughout flight.

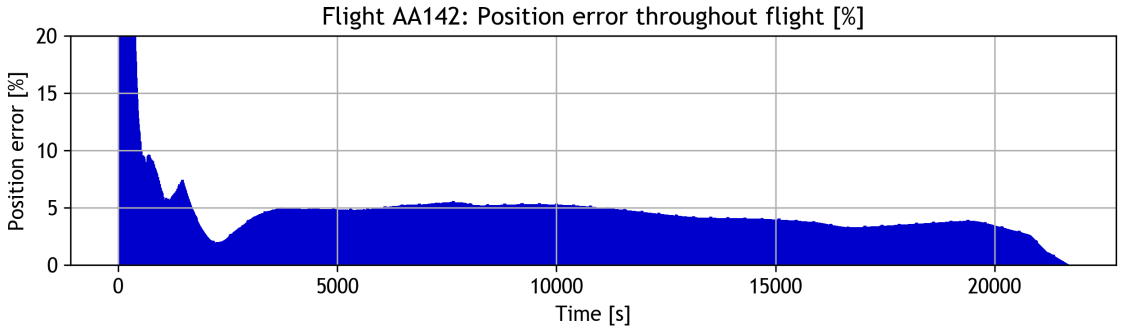

Figure 4.31: Flight AA142 (C) percentage distance error throughout flight.

Table 4.6: Percentage distance error [%].

	Flight AA97 (A)	**Flight UA632 (B)**	**Flight AA142 (C)**
Mean	15.32	5.94	6.30
Median	13.47	3.34	4.46
Standard deviation	27.54	45.50	23.63
Maximum	712.52	1875.35	922.98
Minimum	0	0	0

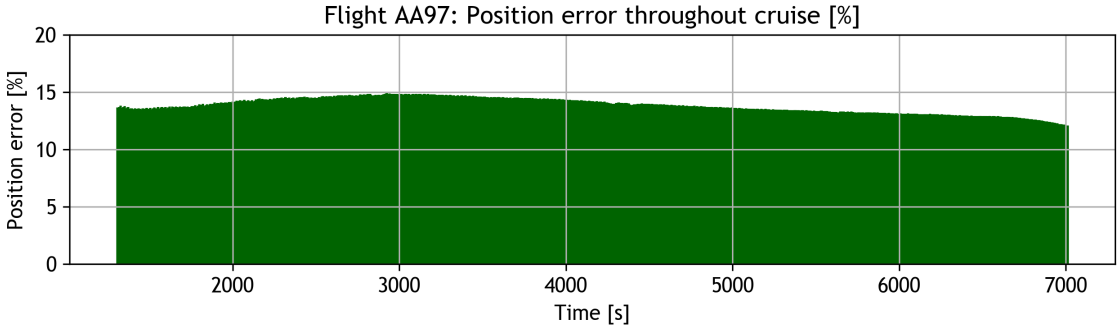

Figure 4.32: Flight AA97 (A) percentage distance error throughout cruise.

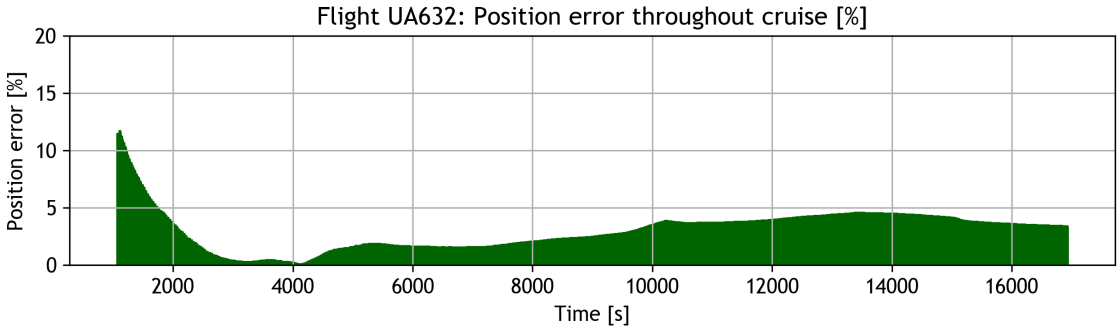

Figure 4.33: Flight UA632 (B) percentage distance error throughout cruise.

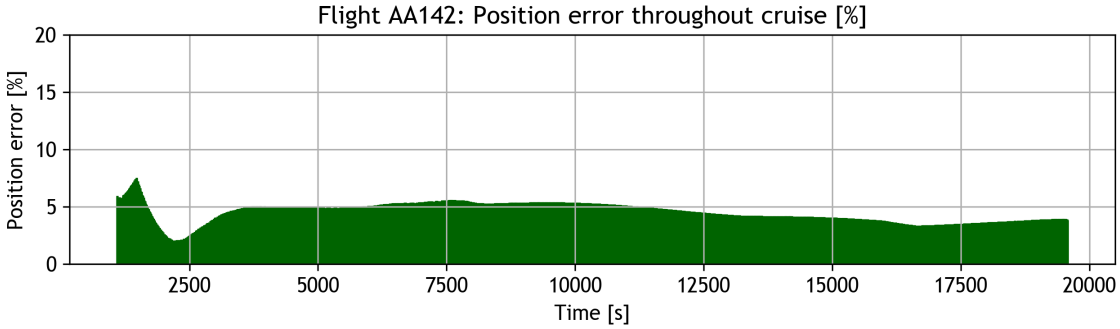

Figure 4.34: Flight AA142 (C) percentage distance error throughout cruise.

Table 4.7: Percentage distance error for the cruise phase [%].

	Flight AA97 (A)	**Flight UA632 (B)**	**Flight AA142 (C)**
Mean	13.77	2.98	4.45
Median	13.77	3.40	4.63
Standard deviation	0.68	1.75	0.86
Maximum	14.83	11.76	7.46
Minimum	12.00	0.08	1.97

Table 4.8: General validation results.

	Flight AA97 (A)	**Flight UA632 (B)**	**Flight AA142 (C)**
Flight time difference from actual flight	+6.58 minutes (+4.67%)	-2.63 minutes (-0.84%)	-10.77 minutes (-3.06%)
Flight time difference from actual flight average	+1.58 minutes (+1.08%)	-11.63 minutes (-3.61%)	+6.77 minutes (+1.84%)
Speed difference average	9.35 m/s	-2.04 m/s	7.02 m/s
Absolute distance average	88.82 km	61.90 km	113.90 km
Percent distance average for the whole flight	15.32 %	5.94 %	6.30 %
Percent distance average for the cruise phase	13.77 %	2.98 %	4.45 %
Takeoff distance error (relative to average)	-252 m (-14.4 %)	-119 m (-6.3 %)	-154 m (5.3 %)
Landing distance error (relative to average)	119.9 m (8.2 %)	-134.5 m (-9.6 %)	-251.11 m (-14.8 %)

These graphs represent the culmination of all errors previously discussed in this chapter. Although the absolute distance differences are somewhat small, each flight's length must also be taken into account. The first set of graphs represent the absolute distance between the real and simulated aircraft from the beginning to the end of the flight. The second set represents the relation between that distance and the total distance traveled so far into the flight. As expected during the initial part of the flight this comparison is very uneven due to the small traveled distance that highly exacerbates this relation. For this reason, both the overall flight and the cruise phase alone were analyzed separately. Although the absolute distance between aircraft generally tends to increase with time, the percentile error does not show the same tendency, oscillating only slightly along the flight.

The overall most accurate flight regarding position along time was flight B with 5.94% of error percentile mean and 61.9 km of absolute mean error. Flight C was less accurate when it comes to position with a 6.3% percentile error and average 113.90 km absolute error mean, which is understandable given the significantly longer flight trajectory. Flight A was the most inaccurate with a 15.32% percentile error and a 88.82 km absolute distance error despite being significantly shorter than the other flights. These differences can be attributed to the large average speed difference error (9.35 m/s) that was probably due to strong wind differences. Flight A was also the flight that had the biggest wind impact, accounting for 20.06% of the flight's duration (compared to flight's B 11.79% and flight's C -5.95%, as seen in the previous chapter), which exacerbates the wind's effect on the overall errors. The percent distance average for the cruise flight is smaller than for the whole flight, mostly due to the climb and descent phase's inaccuracies and the high error during the initial stages of flight.

Regarding flight time, flight B was curiously both the most accurate in this specific flight case with 0.84% relative and a 2.63 minutes absolute error, but also the most inaccurate when comparing flight time average rather than the specific case, at 3.61% relative and 11.63 minutes absolute error. This could be due to seasonal wind differences that are not taken into account

with the flight time average duration. Flight A was the most inaccurate in this specific case with an error of 4.67%, however it was the most accurate flight when compared to the average values with only 1.08% error, which further demonstrates the possibility that this specific flight case had a high chance of unusually strong wind impact.

The takeoff and landing distances error may be due to many different factors, such as lack of information regarding exact values for brake and runway attrition coefficients and, for landing, reverse thrust values.

Chapter 5

Conclusion

The main aim of this study was to create and validate a trajectory prediction tool and to simulate and analyze actual flights. These objectives were accomplished despite some difficulties encountered, as is to be expected with work of this kind. Trajectory prediction in general can take into account a very large number of variables to increase prediction reliability, and it is not feasible to incorporate all of them. The selection of which parameters to incorporate and develop was one of the main difficulties as it is not always easy to evaluate their impact on the overall reliability of the prediction. A balance had to be encountered between simulation complexity, accuracy and speed. With this in mind we can further analyze the results obtained and determine what can be done to improve the prediction reliability.

A huge difficulty that is often somewhat dismissed in trajectory prediction tools is the effect of the atmosphere, more specifically the wind speed variation. The initial idea was to implement a simple wind shear model. However, this proved to be highly inaccurate for high altitudes and it cannot take into account the large effect of geographical position, wind direction and seasonal differences. The solution was to implement a sufficiently accurate and dense wind speed database. The database used was chosen due to its large density of information, both in position and in time. However even this database proved to be slightly inaccurate in certain regions. The only way to improve this area is to use real values of wind direction and intensity along the flight's path, possibly from ADS-B systems, similar to the ones used by Flightradar. This would drastically decrease the trajectory error associated with wind speeds, which is one of the largest and most unpredictable error contributors as seen in the previous section.

Another large error contributor are maneuvers throughout the flight, especially separation and approach maneuvers. Regarding separation maneuvers these are hard to anticipate since they depend on external influences. One way to better improve this aspect is to statistically analyze a certain flight and determine what are the average separation maneuvers for that specific flight. Another much more complex solution would take into account all possible flights that could intercept the current flight and try to emulate the separation maneuvers that would be conducted in a real life setting. As for the approach maneuvers, another statistical study could be conducted to determine what's the average loiter time for landing (if any) for specific flights or airports and the common approach trajectory for that flight.

One of the most obvious error contributors are aircraft model inaccuracies and simplifications. Given the complexity of aircraft flight a strong simplification is needed, which enables the calculation of the forces involved. A more sophisticated aircraft model would definitely increase reliability; however, it would have to be adapted for each individual aircraft and would result in an overall high complexity increase. More accurate aircraft specific information, such as aircraft stability derivatives and thrust lapse rate would also increase reliability, although official values are hard to encounter, meaning an estimation study would be required for each aircraft.

The overall result was satisfactory given the complexity of such a field. However, in order to provide accurate trajectory prediction that could be successfully employed, for example, in the NextGen or SESAR programs a lot of work and new sources of accurate information would be required.

Future works should focus on increasing the trajectory predictor's accuracy and fidelity. This may be done in different ways such as applying a more thorough and detailed aircraft dynamical model with a larger set of aircraft specific information retrieved from, for example, Eurocontrol's base of aircraft data (BADA). The usage of actual atmospheric prediction values instead of average historical values would highly reduce the uncertainty of the weather system on aircraft prediction, despite this being hard to implement on a global scale. Acquiring precise intent information for each flight could greatly reduce the intent associated error, although this is not always possible as it partly depends on unpredictable circumstances. Finally, a different approach to the prediction of separation and approach maneuvers, such as taking into account possible proximity conflicts with other aircraft, is crucial for accurate vertical modeling prediction throughout the flight.

Bibliography

[1] A. Philbin. (2017) Traffic growth and airline profitability were highlights of air transport in 2016. [Online]. Available: https://www.icao.int/Newsroom/Pages/traffic-growth-and-airline-profitability-were-highlights-of-air-transport-in-2016.aspx (Date last accessed 29-September-2017). 1

[2] "Concept of operations for the next generation air transportation system, version 3.2," FAA, Washington DC, Tech. Rep. 0704-0188, sept 2011. 1, 6, 9

[3] L. Stridsman, "Sesar concept of operations step 1," SESAR, Brussels, Tech. Rep. DEC-TR-506, may 2012. 1

[4] R. Lyons, "Complexity analysis of the next gen air traffic management system: Trajectory based operations," *IOS Press*, p. 4514–4522, 2012. 1

[5] (2017) Annual growth in global air traffic passenger demand from 2005 to 2017. [Online]. Available: https://www.statista.com/statistics/193533/growth-of-global-air-traffic-passenger-demand/ (Date last accessed 29-September-2017). 1

[6] "Python language reference," Python Software Foundation. [Online]. Available: https://www.python.org/ 2, 36, 43

[7] "Kivy - open source python library for rapid development of applications that make use of innovative user interfaces, such as multi-touch apps," Kivy Organization. [Online]. Available: https://kivy.org 2

[8] (2017) Ncep/ncar reanalysis monthly means and other derived variables. [Online]. Available: https://www.esrl.noaa.gov/psd/data/gridded/data.ncep.reanalysis.derived.html (Date last accessed 29-September-2017). 2, 15

[9] (2001) Civil jet aircraft design data sets. [Online]. Available: http://booksite.elsevier.com/9780340741528/appendices/default.htm (Date last accessed 29-September-2017). 2, 19, 32

[10] L. R. Jenkinson, D. Rhodes, and P. Simpkin, *Civil jet aircraft design*. Butterworth Heinemann, 2003. 2

[11] (2017) Eurocontrol aircraft performance database. [Online]. Available: https://contentzone.eurocontrol.int/aircraftperformance/default.aspx? (Date last accessed 29-September-2017). 2, 17, 18, 19, 33

[12] "Action plan 16: Common trajectory prediction capability," FAA and EUROCONTROL, Tech. Rep. AP-16, sept 2004. 3, 4, 5

[13] J. Henderson, R. Vivona, and S. Green, "Trajectory prediction accuracy and error sources for regional jet descents," in *AIAA Guidance, Navigation, and Control (GNC) Conference, Boston, USA*, 2013. 5

[14] G. Enea, , and M. Porretta, "A comparison of 4d-trajectory operations envisioned for nextgen and sesar, some preliminary findings," in *28th International Congress of the Aeronautical Sciences, Brisbane, Australia*, 2012. 5, 9, 12

[15] R. Jehlen, “Trajectory based operations (tbo) concept of operations,” ICAO ATMRPP, Tech. Rep. ICAO/ATMRPP WG/27 WP/644, oct 2014. 6, 11

[16] K. Bousson and P. Machado, “4d trajectory generation and tracking for waypoint-based aerial navigation,” vol. 8, pp. 105–119, jan 2013. 6

[17] K. Bousson and T. Gameiro, “A quintic spline approach to 4d trajectory generation for unmanned aerial vehicles,” *International Review of Aerospace Engineering (IREASE)*, vol. 8, no. 1, 2015. 7

[18] B. Musialek, C. F. Munafo, H. Ryan, and M. Paglione, “Literature survey of trajectory predictor technology,” U.S. Department of Transportation, FAA, Washington DC, Tech. Rep. DOT/FAA/TC-TN11/1, nov 2010. 7

[19] D. Boyle and G. Chamitoff, “Robust nonlinear lasso control: A new approach for autonomous trajectory tracking,” Reston, Va., 2003. 8

[20] “Nextgen implementation plan,” NextGen, Washington DC, Tech. Rep., 2016. 8

[21] E. Ulfbratt and J. McConville, “Comparison of the sesar and nextgen concepts of operations,” NCOIC, Tech. Rep., may 2008. 8

[22] (2015) Fact sheet – nextgen. [Online]. Available: https://web.archive.org/web/20150403151639/http://www.faa.gov/news/fact_sheets/news_story.cfm?newsid=8145 (Date last accessed 29-September-2017). 8

[23] (2017) Metroplex: Improving traffic flow in complex airspace. [Online]. Available: https://www.faa.gov/nextgen/snapshots/metroplexes/ (Date last accessed 29-September-2017). 10

[24] (2017) Automatic dependent surveillance–broadcast. [Online]. Available: https://www.faa.gov/nextgen/update/progress_and_plans/adsb/ (Date last accessed 29-September-2017). 10

[25] (2017) In-trail procedures: Saving fuel and boosting pilots’ situational awareness in oceanic airspace. [Online]. Available: https://www.faa.gov/nextgen/snapshots/stories/?slide=52 (Date last accessed 29-September-2017). 10

[26] (2017) About single european sky. [Online]. Available: https://www.sesarju.eu/background-ses (Date last accessed 29-September-2017). 10, 11

[27] “The roadmap for delivering high performing aviation for europe european atm master plan - edition 2015,” SESAR, Tech. Rep. MG-04-15-465-EN-N, 2015. 11

[28] “Introduction to the sesar 2020 programme execution [edition 01.00.00],” SESAR, Brussels, Tech. Rep., apr 2015. 11

[29] (2017) About vision. [Online]. Available: https://www.sesarju.eu/vision (Date last accessed 29-September-2017). 11

[30] R. Raposo, “Topflight b1 demonstration report,” SESAR, Tech. Rep. 02.07, sept 2014. 12

[31] (2017) Topflight project final report. [Online]. Available: https://www.sesarju.eu/newsroom/brochures-publications/topflight-project-final-report (Date last accessed 29-September-2017). 12

[32] “Operational performance assessment,” NextGen, Washington DC, Tech. Rep., 2016. 13

[33] (2002) Wind vector notation conventions. [Online]. Available: http://mst.nerc.ac.uk/wind_vect_convs.html (Date last accessed 29-September-2017). 15

[34] (2010) Flight phase taxonomy. [Online]. Available: https://www.skybrary.aero/index.php/Flight_Phase_Taxonomy (Date last accessed 29-September-2017). 17

[35] R. Mayer, “A flight trajectory model for a pc-based airspace analysis tool,” Reston, Va., 2003. 17

[36] (2016) Airport, airline and route data. [Online]. Available: https://openflights.org/data.html (Date last accessed 29-September-2017). 20

[37] E. Williams. (2012) Aviation formulary v1.46. [Online]. Available: https://www.flightradar24.com (Date last accessed 29-September-2017). 21

[38] W. Gellert and V. N. R. Company, *The VNR concise encyclopedia of mathematics*. Van Nostrand Reinhold Co., 1977. [Online]. Available: https://books.google.pt/books?id=Gx4yAAAAIAAJ 21

[39] *Environmental Technical Manual*, ICAO. 25

[40] Y. S. Chati and H. Balakrishnan, “Aircraft engine performance study using flight data recorder archives,” in *2013 Aviation Technology, Integration, and Operations Conference*, Los Angeles, CA, 2013. 25

[41] H. Vermeille, “Direct transformation from geocentric coordinates to geodetic coordinates,” *J. Geodesy*, vol. 76, no. 8, pp. 451–454, nov 2002. 28

[42] J. Park, D. Evans, K. Murugesan, S. Sekar, and V. Murugesh, “Optimal control of singular systems using the rk-butcher algorithm,” *INT. J. COMPUT. MATH.*, vol. 81, no. 2, pp. 239–249, 2004. 29

[43] (2017) Flightaware. [Online]. Available: https://flightaware.com/ (Date last accessed 29-September-2017). 31

[44] J. D. Hunter, “Matplotlib: A 2d graphics environment,” *Comput. Sci. Eng.*, vol. 9, no. 3, pp. 90–95, 2007. 36, 43

[45] (2017) Flight radar. [Online]. Available: https://www.flightradar24.com (Date last accessed 29-September-2017). 43

Appendix A

Submitted article

F. Lucas and K. Bousson, “Simulation of 4D trajectory navigation”, submitted to Proceedings of the Institution of Mechanical Engineers, Part G: Journal of Aerospace Engineering, October 2017.

Simulation of 4D trajectory navigation

Journal Title
XX(X):1–16

DOI: 10.1177/ToBeAssigned
www.sagepub.com/
SAGE

Francisco Lucas[1], Kouamana Bousson[2]

Abstract

An algorithm to accurately predict 4D trajectory navigation was developed alongside a graphical user interface (GUI) to allow the easy simulation of several trajectories with different parameters. Several simulations were conducted using this tool which were then analyzed and compared with actual flight values in order to validate its accuracy. The need for such a tool emerges from the ever increasing demand regarding the air transportation system, that is expected to maintain positive growth rates up until 2030. The programs of SESAR in Europe and NextGen in the USA were initiated to respond to this need and at their heart lies the implementation of 4D trajectories. A point-mass kinetic model was chosen to simulate the aircraft's movement, as it provides sufficiently accurate results without requiring too much aircraft specific information. A database containing the information of several large turbofan commercial aircraft was compiled. In order to model the effect of the weather on the simulation, a large world wide historical weather database was incorporated into the tool. The intent information required for simulation is the flights course (in waypoints) and some flight phase specific parameters. The tool was created using the Python programming language and the open source library for GUI development Kivy. Three actual flights were simulated and their performance was analyzed. A comparison between the simulated and the actual flight's values was made in order to validate the tool's accuracy. The results were satisfactory with the three flights averaging a 2.27% error regarding average flight duration as well as a 9.19% median error regarding the aircraft's position throughout the flight. Overall the tool proved to be satisfactorily accurate given the amount of possible error sources for flight trajectory prediction however, further improvements are important for implementation in active air traffic management systems.

Keywords

4D-Trajectories; Trajectory navigation; Trajectory simulation; Graphical User Interface

Introduction

Motivation and goals

The global air transportation system is a cornerstone of the world's economy, that in turn is constantly growing. According to ICAO there was a 6% increase of the number of passengers carried on scheduled services in 2016, reaching the 3.7 billion mark. The previous year's relative growth was even more impressive at 7.1%. As a matter of fact, air traffic has sustained an almost constant growth in the last decade, and is expected to maintain positive growth rates up to 2030 (1). However, in order to accompany this constant growth in a sustainable manner the Air Traffic Management (ATM) systems in use today must be updated and drastically transformed. At the heart of this transformation lies the change from clearance based Air Traffic Control (ATC) operations in use today, to trajectory based operations. Trajectory based operations require a change of mentality when it comes to the definition of aircraft trajectories. The implementation of 4 dimensional trajectories (4DT), which are trajectories defined in both time and space, will allow air traffic controllers to properly predict the effect that a disturbance in the air traffic flow will have in the near future, which when combined with the ability to accurately predict trajectories will permit optimal correcting actions to be done accordingly (2) (3) (4). Therefore the ability to predict aircraft trajectories is crucial to properly optimize the ever more complex ATM systems in use today.

The main goal of the present work is to create a tool for aircraft trajectory prediction (TP) and analysis and to use it to study a number of 4D trajectories of certain aircraft. This tool may also be used, to some extent, to study or compare aircraft performance. The tool focuses on large civil transport turbofan powered aircraft. There was a significant effort placed in making the tool user friendly so that it may be used and improved upon by future users.

The TP tool was created using the Python programming language, version 3.4 (5). It contains a graphical user interface (GUI) created with the use of the cross-platform framework for GUI development Kivy, version 1.9.1 (6). The TP tool also contains

[1]Aeronautical Engineering Student in the Department of Aerospace Science at University of Beira Interior, Covilhã, Portugal.
[2]Professor in the Department of Aerospace Science at University of Beira Interior, Covilhã, Portugal.

Corresponding author:
K. Bousson, Calçada Fonte do Lameiro, 6201-001 Covilhã, Portugal.
Email: bousson@ubi.pt

databases containing atmospheric information derived from historical data sets made available by the National Oceanic and Atmospheric Administration (NOAA) (7). A database containing the information of several aircraft was also compiled, which includes both flight phase dependent information as well as actual aircraft characteristics. This information was mainly obtained from the online data set appendices (8) of the book Civil Jet Aircraft Design (9) and from Eurocontrol's vast aircraft performance database (10).

Fundamentals

The main goal of a trajectory predictor is to be able to accurately describe an aircraft's state and position during flight from its initial position to its final destination. Despite existing several different and valid approaches to building a trajectory predictor almost all of them share the following components (11):

1. Initial condition: The aircraft's initial condition must always be included, regardless of the complexity of the used model. The actual parameters necessary will depend on the the used model type.
2. Intent or trajectory information: The information regarding the aircraft's desired trajectory or flight plan can be included in several different forms, but it must always be present. It may come in the form of a full control setting schedule, a flight plan or simply a projection of the state vector with fixed heading and speed. Other important information can also be included such as operational procedures that are flight phase dependent or certain restrictions such as maximum speeds or altitudes.
3. Environmental information: Given the very significant impact of external environmental factors on a flights trajectory they should always be included, even if in simple formats. The most important parameter of this kind is wind velocity.
4. Aircraft information: Relevant aircraft information such as weights or thrust modeling is usually included even if in simple formats. Alternatively some models use fixed speed values for certain phases.

The initial steps of a trajectory predictor involve the treatment of the given information and is usually referred to as the preparation process. A common way to express the flight plan is by a list of waypoints, which are simply named geographical positions. These positions must be processed and converted to actual geographical points in Cartesian or geodetic coordinates before the simulation start, which is known as route conversion. After completing the route conversion the initial intent for the aircraft must be calculated which will depend on the aircraft's initial state. This mechanism is usually known as lateral path initialization. Other steps may also be required depending on the complexity of the predictor such as getting the initial environmental state or applying certain constraints.

Following these initial steps lies the core of trajectory prediction which will take into account the aircraft's current state, follow appropriate aircraft dynamics while considering environmental and aircraft-specific information as well as any other simulation specified constraints to obtain the next aircraft state. The final result will be the aircraft's state and position expressed as a function of time from start to finish.

Dynamical models

Trajectory predictors can employ several types of dynamical systems which in turn require different types of intent or aircraft specific information. Although certain models demonstrate higher fidelity than others the TP accuracy is not solely dependent on the dynamical model used, it highly depends on the input data reliability and the consideration of many operational conditions. Keeping this in mind the following are the most commonly used dynamical systems from the most to the least accurate (11).

1. Six degree of freedom model - This model takes into account the forces and moments that affect the airframe along all axes of motion. These moments are dependent on the aircraft's state and control settings and therefore require knowledge of the control laws that govern the aircraft. This method requires accurate working relationships between the moments and the aircraft's state and control input, normally obtained from the aircraft's manufacturer which often proves difficult to acquire.
2. Point mass model (kinetic) - Unlike the previous model this approach considers the aircraft as a single point and requires only the modeling of the resulting longitudinal forces, thrust and drag, assuming the lift normally compensates the weight. The main difficulty of this method is acquiring information reliable enough to accurately calculate the thrust and drag in different operational conditions. The engines SFC (specific fuel consumption) is also an important parameter to calculate fuel spent as a function of thrust and time. This method provides accurate information for regular large commercial aircraft flights where straining maneuvers are not very common and therefore the calculation of moments is of less importance.
3. Macroscopic model (kinematic) - This simplified model does not calculate the forces acting on the aircraft, therefore being a kinematic approach. It instead uses constant, predetermined fixed values for various parameters that are often flight phase dependent, such as climb/descent rate, accelerations and others that may, for example, be a function of altitude. The main advantage of this model is that it does not require thrust and drag data and can instead use average values from known flights, which in many cases are readily available. This approach is of relatively easy implementation and can provide

acceptable results for already well established flights. However, it lacks flexibility since it requires accurate values for each individual flight phase.

Error sources

Although errors or simplifications of the used TP dynamical model account to significant inaccuracies, there are other outside error sources that are very significant, of which the most significant ones are described below (11) (12).

1. Inaccurate initial condition errors due to, for example, sensor errors or simple lack of detail in communication.
2. Errors in atmospheric models or forecasts.
3. Several types of missing intent information such as separation or approach maneuvers, unreliable course waypoints or inaccurate target speeds. Very often this type of intent information is simply not known before the flight (or not properly communicated) and therefore cannot be used for ground trajectory prediction. Many times, even in-flight trajectory prediction may suffer from this problem when, for example, path changes issued by voice are not inputted into the system.
4. Path deviation will always occur to some extent, when the aircraft deviates from the predicted lateral path.

4D trajectories and trajectory based operations

A 4D trajectory offers precise information about an aircraft's flight path in both space and time, while also taking into account some position uncertainty. These trajectories have different levels of specificity depending on their implementation, but most of them use a system of waypoints specified in latitude and longitude, as well as altitude and, of course, time. The time variable however is somewhat flexible to compensate for uncertainties such as wind speeds or airport queue times. Some trajectories employ controlled time of arrivals (CTA's) which are a system of time windows to cross several waypoints in order to have extra control on traffic flow (13).

Trajectory based operations (TBO) are based on the notion of 4D trajectories and on the planning and execution of those trajectories in a broad, strategical, sense. In a more specific, tactical sense TBO include the adjustment and evaluation of individual trajectories to ensure a synchronized, efficient and safe access to the airspace taking into account weather, environmental, defense, security and departure/arrival airport constraints. These individual trajectories are often combined into aggregate flows and are generated, negotiated and managed by ATM systems. This system allows the reduction of overly conservative and non-optimal actions, without compromising security. With proper integration, it also takes into account the airlines, aircraft's or flight crew's specific needs and limitations and tailors the generated trajectories to their needs and preferences. When conflicts that require controller interference do arrive, they will be controlling the overall flow of traffic instead of an individual aircraft taking into account not only the immediate effects on traffic, but the long term effects as well. This system also allows for efficient high density arrival/departure operations, improving airport efficiency and capacity at times of peak demand. Current aircraft separation operations are managed by air traffic controllers using radar screens to visualize current trajectories and making operational judgments to resolve conflicts, however further use of TBO will change this process by inserting a much higher degree of automation and support for these maneuvers and in some cases it may be possible to delegate the separation maneuvers to the aircraft's crew. The main benefits of TBO are the following (2) (14):

1. Capacity increase - Proper and global use of TBO will allow a very significant increase in capacity of the airspace, even in high traffic regions. The combination of proper trajectory planning that takes into account all requirements of the users will allow access to more of the airspace more of the time. Part of this capacity increase comes from the reduction of excessive separation without compromising security, thanks to the predictability of the system. High-density arrival/departure procedures will also highly benefit from this system.
2. Efficiency and environment - The operational management of TBO allow for a much more efficient control and spacing of flights, which will result in more consistent flight schedule integrity. In departure/arrival zones this increase in predictability and efficiency will allow an increased use of noise sensitive flights paths. While the increased efficiency will reduce fuel consumption the superior predictability will allow for a closer to optimal fuel loading.
3. Reduced cost per operation - After the initial implementation cost TBO will increase air service providers overall productivity which will result in a general reduction of per-operation costs.

Previous works

There has been great activity in the past few years regarding trajectory prediction due to the development of the NextGen and SESAR programs and their innovations regarding flight management systems (FMS) and Automatic Dependent Surveillance – Broadcast (ADS-B) capabilities that provide accurate details useful for trajectory prediction. Most existing trajectory predictors are used as a tool to be employed within the Air Traffic Management system to facilitate both automation and decision making. Aircraft separation is an especially important component that depends on decision making. Existing algorithms to predict aircraft separation and associated conflicts are mostly simplified and consider the aircraft to have constant altitude, velocity and acceleration however, effort is being made to accurately predict conflicts regarding aircraft with transitioning altitudes. From an extensive literary review (15), it was observed that

the majority of papers in this field are concerning lateral, longitudinal and vertical profiles as well as flight plan and surveillance. Out of the 282 papers reviewed 20 of them shown special promise due to their innovative approaches in the areas of holding, modeling turns, vertical modeling and general mathematical flight models. Despite this, there are many sub themes related to the global trajectory prediction theme that have been the subject of research. The vast majority of these papers focused on methods for estimating flight state variables, and not TP as a whole. The broadcasting of real time meteorological data combined with on board sophisticated flight systems was the major driver for a great part of these works, as well as the shift toward autonomous flight rules when, for example, aircraft separation could be handled by the crew and not by an air traffic controller, which would require great TP capabilities combined with somewhat autonomous conflict handling. When it comes to the mathematical models used, the majority of them were of the point-mass type, mostly due to the reasons disclosed in the previous chapter. Another somewhat common model was the kinematic model, that does not calculate forces and focuses only predefined values. A full sin degree of freedom model was only found once (16) despite being the most accurate if employed correctly. The majority of existing papers on this subject are of the academic level which is reflected on their low levels of maturity, since it requires many resources and years of research, prototyping, testing and validation for these concepts to be introduced in the operational system. Despite the tendency of moving some of the responsibility of aircraft separation from the ground to the cockpit the air traffic controller is still, and will remain to be, the final decision maker to such procedures, hence the need to track aircraft during all stages of flight. It is obvious that TP has greatly benefited from modern computer capabilities and the availability of accurate data that allows TP tools to take into account different aircraft performances as well as other external factors such as weather and separation requirements. This results in a direct increase of TP fidelity that can lead to a lesser separation standard and the resulting increase in overall flight space capacity and flight delay reduction. Some future areas of research that could prove to be very beneficial are vertical modeling, hold modeling and models of closure rates may improve overall TP and conflict resolution fidelity.

Methods and Algorithms

Weather model

The unpredictability of the weather system presents a real difficulty when it comes to trajectory prediction. Without resorting to real weather data of the specific time and place (which is very hard to acquire given the altitude of commercial flights) the second-best option is to utilize historical values or to use a prediction model. However, unlike temperature and atmospheric pressure the relation between wind speed and altitude is hard to be modeled at high altitudes as it depends widely on geographical position and other factors. Given the difficulties of implementing an accurate wind model and of acquiring accurate weather values for the specific date and place of the flights, the best solution was found to be the use of reliable historical values. The weather database employed requires to have wind velocity information of different altitudes as well as geographical positions. Another important factor is the ability to access data relative to different times of the day and year. The database employed was NCEP/NCAR (National Center for Environmental Prediction and National Center for Atmospheric research) Reanalysis 1: pressure, made available by NOAA (National Oceanic and Atmospheric Administration) (7). This database provided all the required information in various, easily accessible, netCDF4 format files. The available variables and temporal/spatial coverage was ideal as can be seen by its relevant characteristics in below.

1. **Variables used**: Air temperature, uwind, vwind*
2. **Temporal coverage**: 4 times daily values from January 1, 1948 to the present
3. **Spatial coverage**: 2.5x2.5 degrees global grid (144x73 resolution)
4. **Altitude Levels**: 17 pressure levels from 1000 mb to 10 mb

This database was made possible by the cooperation between the NCEP and the NCAR in creating this project that comprises a long record of global analysis of atmospheric fields to support climate monitoring communities. The data utilized on this project was recovered from land surface devices, ship, rawinsonde (radiosondes tracked by a radio direction finding device to determine wind velocity), pibal (also known as ceiling balloon or pilot balloon), aircraft, satellite and other sources. The data assimilation system employed eliminates perceived climate jumps associated with changes in the data assimilation system. This database has shown to be especially accurate near and around mainland USA, mainly due to the larger availability of information sources in this area. Given its very large temporal and spatial density, in order to make the database file size smaller and faster to process a new database was derived by calculating the average variable value of each month at the 4 available times of day (6 hours apart). This allowed to vastly reduce the file size while also allowing the user to choose the approximate time of day and month of the flight.

Flight phase explanation

There are several accepted terms for each flight phase, that depend on their use as well as the organization that defined them. The flight phase terminology and definition used for the TP tool were adapted from

*Where uwind is the U component of the wind that is positive for a west to east flow (eastward wind) and vwind is the V component of the wind that is positive for a south to north flow (northward wind) (17).

IATA's (International Air Transport Association) taxonomy (18), ICAO's (International Civil Aviation Organization) Accident/Incident Data Reporting (ADREP) system (18) as well as Eurocontrol's flight phase definition as used on their aircraft performance database (10). The adapted BADA flight phases as defined in (19) were also used. Each different flight phase requires several parameters for an accurate simulation such as target speed, target altitude or climb/descent rates. These values will always be respected unless it is not possible to do so. All climb and descent phases have a pre-determined thrust setting that will be maintained constant unless it must be altered in order to, for example, respect speed constraints, target altitudes or rates of climb/descent. The used terminology for each flight phase is the following:

1. **Takeoff**: This phase combines both the takeoff roll as well as the rotation and the takeoff phases. This phase's thrust setting is constant at the maximum value. The parameters this phase requires are rotation speed and initial obstacle altitude. The phase ends when the initial obstacle altitude is reached.
2. **Initial Climb**: During the initial climb the thrust setting is set to be slightly less than the maximum value in order to minimize the increased stress the engines are subject to at maximum power setting. This phase is the steepest of all climb phases and lasts until its target altitude is reached. It requires initial climb target speed, altitude and rate of climb.
3. **On Course Climb**: The on course (or en route) climb starts when the aircraft has reached a high enough altitude to safely proceed "on course" to its target destination. It requires on course climb target speed, altitude and rate of climb.
4. **Secondary Climb**: The secondary climb is a continuation of the en route climb, that is usually slightly less steep. It requires secondary climb target speed, altitude and rate of climb.
5. **Mach Climb**: The mach climb (also called cruise climb) is the final climb phase before reaching cruise altitude, and its generally the smoothest of all climb phases. Usually most altitude related airspeed restrictions no longer apply at this altitude so the aircraft will accelerate to high speeds, close to cruising speed. As the altitude increases it is necessary to gradually reduce the flight path angle in order to ensure a close to constant speed. This phase requires mach climb target Mach number, altitude and rate of climb.
6. **Cruise**: During cruise the aircraft is leveled off and unlike the previous phases it's power setting is adjusted to maintain the cruise phase desired speed. The cruise phase ends when the aircraft is close enough to the airport as to ensure a smooth descent. This phase requires target Mach number and distance from airport to initiate descent.
7. **Initial Descent**: At the start of the initial descent the power setting will be set to idle and a descending flight path is taken. This phase is usually flown at high, close to cruise, speeds. It requires target Mach number, altitude and rate of descent.
8. **Main Descent**: During this phase it is sometimes required for the aircraft to level off to slow down to its target speed. Once a certain altitude has been reached it is safe to extend flaps, which are crucial to reach safe approach and landing speeds. This phase requires target speed, altitude and rate of descent.
9. **Approach Descent**: The final descent phase is also set to be flown at idle power, however it is often required to slightly increase power for approach maneuvers. During this phase it is essential to reduce the aircraft's speed to a safe speed for landing. This phase requires approach descent target speed.
10. **Landing**: During landing the aircraft is leveled off and its thrust is set to reverse mode. The simulation ends when, during this phase, the aircraft's speed reaches zero.

Aircraft information

The aircraft information employed is divided in two main areas: aircraft parameters and aircraft flight plan typical values. The aircraft parameters were mostly retrieved from the book Civil Jet Aircraft Design data sets that contained accurate information regarding the majority of large civil transport aircraft in use today (8). The aircraft typical flight plan values were retrieved from Eurocontrol's Aircraft Performance database (10). Using these sources a database of several aircraft was created and included on the TP tool, allowing the user to easily simulate several civil transport aircraft in use today. In order to contain this information the JSON (JavaScript Object Notation) file format was chosen due to its lightweight and simplicity of use, as well as its capabilities of being both easily readable and writable for humans and for machines to parse and generate. The tool also allows the user to create a new aircraft entry based on existing entries or to create a completely new entry.

Table 1. Required aircraft parameters for simulation.

Parameter name	Parameter type
Maximum take-off weight [kg]	Weights
Fuel Weight [kg]	Weights
Number of engines	Engines
Maximum sea level thrust [N]	Engines
Take-off SFC [kg/s/N]	Engines
Cruising SFC [kg/s/N]	Engines
Engine idle thrust percentage	Engines
Wing span [m]	Dimensions
Wing surface area [m^2]	Dimensions
Flap to wing span ratio	Dimensions
Takeoff lift coefficient	Aerodynamic
Maximum lift coefficient	Aerodynamic
Parasitic drag coefficient	Aerodynamic
Never exceed speed (V_{NE}) [m/s]	Safety
Maximum flight path angle [°]	Safety

Waypoint determination

The TP tool allows the user to simulate flight solely between a starting and a finishing waypoint and also to simulate a trajectory between a larger number of given waypoints, while calculating intermediate waypoints between them as needed, in order to approach the path to a orthodromic trajectory between intermediate waypoints. In order to approximate the trajectory between two given points to a orthodromic one, intermediate waypoints are calculated on a great circle (or orthodrome) between those two points. The amount of waypoints calculated depends on the position of the two original waypoints. The algorithm below calculates the latitude and longitude of a point between the two given points that is at a fraction of the total distance between them on the same orthodrome. The only requirement is that the initial points are not antipodal, as that would cause the route to be undefined. In the algorithm below f is the fraction of the distance between the given points, d is the distance in degrees between the given points, λ_x and φ_x are the latitude and longitude of the given points and finally λ_f and φ_f are the coordinates of the calculated intermediate points (20).

1. A:
$$A = \frac{sin(d(1-f))}{sin(d)} \tag{1}$$
2. B:
$$B = \frac{sin(fd)}{sin(d)} \tag{2}$$
3. x:
$$x = Acos(\lambda_1)cos(\varphi_1) + Bcos(\lambda_2)cos(\varphi_2) \tag{3}$$
4. y:
$$y = Acos(\lambda_1)sin(\varphi_1) + Bcos(\lambda_2)sin(\varphi_2) \tag{4}$$
5. z:
$$z = Asin(\lambda_1) \tag{5}$$
6. Intermediate point latitude, λ_f:
$$\lambda_f = atan2(z, \sqrt{x^2 + y^2}) \tag{6}$$
7. Intermediate point longitude, φ_f:
$$\varphi_f = atan2(y, x) \tag{7}$$

The angular distance d, between the given points is calculated in the following way, where the point P is the elevated pole, A and B are the given points:

1. AB longitude variation, $\Delta\varphi$:
$$\Delta\varphi = \varphi_2 - \varphi_1 \tag{8}$$
2. Angular distance between A and P, PA*:
$$PA = 90 \pm \lambda_1 \tag{9}$$
3. Angular distance between B and P, PB*:
$$PB = 90 \pm \lambda_2 \tag{10}$$
4. C_{AB}:
$$C_{AB} = cos(PB)cos(PA) \tag{11}$$
5. Angular distance between A and B, d:
$$d = acos(cos(\Delta\varphi)sin(PA)sin(PB) + C_{AB}) \tag{12}$$

In order to determine when a intermediate waypoint is needed an iterative process determines the fraction between the initial point and the final point by calculating the Givry correction between the initial point and the would be intermediate point and comparing it to a maximum value, whose default is set to 10º. If the Givry correction is larger than the maximum value that intermediate waypoint is integrated in the trajectory path. In order to calculate the Givry correction (γ_G) between two waypoints only their coordinates are required, as can be seen below where A and B are the waypoints used:

$$\gamma_G = \frac{\Delta\lambda_{AB}}{2} sen\varphi_m \tag{13}$$

The medium latitude between points A and B (φ_m) is given by:

$$\varphi_m = \frac{1}{2}(\varphi_A + \varphi_B) \tag{14}$$

Main algorithm

In this section the main algorithm's loop will be explained step by step. Before the initiation of the loop a verification of the user input is applied, to make sure its valid. The required parameters are the aircraft characteristics described above, as well as the flight path waypoints or, at least, the initial and final waypoints. The month and time of day of the simulation, as well as attrition coefficients for the takeoff and landing phases should also be provided.

1. **Time Step Calculation**: Given the nature of commercial aircraft flights a variable time step is valuable for their efficient (fast) simulation. This is due to the long duration of the cruise flight phase when maneuvers are limited and overall speed and acceleration values are somewhat constant. Taking this fact into account a variable time step is used whose value depends mostly on the current flight phase and the distance to the target waypoint, diminishing the closest the aircraft is to the waypoint. Smaller values of time step are especially important during ground phases for accurate calculation of landing and takeoff distances.

*When calculating the angular distance of A and B from the elevated pole P (PA and PB), the mathematical operator depends on which elevated pole is selected (North or South) and on what hemisphere the points A and B are on. If the selected pole and the point's hemisphere is the same the operator is minus, otherwise its plus.

2. **Update climate state**: When the aircraft crosses the spatial grid of the weather database new values must be retrieved from it. This is done by checking the aircraft's current position and comparing it to its last position. Even if new database entries are not required, the weather database parameters are interpolated between entries to improve accuracy and to avoid sudden steep leaps in values.
3. **Available Thrust**: In this step, the maximum available thrust is calculated (at full throttle) for the current simulation state. As stated before, these simulations are based on high bypass ratio turbofan engines, since these are the most widely used for large civil transportation aircraft. These engine's thrust varies significantly with speed and altitude. Although it varies with every engine, it can be estimated by the equation below, where M is the Mach number, T_0 is the maximum available thrust at sea level and $\rho(h)$ and ρ_0 is the air density at the current altitude and at sea level, respectively. When $M < 0.1$, $M = 0.1$ should be used.

$$T_A = \frac{0.1}{M} T_0 \frac{\rho(h)}{\rho_0} \tag{15}$$

4. **Drag**: The current total drag is calculated in this step, by combining the parasitic and lift induced drag. This tool only takes into account subsonic drag since it's focus is to simulate large transport aircraft whose highest Mach numbers during cruise are usually between 0.79 and 0.86. The parasitic and induced drags are calculated below where V is the current speed, W is the aircraft weight, S is the wing surface area, C_{D0} is the parasitic drag coefficient and γ is the aircraft flight path angle.

   (a) Parasitic Drag (D_0):

$$D_0 = \frac{1}{2}\rho V^2 S C_{D0} \tag{16}$$

   (b) Induced Drag (D_i):

$$D_i = \frac{KW^2 cos^2\gamma}{\frac{1}{2}\rho V^2 S} \tag{17}$$

   (c) Total Drag (D):

$$D = D_0 + D_i \tag{18}$$

   The parameter K is the induced drag coefficient and can be calculated with the equation bellow where AR is the wing aspect ratio, e is the Oswald efficiency number and K_p is the airfoil's induced drag factor.

$$K = \frac{1}{\pi ARe} + K_p \tag{19}$$

5. **Current Thrust and Power Setting**: The way thrust and power setting is calculated in this simulation depends on the current flight phase. In phases where the power setting is constant, the current thrust is simply calculated with that power setting value (δ) and the available thrust (T_A). The power setting values range from 0 (zero thrust) to 1 (maximum thrust), although during flight the minimum power setting acceptable is the idle power setting, whose default value is set to be 0.1, but may be changed by the user. The default thrust setting values used are ICAO's standard values in the Landing and Takeoff (LTO) cycle, which were defined for aircraft emission testing (21), and are shown below. These values however, are only general approximations and sometimes differ significantly from the actual used values, which could result in a significant source of intent prediction error (22).

$$T = \delta T_A \tag{20}$$

   - Takeoff: During takeoff the power setting is constant and set to the maximum value.
   - Climb Phases: During climb the default power setting is set to slightly less than maximum value, at 0.85. It remains at this value unless more thrust is required to reach the current phase's target altitude.
   - Cruise: Unlike the previous phases the power setting during this phase is not constant or predetermined. During the beginning of cruise the thrust setting is kept at the previous phase's setting while accelerating to the cruise phase target Mach number. Once the cruise target Mach number is reached the current thrust is set to be equal to the required thrust to maintain the current Mach number, and is updated every iteration, causing a changing power setting. In other words the required thrust is approximately equal to the previously calculated drag, in order to maintain a constant Mach number as the speed of sound varies only slightly on constant altitude.
   - Descent Phases: During the descent phases the power setting is set to idle, except when the current aircraft speed is less than the phases target speed or the aircraft's stall speed. In this case the current thrust is set to the required thrust to maintain constant speed, much like during the cruise phase, except in this phase the weight component must be taken into account.
   - Landing: During the landing phase the thrust is set to reversed mode, with an arbitrary value of percentage of available thrust that is user dependent.

6. **Flight Path**: The first step to calculate the flight path angle is calculating the desired flight path, called the reference flight path. This angle is calculated based on the excess thrust, the difference between current thrust and the required thrust to maintain this phase's target speed.

$$\gamma_{ref} = asin\left(\frac{T - T_r}{W}\right) \quad (21)$$

One exception to this happens if during the start of a descent phase a deceleration is required to reach the phases target speed, in which case the aircraft is leveled (γ=0) until that speed is reached. Another exception is during the final approach phase in which the descent angle must be smoother, and is therefore calculated based on the proximity to the airport, where h is the aircraft's altitude and d_a is the absolute distance to the airport.

$$\gamma_{ref} = asin\left(\frac{h}{d_a}\right) \quad (22)$$

After calculating the reference flight path the actual angle is calculated. In order to avoid instant variations of the flight path angle it is calculated using an arbitrary maximum flight path angle rate of change. The maximum value of the flight path angle is limited by the user input maximum flight path angle.

7. **Acceleration**: The acceleration is calculated in two separate ways: on the ground (takeoff and landing) and during flight.

   - During flight:

$$a = \frac{T - D - Wsin(\gamma)}{M_a} \quad (23)$$

   - On the ground:
     - Ground induced drag compensation, ϕ: This parameter compensates the reduced induced drag due to the proximity between the ground and the wing. The parameter h_g is the distance between the wing and the ground and b is the wing span.

$$\phi = \frac{\left(\frac{16h_g}{b}\right)^2}{1 + \left(\frac{16h_g}{b}\right)^2} \quad (24)$$

     - C_{Lg}: The lift coefficient during ground acceleration or deceleration C_{Lg} is assumed to be constant at 0.8, although different values can be set by the user.
     - L_g:

$$L_g = \frac{1}{2}\rho V^2 S C_{Lg} \quad (25)$$

     - D_g: The ground drag value takes into account the flaps contribution separately with the parameter C_{d0_f}.

$$D_g = \frac{1}{2}\rho V^2 S(C_{d0} + C_{d0_f} + \phi K {C_{Lg}}^2) \quad (26)$$

     - Ground acceleration, a: Where μ is the floors attrition coefficient that has different values for landing or takeoff. These values can be set by the user, but are usually between 0.03 and 0.08 during takeoff and between 0.06 and 0,5 during landing, when brakes are taken into account.

$$a = g\left(\frac{T}{W} - \mu\right) - \frac{g}{W}(D_g - \mu L_g) \quad (27)$$

8. **Trajectory Angle**: The calculation of the trajectory angle is divided in three parts: the initial reference trajectory angle ψ_{ref}, the corrected reference trajectory angle that takes into account the atmospheric winds effect ψ_{ref_c} and finally the actual trajectory angle ψ that is calculated using the pre-defined trajectory angle rate of change and ψ_{ref_c}.

   (a) Initial reference trajectory angle, ψ_{ref}: This initial step requires only the aircraft position and its current target waypoint position, and it is given by:

$$\psi_{ref} = arctan_2(\Delta\lambda, \Delta\varphi) \quad (28)$$

   - Where $\Delta\lambda$ is the differential longitude, in degrees, where λ_w is the target waypoint's longitude and λ is the current longitude:

$$\Delta\lambda = \lambda_w - \lambda \quad (29)$$

   - And where $\Delta\varphi$ is the differential latitude:

$$\Delta\varphi = \varphi^{(2)} - \varphi^{(1)} \quad (30)$$

$$\varphi^{(1)} = ln\left(\left|tan\left(\frac{\varphi}{2} + 45^o\right)\right|\right) \quad (31)$$

$$\varphi^{(2)} = ln\left(\left|tan\left(\frac{\varphi_w}{2} + 45^o\right)\right|\right) \quad (32)$$

   (b) Corrected reference trajectory angle, ψ_{ref_c}: In order to correct the current trajectory to take into account the atmospheric winds a wind correction angle ψ_{cor} must be calculated. The first step is to calculate the current wind angle and the wind intensity from the atmospheric parameters u_w and v_w.

   i. Wind angle, ψ_w:

$$\psi_w = atan^2(u_w, v_w) \quad (33)$$

   ii. Wind intensity, W_i:

$$W_i = \sqrt{{u_w}^2 + {v_w}^2} \quad (34)$$

   iii. Wind correction angle, ψ_{cor}: Knowing the wind intensity, the aircraft's speed, the wind angle and the initial reference trajectory angle we can now calculate the

wind correction angle:

$$\psi_{cor} = asin\left(\frac{W_i * sin(\psi_{ref} - \psi_w)}{V}\right) \tag{35}$$

iv. Corrected reference trajectory angle, ψ_{ref_c}:

$$\psi_{ref_c} = \psi_{cor} + \psi_{ref} \tag{36}$$

(c) Final trajectory angle, ψ: After calculating the corrected reference trajectory angle, ψ_{ref_c}, the actual current trajectory is calculated. In order to avoid sudden instant variations of the trajectory angle it is calculated using an arbitrary trajectory angle rate of change.

It is important to note that during the initial climb phase the trajectory stays constant, only beyond a certain altitude does the aircraft begin to adjust it's trajectory to reach the target waypoint. During ground phases the wind effects are not taken into account.

9. **True Speed**: In this step, we simply use the calculated acceleration and calculate the current iteration's speed. We also update the iteration's Mach number, where c is the speed of sound retrieved from the current climate state.

$$V = V + a * t \tag{37}$$

$$M = \frac{V}{c} \tag{38}$$

10. **Mass Flow**: Knowing the specific fuel consumption (SFC, as c_{SFC}) the aircraft's current fuel consumption and consequently its mass variation is calculated here. The value of SFC used is interpolated between the aircraft engine's SFC values at sea level (takeoff) and at cruise altitude.

(a) Mass flow, $\dot{m}$:

$$\dot{m} = c_{SFC}T \tag{39}$$

(b) Spent fuel mass, M_{fuel}:

$$M_{fuel} = M_{fuel} + \dot{m}t \tag{40}$$

(c) Aircraft mass, M_a:

$$M_a = M_a + \dot{m}t \tag{41}$$

11. **Aircraft Position**: In order to calculate this iteration's change in position the effects of the aircraft's true speed and of the wind are calculated separately. This allows us to easily set the wind effect to zero if required, for example when the aircraft is on the ground. The longitude, latitude and altitude change of this iteration are also calculated separately and the aircraft's position is updated in the end and converted to geodetic coordinates. The following equations are valid for both true aircraft speed and wind speed, therefore V can refer to either of these speeds.

- Latitude variation, $\Delta\lambda$:

$$\Delta\lambda = \left(\frac{Vcos\psi}{6371008}\right)t \tag{42}$$

- Longitude variation, $\Delta\varphi$:

$$\Delta\varphi = \left(\frac{Vsin\psi}{cos\lambda 6371008}\right)t \tag{43}$$

- Altitude variation, Δh:

$$\Delta h = Vsin\gamma t \tag{44}$$

Using the equations above for both true aircraft speed and wind speed the last step is simply adding the resulting position variation to the current aircraft's position. The differential equations above were solved using the Runge Kutta-Butcher algorithm (23).

12. **Target Verification**: With the newly updated aircraft position it is necessary to verify if we have reached the current target waypoint, by calculating the distance between the aircraft and that target waypoint and comparing to an arbitrary interval value. If the target waypoint has been reached the next waypoint on the list is targeted. When the final waypoint has been reached, the current flight phase is landing and the aircraft's speed is 0, it means the aircraft has landed and the simulation is successful.
13. **Elapsed Time**: The final step of the iteration is to update the elapsed time (T_e) with the current simulation step (t).

$$T_e = T_e + t \tag{45}$$

Simulation

General information

Several simulations were performed using the created TP tool, most of them during development in order to improve upon its results. This chapter will contain three simulations made using the most recent iteration of the tool, divided in two sections: the information required for simulation (flight intent, aircraft information and other relevant factors) and the actual simulation results. The flights were chosen based on their length (a short, medium and long flight), aircraft model, available course information and the availability of actual flight information to be used in the tool's validation discussed on the next chapter. All simulations were conducted on a laptop PC with an Intel Core i7 Processor (8x 2.60 GHz) and 16gb DDR5 RAM running the Windows 10 operating system.

The information required for simulation that was discussed on the previous chapter is shown here for all three flights. Flights departing from or arriving to the USA were preferred because their flight plan was of easier access and the atmospheric database employed seems to be more accurate in this region. The majority of the flight plan information was retrieved from the website flightaware.com, who in turn obtains it from

several government sources, airlines, commercial data providers and ADS-B receivers (24).

Table 2. Flight AA97 general information.

	Flight A (short distance)
Flight number	AA97
Departure airport	Miami, MIA/KMIA
Arrival airport	Houston, IAH/KIAH
Date	March 7, 2017, 10:29 (UTC)
Aircraft Model	Airbus A319-115
Flight time	2 hours 21 minutes
Average flight time	2 hours 26 minutes
Great circle distance	1549.4 km

Table 3. Flight UA632 general information.

	Flight B (medium distance)
Flight number	UA632
Departure airport	Washington, IAD/KIAD
Arrival airport	Los Angeles, LAX/KLAX
Date	March 7, 2017, 7:48 (UTC)
Aircraft Model	Boeing 757-224
Flight time	5 hours 13 minutes
Average flight time	5 hours 22 minutes
Great circle distance	3674.0 km

Table 4. Flight AA142 general information.

	Flight C (long distance)
Flight number	AA142
Departure airport	New York, JFK/KJFK
Arrival airport	London, LHR/EGLL
Date	March 9, 2017, 15:33 (UTC)
Aircraft Model	Boeing 777-223 (ER)
Flight time	5 hours 52 minutes
Average flight time	6 hours 8 minutes
Great circle distance	5539.5 km

General results

This subsection will contain an analysis and comparison of the most important flight parameters between the three simulated flights. All of the following data was taken directly from the TP tool and edited using Python programming language (5), more specifically using the matplotlib package (25) to generate the plots.

Table 5. General simulation results.

	Flight A	**Flight B**	**Flight C**
Total flight time	2h 28m	5h 12m	6h 2m
Distance traveled [km]	1580.42	3831.47	5676.31
Fuel spent [kg]	4846.92	16872.09	38268.11
Fuel spent [% of total]	37.23	41.98	53.77
Takeoff roll distance [m]	1498.17	1780.83	2745.64
Landing distance [m]	1469.87	1265.47	1448.89
Simulation time [s]	2.13	4.02	4.00

Both the flight time and distance traveled were near the expected results. The fuel spent as a percentage of total aircraft fuel was slightly lower than expected, however this will be discussed in further detail later on the chapter. The takeoff roll and landing distances were also in the acceptable range, the comparison between them and their expected actual values will be present in the validation chapter. Finally the simulation time was acceptable, however further optimization might be required if the need to simulate a very large number of trajectories arises.

Wind impact

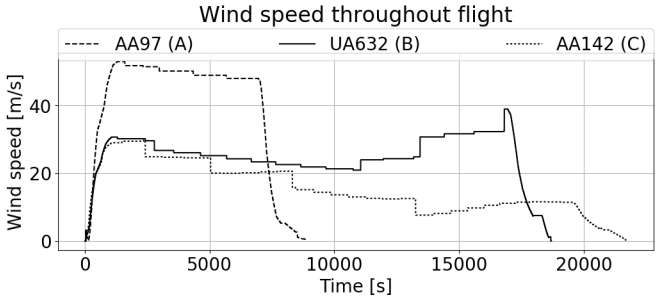

Figure 1. Simulated wind speed throughout the flight for all three cases.

Table 6. Overall wind impact on flight.

	Flight A	**Flight B**	**Flight C**
Duration impact [minutes]	24.66	32.86	-17.9
Duration impact [%]	20.06 %	11.79 %	-5.95 %
Fuel spent impact [kg]	752	1514	-1678
Fuel spent impact [%]	18.36 %	9.85 %	-4,38 %

As expected it can be observed that the wind increases with altitude, however it's also vastly dependent on the geographic position, especially in the case on the transatlantic flight AA142 where the wind speed diminishes significantly while at the same altitude during cruise. Both flight AA97 and flight UA632 had strong headwinds which delayed the flight, while flight AA142 had a significant tailwind. The wind impact on the flights duration was of approximately +20.06% for the AA97 flight, +11.79% for the UA632 flight and -5.95% for the AA142 flight. An obvious consequence of the impact of flight time is the effect of fuel consumption which was significant for all flights, as shown on table 6. The heavy impact of the wind on the shorter flight A will lead to some difficulties in its accurate prediction, as the values used are averages, which may vary heavily over time. These significant impacts easily justify the need to take wind speed into account for trajectory prediction and optimization.

Validation

To validate the used methods of trajectory prediction the three flight trajectories discussed on the previous chapter were compared with values from actual flights. These actual values were obtained from the website flightradar24.com which in turn acquired them mostly from automatic dependent surveillance-broadcast (ADS-B). Aircraft equipped with ADS-B capabilities (roughly 70% of all commercial passenger

aircraft) get their current position from a GPS source while a transponder transmits this information (and more) to nearby receivers which in turn feed the data to its final destination. The information required for this vlidation was the aircraft's ground speed and its location (latitude, longitude and altitude). This information is received by the ADS-B system in intervals of varying lengths from usually 5 to 50 seconds when there is good coverage. This temporal density allows an accurate comparison with the simulation's results. Due to the limitations of the on-board transponders and ground receivers range some remote areas of the globe are not covered by the system even though flightradar24 maintains over 7000 receivers worldwide (26).

In order to provide an accurate comparison the values for both the simulations and the actual flights were interpolated in 10 second intervals and the absolute differences between them, as well as the original values themselves, were plotted. Like in the previous chapter the information was edited using Python programming language (5), specifically pyplot from the matplotlib library (25).

Altitude

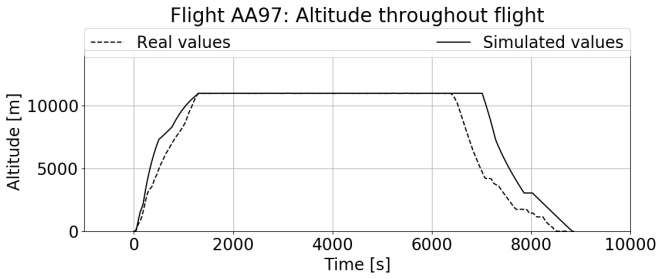

Figure 2. Flight AA97 (A) actual and simulated altitude throughout flight comparison.

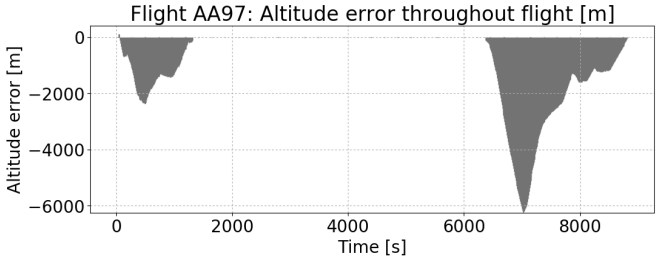

Figure 3. Flight AA97 (A) altitude error throughout flight.

Table 7. Altitude general error.

	Flight A	**Flight B**	**Flight C**
Mean	-833.66	-225.92	-1302.23
Median	-7.95	-8.66	-1269.78
Standard deviation	1375.51	1798.87	924.85
Maximum	95.10	6646.04	128.01
Minimum	-6256.01	-3942.59	-4441.49

The main differences in altitudes are a result of flight planning and aircraft separation maneuvers. For

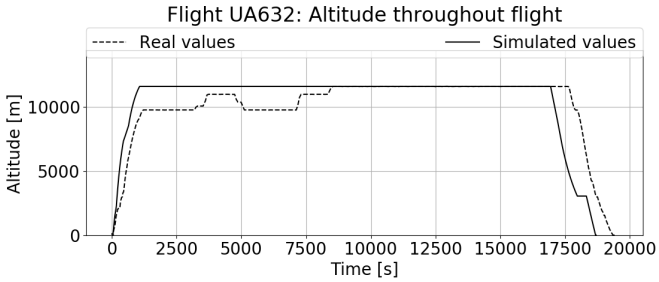

Figure 4. Flight UA632 (B) actual and simulated altitude throughout flight comparison.

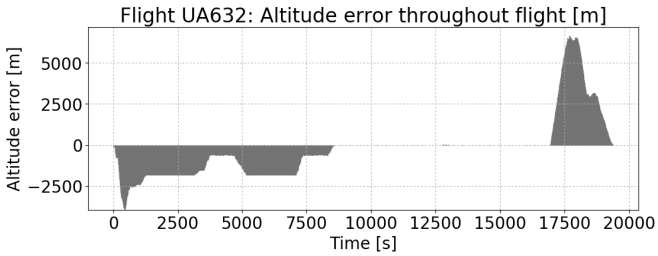

Figure 5. Flight UA632 (B) altitude error throughout flight.

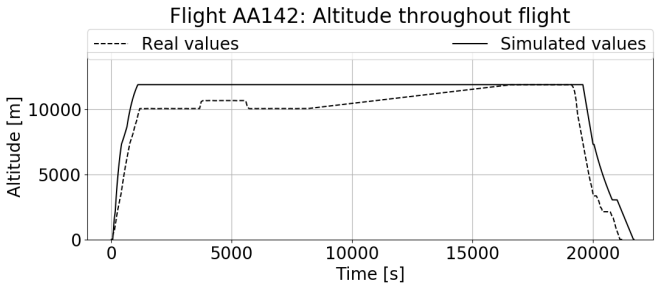

Figure 6. Flight AA142 (C) actual and simulated altitude throughout flight comparison.

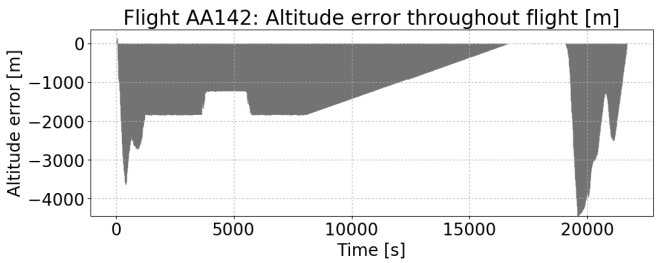

Figure 7. Flight AA142 (C) altitude error throughout flight.

longer flights it is usual for aircraft to fly at non-optimal altitudes in order to meet aircraft separation requirements. During flight the aircraft will climb or descent to the optimal cruise altitude when possible. These changes in altitude are hard to predict beforehand and present a significant difficulty for flight prediction tools. It is also important to note that the transatlantic flight A had no ADS-B coverage throughout some of its duration (approximately between the 8000s and 16000s flight times), which resulted in the linear altitude change during those times, that did not occur that way and is only a simplification.

It can be observed that during climb for all three cases the simulated flight climb gradient was almost

always significantly higher than the actual one. The only exceptions are during the initial climb phase when the climb gradients remains approximate and during the final climb phases of flight A when the simulated climb gradient was significantly lesser than the actual flight. This can be partly explained by an overestimation of the available thrust during the climb phases. Another significant source of error is that the difference of the climb gradient between climb phases is not as big as expected. It can be seen, especially on flight A, that the actual climb gradient remains almost constant throughout climb, while there is a significant difference in climb gradient between the initial and final simulated climb phases.

Regarding the differences between the times to initiate the descent, they can be attributed to the overall ground speed differences during flight and also to the exact distance to reach the airport required to start the descent phase, which is hard to emulate accurately as it depends on several factors.

During the final descent phases, it can be seen in both the actual and simulated cases that there are periods of time when the altitude is maintained constant. In the simulated cases this is to decrease the aircraft's speed before continuing the descent. In the actual cases, however, these periods of time may also be due to loitering periods while waiting for landing clearance or due to approach maneuvers to position the aircraft for the final approach and landing. The final approach phase trajectory and altitudes differ greatly from the simulated values, due to these operations that are not taken into account in the simulation, as it would require case specific intent information, that is very hard to accurately generalize for all flights.

Speed

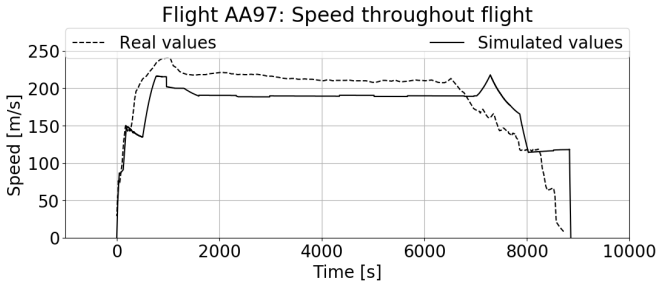

Figure 8. Flight AA97 (A) actual and simulated ground speed throughout flight comparison.

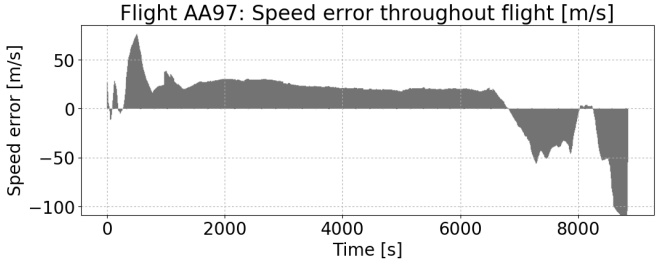

Figure 9. Flight AA97 (A) absolute speed error during flight.

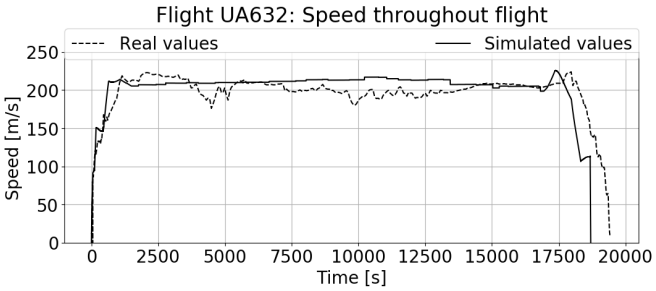

Figure 10. Flight UA632 (B) actual and simulated ground speed throughout flight comparison.

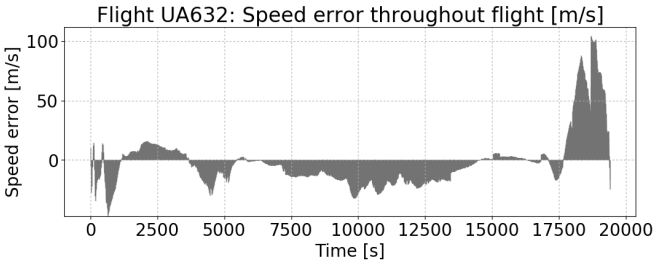

Figure 11. Flight UA632 (B) absolute speed error during flight.

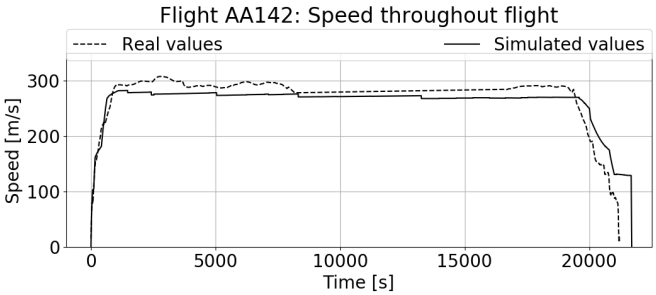

Figure 12. Flight AA142 (C) actual and simulated ground speed throughout flight comparison.

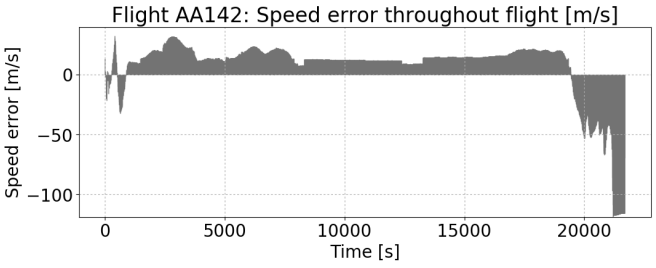

Figure 13. Flight AA142 (C) absolute speed error during flight.

In most cases the speed errors can be largely attributed to wind speed oscillations. During the climb phases, it can clearly be seen that initially the speeds are very approximate to each other. However, this ceases to be the case during the final mach climb phase. This is especially true in flight's A and B cases. This can be partly due to the higher flight path (and consequently climb gradient) of the simulated cases, which was discussed in the previous section as well as

Table 8. Speed general error.

	Flight A	**Flight B**	**Flight C**
Mean	9.35	-2.04	7.02
Median	20.64	-5.00	13.84
Standard deviation	31.96	23.09	25.69
Maximum	76.15	104.21	32.03
Minimum	-108.52	-47.05	-118.80

an abrupt change in the wind database values between flight levels.

During the descent phase, there are two main issues. The first is that the actual descent takes place at different times. This is due to the speed differences throughout the flight and also due to differences in distance between aircraft and airport to begin the initial descent, as mentioned before. The second issue is similar to that of the climbing phases, in that the descent angle is most likely different between cases. The period of time during the simulated descent when the speed remains nearly constant which does not occur in the actual case (except slightly in flight's A case), can be attributed to a descent angle during this time that adjusts itself to maintain the speed approximately constant while descending, which does not occur in the actual case.

Position

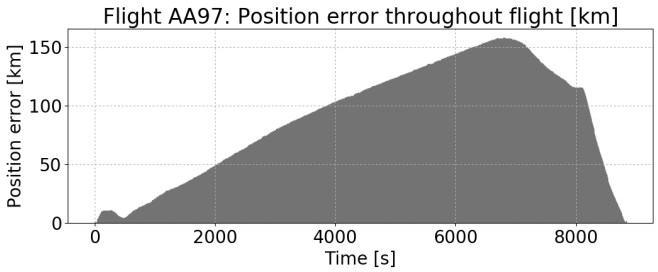

Figure 14. Flight AA97 (A) absolute distance error throughout flight.

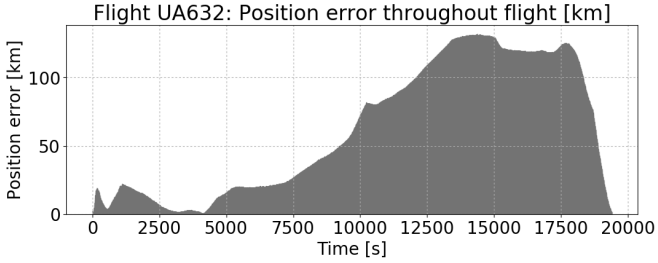

Figure 15. Flight UA632 (B) absolute distance error throughout flight.

These graphs represent, in a way, the culmination of all errors previously discussed in this chapter. Although the absolute distance differences are somewhat small, the flight length must also be taken into account. The first set of graphs represent the absolute distance between the actual and simulated aircraft from the beginning to the end of the flight. The second set represents the relation between that distance and

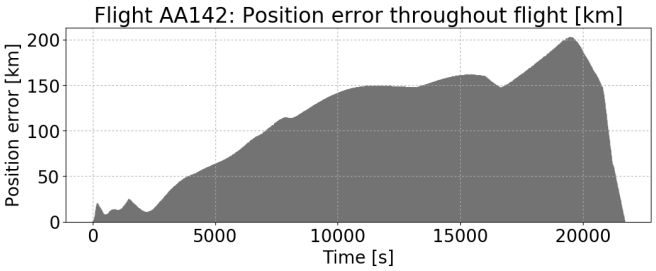

Figure 16. Flight AA142 (C) absolute distance error throughout flight.

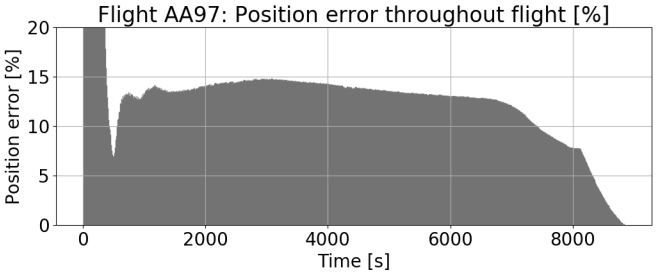

Figure 17. Flight AA97 (A) percentage distance error throughout flight.

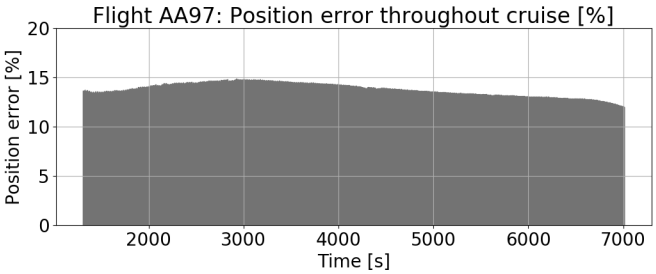

Figure 18. Flight AA97 (A) percentage distance error throughout cruise.

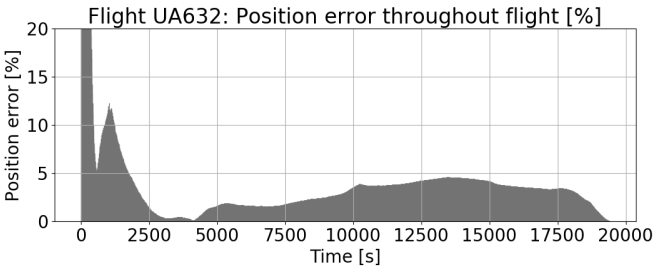

Figure 19. Flight UA632 (B) percentage distance error throughout flight.

the total distance traveled so far into the flight. As expected, during the initial part of the flight this fraction is very high due to the small traveled distance that highly exacerbates this relation. For this reason, both the overall flight and the cruise phase alone was analyzed. Although the absolute distance between aircraft generally tends to increase with time, the percentile error does not show the same tendency, oscillating only slightly along the flight.

The overall most accurate flight regarding position along time was flight B with 5.94% of error percentile mean and 61.9 km of absolute mean error. Flight

Table 10. Absolute distance general error.

	Flight A	Flight B	Flight C
Mean	88.82	61.90	113.90
Median	98.40	48.88	141.44
Standard deviation	48.90	47.81	57.36
Maximum	157.73	131.88	203.00
Minimum	0.38	0.63	1.17

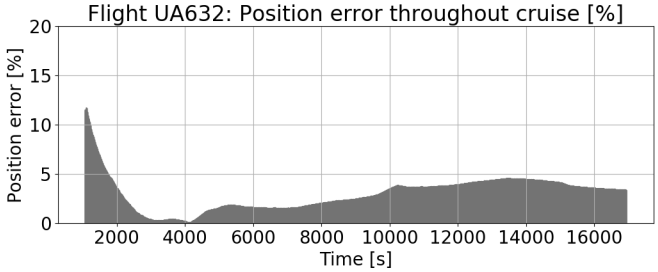

Figure 20. Flight UA632 (B) percentage distance error throughout cruise.

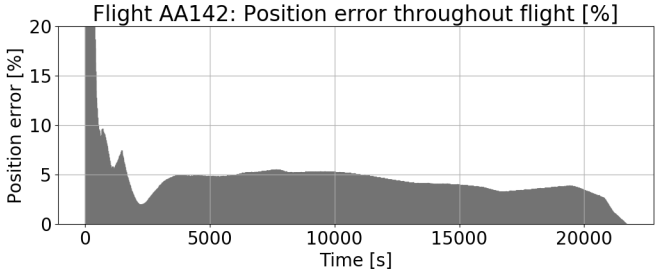

Figure 21. Flight AA142 (C) percentage distance error throughout flight.

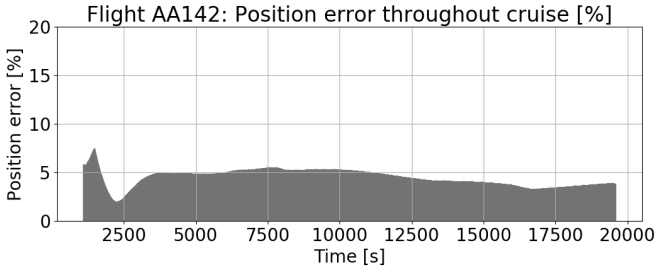

Figure 22. Flight AA142 (C) percentage distance error throughout cruise.

C had less accuracy with a 6.3% percentile error and average 113.90 km absolute error mean, however this is understandable due to the significantly longer trajectory. Flight A was the most inaccurate with a 15.32% percentile error and a 88.82 km absolute distance error despite being significantly shorter than the others. These differences can be attributed to the large average speed difference (9.35 m/s) that was probably due to strong wind differences. Flight A was also the flight that had the biggest wind impact, accounting for 20.06% of the flights duration (compared to flight's B 11.79% and flight's C -5.95%), which exacerbates the wind's effect on the overall errors. As expected, the percent distance average for the cruise flight is smaller than for the whole flight, due to the climb and descent phases inaccuracies and the high error during the initial stages of flight.

Regarding flight time, flight B was curiously both the most accurate in this specific flight case with 0.84% relative and a 2.63 minutes absolute error, but also the most inaccurate when comparing flight time average rather than the specific case, at 3.61% relative and 11.63 minutes absolute error. This could be due to seasonal wind differences that are not taken into account with the flight time average duration. Due to the reasons discussed before, flight A was the most inaccurate in this specific case with an error of 4.67%, however it was the most accurate flight when compared to the average values with only 1.08% error, which further demonstrates the possibility that this specific flight case had a high chance of unusual wind impact.

The takeoff and landing distances error may be due to many different factors, such as lack of information regarding exact values for brake and landing/takeoff runway attrition (which is influenced by the weather) and, in the case of the landing, reverse thrust values.

Table 11. Percentage distance error.

	Flight A	Flight B	Flight C
Mean	15.32	5.94	6.30
Median	13.47	3.34	4.46
Standard deviation	27.54	45.50	23.63
Maximum	712.52	1875.35	922.98
Minimum	0	0	0

Table 12. Percentage distance error for the cruise phase.

	Flight A	Flight B	Flight C
Mean	13.77	2.98	4.45
Median	13.77	3.40	4.63
Standard deviation	0.68	1.75	0.86
Maximum	14.83	11.76	7.46
Minimum	12.00	0.08	1.97

Table 9. General validation results.

	Flight A	Flight B	Flight C
Flight time difference from actual flight	6.58 minutes (4.67%)	2.63 minutes (0.84%)	9.77 minutes (2.78%)
Flight time difference from actual flight average	1.58 minutes (1.08%)	11.63 minutes (3.61%)	7.77 minutes (2.11%)
Speed difference average	9.35 m/s	-2.04 m/s	7.02 m/s
Absolute distance average	88.82 km	61.90 km	113.90 km
Percent distance average for the whole flight	15.32 %	5.94 %	6.30 %
Percent distance average for the cruise phase	13.77 %	2.98 %	4.45 %
Takeoff distance error (relative to average)	-252 m (-14.4 %)	-119 m (-6.3 %)	-154 m (5.3 %)
Landing distance error (relative to average)	119.9 m (8.2 %)	-134.5 m (-9.6 %)	-251.11 m (-14.8 %)

Conclusion

The main aim of this study was to create and validate a trajectory prediction tool and to simulate and analyze actual flights. These objectives were accomplished despite some difficulties encountered, as is to be expected with work of this kind. Trajectory prediction in general can take into account a very large number of variables to increase prediction reliability, and it is not feasible to incorporate all of them. The selection of which parameters to incorporate and develop was one of the main difficulties as it is not always easy to evaluate their impact on the overall reliability of the prediction. A balance had to be encountered between simulation complexity, accuracy and speed. With this in mind we can further analyze the results obtained and determine what can be done to improve the prediction reliability.

A huge difficulty that is often somewhat dismissed in trajectory prediction tools is the effect of the atmosphere, more specifically the wind speed variation. The initial idea was to implement a simple wind shear model. However, this proved to be highly inaccurate for high altitudes and it cannot take into account the large effect of geographical position, wind direction and seasonal differences. The solution was to implement a sufficiently accurate and dense wind speed database. The database used was chosen due to its large density of information, both in latitude/longitude and altitude. However even this database proved to be slightly inaccurate in certain remote regions. It could also not handle the sudden changes in wind speed that can have a drastic effect in flight speed. The only way to improve this area is to use actual values of wind direction and intensity along the flights path, possibly from ADS-B systems, similar to the ones used by Flightradar. This would drastically decrease the trajectory error associated with wind speeds, which is one of the largest and most unpredictable error contributors as seen in the previous section.

Another large error contributor are maneuvers throughout the flight, especially separation and approach maneuvers. Regarding separation maneuvers these are hard to anticipate since they depend on external influences. One way to better improve this aspect is to statistically analyze a certain flight and determine what are the average separation maneuvers for that specific flight. Another much more complex solution would take into account all possible flights that could intercept the current flight and try to emulate the separation maneuvers that would be conducted. As for the approach maneuvers, another statistical study could be conducted to determine what's the average loiter time for landing (if any) for specific flights or airports and the common approach trajectory for that flight.

Some of the most obvious error contributors are the aircraft model inaccuracies and simplifications. Given the complexity of aircraft flight a strong simplification is needed, which enables the calculation of the forces involved. A more sophisticated aircraft model would definitely increase reliability; however, it would have to be adapted for each individual aircraft and would result in an overall high complexity increase. More accurate aircraft specific information, such as aircraft C_{D0} and thrust lapse rate would also increase reliability, although official values are hard to encounter, meaning an estimation study would be required for each aircraft.

The overall result was satisfactory given the complexity of such a field. However, in order to provide accurate trajectory prediction that could be successfully employed, for example, in the NextGen or SESAR programs a lot of work and new sources of accurate information would be required.

Future works should focus on increasing the trajectory predictor's accuracy and fidelity. This may be done in different ways such as applying a more thorough and detailed aircraft dynamical model with a larger and more detailed source of aircraft specific information retrieved from, for example, Eurocontrol's base of aircraft data (BADA). The usage of actual atmospheric prediction values instead of average historical values would highly reduce the uncertainty of the weather system on aircraft prediction, however this would be hard to implement on a global scale. Finally, a different approach to the prediction of separation and approach maneuvers, such as taking into account possible proximity conflicts with other aircraft, is crucial for accurate vertical modeling prediction throughout the flight.

Funding

This research is supported by the Associated Laboratory for Energy, Transportation and Aeronautics (LAETA) of the Portuguese Foundation for Sciences and Technology (FCT).

Declaration of conflicting interests

The authors declare that there is no conflict of interest.

References

[1] A. Philbin. (2017) Traffic growth and airline profitability were highlights of air transport in 2016. [Online]. Available: https://www.icao.int/Newsroom/Pages/traffic-growth-and-airline-profitability-were-highlights/-of-air-transport-in-2016.aspx (Date last accessed 29-September-2017).

[2] "Concept of operations for the next generation air transportation system, version 3.2," FAA, Washington DC, Tech. Rep. 0704-0188, sept 2011.

[3] L. Stridsman, "Sesar concept of operations step 1," SESAR, Brussels, Tech. Rep. DEC-TR-506, may 2012.

[4] R. Lyons, "Complexity analysis of the next gen air traffic management system: Trajectory based operations," *IOS Press*, p. 4514–4522, 2012.

[5] "Python language reference," Python Software Foundation. [Online]. Available: https://www.python.org/

[6] "Kivy - open source python library for rapid development of applications that make use of innovative user interfaces, such as multi-touch apps," Kivy Organization. [Online]. Available: https://kivy.org

[7] (2017) Ncep/ncar reanalysis monthly means and other derived variables. [Online]. Available: https://www.esrl.noaa.gov/psd/data/gridded/data.ncep.reanalysis.derived.html (Date last accessed 29-September-2017).

[8] (2001) Civil jet aircraft design data sets. [Online]. Available: http://booksite.elsevier.com/9780340741528/appendices/default.htm (Date last accessed 29-September-2017).

[9] L. R. Jenkinson, D. Rhodes, and P. Simpkin, *Civil jet aircraft design*. Butterworth Heinemann, 2003.

[10] (2017) Eurocontrol aircraft performance database. [Online]. Available: https://contentzone.eurocontrol.int/aircraftperformance/default.aspx? (Date last accessed 29-September-2017).

[11] "Action plan 16: Common trajectory prediction capability," FAA and EUROCONTROL, Tech. Rep. AP-16, sept 2004.

[12] J. Henderson, R. Vivona, and S. Green, "Trajectory prediction accuracy and error sources for regional jet descents," in *AIAA Guidance, Navigation, and Control (GNC) Conference, Boston, USA*, 2013.

[13] G. Enea, , and M. Porretta, "A comparison of 4d-trajectory operations envisioned for nextgen and sesar, some preliminary findings," in *28th International Congress of the Aeronautical Sciences, Brisbane, Australia*, 2012.

[14] R. Jehlen, "Trajectory based operations (tbo) concept of operations," ICAO ATMRPP, Tech. Rep. ICAO/ATMRPP WG/27 WP/644, oct 2014.

[15] B. Musialek, C. F. Munafo, H. Ryan, and M. Paglione, "Literature survey of trajectory predictor technology," U.S. Department of Transportation, FAA, Washington DC, Tech. Rep. DOT/FAA/TC-TN11/1, nov 2010.

[16] D. Boyle and G. Chamitoff, "Robust nonlinear lasso control: A new approach for autonomous trajectory tracking," Reston, Va., 2003.

[17] (2002) Wind vector notation conventions. [Online]. Available: http://mst.nerc.ac.uk/wind_vect_convs.html (Date last accessed 29-September-2017).

[18] (2010) Flight phase taxonomy. [Online]. Available: https://www.skybrary.aero/index.php/Flight_Phase_Taxonomy (Date last accessed 29-September-2017).

[19] R. Mayer, "A flight trajectory model for a pc-based airspace analysis tool," Reston, Va., 2003.

[20] E. Williams. (2012) Aviation formulary v1.46. [Online]. Available: https://www.flightradar24.com (Date last accessed 29-September-2017).

[21] *Environmental Technical Manual*, ICAO.

[22] Y. S. Chati and H. Balakrishnan, "Aircraft engine performance study using flight data recorder archives," in *2013 Aviation Technology, Integration, and Operations Conference*, Los Angeles, CA, 2013.

[23] J. Park, D. Evans, K. Murugesan, S. Sekar, and V. Murugesh, "Optimal control of singular systems using the rk-butcher algorithm," *INT. J. COMPUT. MATH.*, vol. 81, no. 2, pp. 239–249, 2004.

[24] (2017) Flightaware. [Online]. Available: https://flightaware.com/ (Date last accessed 29-September-2017).

[25] J. D. Hunter, "Matplotlib: A 2d graphics environment," *Comput. Sci. Eng.*, vol. 9, no. 3, pp. 90–95, 2007.

[26] (2017) Flight radar. [Online]. Available: https://www.flightradar24.com (Date last accessed 29-September-2017).